AHRI Project 8013:
A Study of Methods to Represent Compressor Performance Data over an Operating Envelope Based on a Finite Set of Test Data

Final Report
May, 2015

Prepared by:
Dr. Vikrant Aute, Cara Martin,
Dr. Reinhard Radermacher
Optimized Thermal Systems, Inc.
5000 College Avenue, Suite 3105
College Park, MD 20740

Prepared for:
Air-Conditioning, Heating, and Refrigeration Institute (AHRI)
2111 Wilson Boulevard, Suite 500
Arlington, VA 22201

© 2015 AHRI

Executive Summary

Optimized Thermal Systems, Inc. (OTS) was selected to work with the Air-Conditioning, Heating, and Refrigeration Institute (AHRI) and the associated Project Committee on Project 8013: *A Study of Methods to Represent Compressor Performance Data over an Operating Envelope Based on a Finite Set of Test Data*. Work was conducted between August 2013 and February 2015. The project included a thorough review of the existing method to represent compressor performance data for positive displacement compressors, currently outlined per ANSI/AHRI Standard 540-2004 (AHRI-540), and identify a new method(s), if appropriate, to account for system uncertainties and existing errors in data representation.

Multiple factors contribute to inaccuracies with the current AHRI-540 methods including measurement uncertainty, regression uncertainty, compressor to compressor variation, and operation outside of the normal operating envelope (extrapolation). An improvement in the method for representing data will likely enable an improvement in the accuracy of the product ratings without increasing the cost of generating the data.

In order to analyze the existing data representation method and evaluate potential alternatives, members of the project committee provided as many raw compressor data sets as feasible. These were used to conduct an uncertainty analysis, assess the accuracy of the AHRI-540 method, assess the accuracy of four identified alternative methods, evaluate the effect of sample size, and evaluate the effect of superheat.

In addition to the request for raw compressor data, participating project committee manufacturers were asked a series of questions regarding their practices and procedures in testing compressors and developing a representative compressor performance map from the collected data. Most manufacturers indicated that more than fourteen test points were used to develop their compressor maps (a minimum of eleven points are needed to develop the AHRI-540 10-coefficient model). Most manufacturers also account for unit to unit variation, testing at least three separate units of the same compressor model. But of those surveyed, all manufacturers indicated that testing is performed as close to the operating envelope as possible and that no validation is conducted for any extrapolated data points.

Prior to completing any analyses, a comprehensive literature review was conducted to identify alternative compressor models and data representation methods. Four models in addition the AHRI540 baseline method were selected for review and analysis. These included a variation of the AHRI540 model (MPOLY) and models as presented by Qiao et al. (2014) [QIAO], Jahnig et al. (1999) [KLEIN], and Navarro et al. (2007) [EMILIO].

Before the alternative methods were evaluated, a regression uncertainty analysis was conducted using a Monte Carlo simulation method. Results showed that the average uncertainty in mass flow rate prediction can be as high as 4% and that in power prediction can be as high as 5%. The worst case maximum absolute error in predicted mass flow rate across all data sets was 17% and that for power was 9%. Error in predicted power and mass flow rate is higher for larger capacity compressors. For most compressors, the high errors occur in the region of the envelope with low suction and low discharge dew point temperatures.

Three data sets were available for comprehensive comparison of the AHRI540 model predictions over the entire operating envelope and beyond (for extrapolation). It was observed that within the operating envelope, the AHRI540 model predicted the mass flow rate and power within an average error of 1%. But for extrapolated areas, (10°F outside the operating envelope on suction and discharge dew point), the worst case errors were as high as 9% in power and 8% in mass flow prediction. This indicates that the AHRI540 performance map is not suitable for extrapolation purposes.

In reviewing the AHRI540 baseline model and the selected alternatives, the accuracy in predicting behavior varied significantly. For most of the data sets, the average errors in mass flow rate prediction were better than 2% and the maximum absolute errors were of the order of 2.5% for the AHRI540, MPOLY and QIAO models. The KLEIN and EMILIO models resulted in average errors in mass flow rate predictions on the order of 3%, but the maximum errors were more than 7%. In the case of power prediction, the AHRI540 and MPOLY models showed average errors of 3%, the QIAO model had errors around 4%, and the KLEIN and EMILIO models exhibited errors greater than 15%. Error metrics were also analyzed with regards to compressor type, compressor capacity and refrigerants. In general, the QIAO and the MPOLY models were found to be more suited for rotary and reciprocating compressors than scroll compressors.

In addition to reviewing the models for accuracy in predicting power and mass flow rate, a study of sampling method considering different sample sizes and multiple sampling methods was conducted. This analysis was presented with several challenges, particularly since the compressor operating envelope is a non-rectangular domain. A sampling method using Latin Hypercube Design (LHS) and a proposed alternative sampling method based on design of experiments (PDOE) were evaluated. In general, both the LHS and PDOE methods yielded similar errors in mass flow rate for all models for samples sizes of 12, 14 and 16. Thus, for mass flow rate, it is possible to build a model with 12 systematically selected test points. For power prediction, the average error for the LHS and PDOE methods using AHRI540, QIAO and MPOLY was lower than 2% for all sample sizes. The KLEIN and EMILIO models exhibited significantly higher errors.

Lastly, a study on the effect of superheat was conducted. In general, the error in predicted mass flow rate for superheat values different than the map superheat has a strong correlation with the ratio of suction densities. The same is true for errors in power prediction, except for the QIAO model. The Dabiri and Rice (1981) superheat correction was found to work well for the AHRI540 map. The QIAO model shows good average prediction, but very high maximum errors. The AHRI540 model produces the best predictions in power for alternate superheat cases, however, even better than the corrected model. All of the other models exhibit significantly high errors making them unusable for any prediction task.

Based on the results of the analysis conducted for this Project, the following conclusions are drawn:

1. Reducing the measurement uncertainty is important. Particular attention must be paid for measurements involving low suction and low discharge dew point temperatures.

2. The regression uncertainty has an additive effect on the overall model prediction when the measurement uncertainty is factored into the overall model uncertainty.
3. In order or reduce the regression uncertainty, numerically stable and linearly regressed models should be selected.
4. There is potential for reducing the number of tests used to develop the performance map for a compressor.
5. The use of a systematic design of experiments (DOE) method is recommended for selection of samples once an operating envelope is determined. Adaptive DOE methods are available in the literature that can improve model accuracy for the same number of tests.
6. It is possible to develop a test matrix with less than 16 points that will also be suitable for different superheat values and for reasonable extrapolation. Such a test matrix would involve tests at multiple suction superheat values. Evaluating this approach is recommended for future work.

Table of Contents

Nomenclature

Symbol	Definition
a1 – a18	Regression coefficients
$b_1 - b_9$	Regression coefficients
d, e	Regression coefficients
f	Regression coefficient / frequency
C	Clearance volume ratio
h	Enthalpy
k	Isentropic exponent
$\dot{m}$	Mass flow rate
m	Polytropic exponent
n	Polytropic exponent
p	Pressure
T	Temperature
$\dot{V}$	Volume flow rate
V	Swept volume
Greek Symbols	
α	Loss factor
δ	Dimensionless diameter/small fraction of the property
ρ	Density
$\emptyset$	Normalized frequency
φ	Pressure ratio
ϑ	Specific volume
η	Efficiency
Subscripts	
amb	Ambient
comb	Combined
comp	Compressor
c, cond	Condenser
dis, ex	Discharge / Exit / Outlet
e, evap	Evaporator
isen	Isentropic
loss0	Constant Loss
mech	Mechanical
nominal	Nominal

su, suc, suction, in	Compressor Suction / Inlet
sh	Compressor Shaft
vol	Volumetric

Acronyms

AAPE	Average Absolute Percent Error
AHRI	Air-Conditioning, Heating and Refrigeration Institute
COP	Coefficient of Performance
COV	Coefficient of Variance
DOE	Design of Experiments
EMILIO	Method proposed in Navarro et al. (2007)
HVAC&R	Heating, Ventilation, Air-Conditioning, and Refrigeration
KLEIN	Method proposed in Jahnig et al. (1999)
LHS	Latin Hypercube Design / Sampling
MAEP	Maximum Absolute Error Percent
MAPE	Maximum Absolute Percent Error
MPOLY	Variation of AHRI Standard 540 Method
OTS	Optimized Thermal Systems, Inc.
PDOE	Polygon Design of Experiments
QIAO	Method proposed in Qiao et al. (2014)
RPM	Revolutions Per Minute
RRMSE	Relative Root Mean Square Error

1 Introduction

In August 2013, the Air-Conditioning, Heating, and Refrigeration Institute (AHRI) solicited proposals for Project 8013: *A Study of Methods to Represent Compressor Performance Data over an Operating Envelope Based on a Finite Set of Test Data*. The project was to include a thorough review of the existing method to represent compressor performance data for positive displacement compressors, currently outlined per ANSI/AHRI Standard 540-2004, and identify a new method(s) to account for system uncertainties and existing errors in data representation. Optimized Thermal Systems, Inc. (OTS) was selected to complete the compressor performance data study. This report summarizes the findings and recommended outcomes of the project. The original project scope of work is outlined in Appendix A.

2 Background

The current performance rating standard for positive displacement compressors requires manufacturers to report tabular performance data over a specified operating envelope. The data is usually generated using a 10-coefficient third order polynomial equation. The coefficients for the equation are derived from measured and/or extrapolated values using the method of "Least Squares". This equation is also frequently used by manufacturers to represent the tabular data in a form suitable for use in simulation programs.

The original intent of this reporting method was to provide a consistent and uniform way of presenting performance data to enable manufacturers to evaluate different compressors for a particular application. Manufacturers also desire to use compressor performance with simulation tools to calculate system performance values for rating purposes. The current equation that is used to represent the data does not, however, always provide sufficient accuracy to meet the need for product rating.

A number of factors contribute this inaccuracy. One source of uncertainty, for example, is the skewing and shifting of the data based curve to go through the two primary air conditioning rating points. There is no certification of the final curve other than the two rating points, so significant errors may be generated throughout the remainder of the map. Due to the costs involved with collecting the measured data, there is a desire to use the fewest number of data points. No specific information is provided to understand the impact of the number and distribution of measured test points to achieve a particular level of accuracy. Other sources of uncertainty are associated with the variation of measurement reproducibility across the application envelope as well as the compressor to compressor variation. An improvement in the method for representing data will likely enable an improvement in the accuracy of the product ratings without increasing the cost of generating the data.

3 Project Objectives

The purpose of this project is to improve the method used to represent compressor data and to quantify uncertainty. It will advance the state of the art by providing a comparison of the accuracy of different methods to represent the data and a methodology for quantifying the resulting accuracy for a specific application to better understand requirements for rating

accuracy. A statement of expected accuracy for compressors would be useful in arguments over certification and enforcement tolerances. This study should also provide information to help define future work based on the difference between the resulting levels of accuracy and desired levels.

Specifically, the objectives for this project include:

1. Determine the optimal method to represent performance data over the application envelope, which maximizes accuracy for a given number of test points; and,

2. Develop an estimate of the level of uncertainty in each method as a function of measurement reproducibility and/or product to product variation especially at the typical rating points given in the standard.

4 Test Data Used for Analysis

In order to evaluate the current method of developing a representative compressor performance map from experimental data, member companies of the project committee provided raw compressor data, published coefficient information, and information on the methodologies used to test compressors and develop representative performance maps. An overview of the requested and collected data, as well as the responses received on the manufacturer survey are presented in the subsections below.

4.1 Raw Compressor Data

The existing AHRI Standard 540 includes single and variable positive displacement compressors for five different applications. In order to conduct a comprehensive review of the effectiveness of the existing method, data for the full reach of the Standard was requested. The ideal data set for project analysis consists of every possible combination of the parameters presented in Table 1.

Table 1: Ideal Compressor Data Set

Compressor Type	Application	Refrigerant	Capacity
Reciprocating	Air cooled A/C & HP	Pure fluid (eg.:R134a)	Low
Rotary	Evap cooled A/C & HP	Mixture (eg.:R410A)	Medium
Scroll	Water cooled A/C & HP		High
Screw	Refrigeration		

Members of the project committee provided as many raw compressor data sets as feasible. Actual data sets collected and used for the analysis of this project are summarized in Table 2.

Table 2: Received Data Set Used for Project Analysis

Compressor Type	Application	Refrigerant	Capacity Range [Btu/hr]	Number of Data Sets	Number of Units Per Model
Reciprocating	A/C & HP	R410A	2,285 – 65,099	9	2-3
Reciprocating	A/C & HP	R22	5,075 – 36,079	2	3
Scroll	A/C & HP	R410A	6,013 – 776,125	8	1
Rotary	A/C & HP	R410A	3,838 – 44,427	2	1
Rotary	A/C & HP	R134a	1,523 – 18,695	2	1
Rotary	A/C & HP	R407C	4,813 – 20,851	1	1
Reciprocating	Low Temp	R404A	1,816 – 10,331	1	1
Reciprocating	High Temp	R407C	5,611 – 40,906	1	1
Reciprocating	High Temp	R134a	2,929 – 12,739	1	1
Reciprocating	Medium Temp	R404A	2,564 – 13,483	1	1
Scroll	Low Temp	R404A	4,844 – 19,970	1	1
Screw	A/C & HP	R134a	Too few data points to perform fitting. AHRI coefficients not provided.		
Reciprocating	Medium Temp	R410A			
Reciprocating	Low Temp	R134a			
Reciprocating	Low Temp	R404A			
Total complete data sets available for analysis : 29					

As can be seen from the table, data received accounted for three types of compressors (reciprocating, rotary and scroll) over a complete capacity range for both pure fluids (R134a and R22) and mixed refrigerants (R404A and R410A). Data for multiple compressors of the same model were also acquired to evaluate the impact of unit to unit variation.

Prior to receiving data, OTS and the project committee agreed on the parameters to include and the format for each compressor data set. Data generally included compressor geometry, operating conditions (pressure, temperature, mass flow rate, superheat, etc.), performance, instrument uncertainties, and Standard 540 coefficients. A comprehensive list of the data points requested is provided in Appendix B.

For some data sets, it was observed that there were differences between the provided coefficients and those calculated by OTS using the raw data provided. This is likely due to the exclusion of some raw data not identified to OTS. For purposes of analysis, if a difference in coefficients existed, the calculated coefficients from the raw data provided were used rather than the published coefficients.

Lastly, the data provided for R404A and R407C compressors was based on variable superheat as opposed to the constant (20°F) superheat for all other data sets. These were still included in the analysis.

4.2 Manufacturer's Survey

In addition to the request for raw compressor data, manufacturers were asked a series of questions regarding their practices and procedures in testing compressors and developing a representative compressor performance map from the collected data. A list of the survey questions and a summary of the responses are included in Appendix C. OTS received input from a total of six manufacturers.

While the number of responses received is statistically insignificant to draw any specific conclusions, input provided by the manufacturers regarding the methodology used to develop representative compressor performance maps provides some insight on the need for a review, and possibly replacement, of the existing standard.

Manufacturers were asked about the number of test points used to generate the compressor map, including the number of test points used, the total number of tests conducted for a single compressor, and the number of units tested for the same model. Given that the AHRI Standard 540 is a 10-coefficient model, the minimum number of test points required to generate a performance map would be eleven. Most manufacturers indicated that more than fourteen test points were used to develop their compressor maps. One manufacturer, however, indicated that only five to ten test points were used to generate a compressor map, which is mathematically challenging and will lead to further inaccuracies. Most manufacturers account for unit to unit variation, testing at least three separate units of the same compressor model. Two manufacturers responding to the survey indicated that only one or two units may actually be tested for developing map data.

Determining the performance envelope is important in establishing a boundary for the collected data and understanding testing and operating limits. Manufacturers confirmed that the performance envelope is application specific. In order to aid in comprehensive analysis for the purposes of the study, the project committee assisted OTS in establishing appropriate envelope limits for each of the five applications included in Standard 540.

One of the motivating concerns for the project was the potential for extrapolation and data shifting and understanding the impact this has on the accuracy of the compressor performance data representation. As such, manufacturers were asked about any extrapolation and/or data shifting practices. All manufacturers indicated that testing is performed over the full rating conditions, as close to the operating envelope as possible. No manufacturers test at or beyond the operating envelope and two manufacturers indicated that extrapolation is used for extremely high or low temperatures. No validation is conducted for any extrapolated data points. Another two manufacturers indicated that data can be skewed / shifted to the rating points by repeating the data for those points in the data reduction process.

All of the manufacturers surveyed indicated that compressor testing is completed in house. Measurement accuracy, however, varied widely between the manufacturers such that a general

trend could not be identified. As such, measurement uncertainties for the uncertainty analysis presented in Section 5 uses the minimum required accuracies per ASHRAE Standard 23.

Refrigerant purity surfaced as another manufacturer concern during early discussions of the project. When surveyed, responses were split. Three manufacturers indicated that refrigerant used for compressor testing was regularly replaced. The other manufacturers indicated that the refrigerant was not routinely checked, though all manufacturers use virgin refrigerant to the extent possible.

5 Uncertainty Analysis and Results

Correlations based on experimental data are widely used in the HVAC&R field. Common examples are the AHRI 10-coefficient compressor map, heat transfer and pressure drop correlations for various surfaces, etc.

Experimental measurements involve uncertainty due to various sources and it is important to characterize the effect of measurement uncertainties on the regression coefficients (Coleman and Steele, 2009). This helps us to better understand the effect of measurement uncertainty on the values predicted by the compressor map and the corresponding uncertainty when the map is used for system rating. The uncertainty information can then be used in understanding the effect of tolerances used in the various rating and enforcement tests.

5.1 Sources of Uncertainty

The following are the sources of uncertainty in the performance rating/testing of manufactured products:

a. Manufacturing/product tolerances
b. Testing procedures
c. Instrument accuracies (a.k.a. measurement uncertainty)
d. Random uncertainty during testing (e.g., one unit tested repeatedly at the same lab)
e. Testing location (variability between laboratories, testing the same unit)

Table 3 below shows the various uncertainties and the type of data required to quantify these uncertainties.

Table 3: Uncertainty types and data required for quantification

No.	Uncertainty Type	Data Required for Quantification
1.	Measurement uncertainty (systematic)	Measured data from the laboratory Instrument accuracies Data reduction procedure
2.	Measurement uncertainty (random)	Multiple measurements (e.g., 30 second interval at steady state)
3.	Environmental uncertainty (random)	Data for one unit tested repeatedly in the same laboratory under the same test setup
4.	Variability between laboratories (random)	Data for one unit tested in multiple laboratories under the same test set up
5.	Manufacturing/product variation (random)	Data for multiple units of the same model tested in the same laboratory under the same test setup

5.2 Systematic Uncertainty Analysis

The typical data used in the map are measured temperatures, mass flow rate and power consumption. These are all measured quantities (and not derived) and hence no uncertainty propagation is required. The uncertainty due to regression is analyzed in Section 5.3.

5.3 Regression Uncertainty Analysis

5.3.1 Overview

Conventional uncertainty propagation is carried out using the Taylor series expansion method (Coleman and Steele, 2009). But such an approach is not applicable to the case where-in measured data (e.g., suction and discharge temperature, power, mass flow rate) are used as a part of regression to predict certain parameters of interest. Coleman and Steele (2009) describe an approach for one-input-one-output case using closed form expressions. Based on similar analysis expressions for regression uncertainty can be derived for 2-input-1-output case. An example of such a case is the prediction of compressor power based on the suction and discharge dew point temperatures. Such mathematically rigorous derivation is beyond the scope of this project and as such it is proposed to use the Monte Carlo simulation method.

In the case of compressor testing, the measured quantities include, the suction and discharge dew point temperatures, the power consumption and the mass flow rate. The ASHRAE Standard 23 provides the required measurement accuracies for these quantities. These accuracies are depicted in Table 4 below.

Table 4: Measurement accuracies

Quantity	Accuracy
Temperature	0.5°F
Power	1% of measured value
Mass flow rate	1% of the measured value

During the course of actual experiments, there are random errors as well, which are included in the measurements, but are not quantitatively identified.

5.3.2 Approach

For the purposes of Monte Carlo analysis, the various measurement errors are assumed to be normally distributed with a mean value as the measured value reported in the data sets and the standard deviation as the accuracy value reported in the previous table. Theoretically speaking, the use of accuracy values as standard deviation is not advisable, since the actual standard deviation will be lower. But it is used here to account for the overall measurement uncertainties including both systematic and random errors.

Furthermore, conducting the Monte Carlo analysis with lower values of the standard deviation will not change the location of the points with highest and lowest prediction errors on the compressor operating envelope (plot of Te and Tc).

In order to determine the number of simulation runs required for a good estimate of the mean and standard deviation, the Monte Carlo analysis was carried out for several datasets with a varying number of simulation runs ranging from 1000 to 100,000. Results are depicted in Table 5 below.

Table 5: Effect of simulation runs in Monte Carlo analysis

Simulation Run Count	Power Error in Mean [%]	Power COV [%]	Mass flow rate Error in Mean [%]	Mass flow rate COV [%]
1,000	0.1285	0.5611	0.7841	0.7000
5,000	0.1660	0.5679	0.7489	0.7145
10,000	0.1582	0.5606	0.7751	0.7077
20,000	0.1685	0.5636	0.7748	0.7135
50,000	0.1640	0.5648	0.7813	0.7157
100,000	0.1673	0.5655	0.7720	0.7164

The case with 100,000 runs takes approximately 30 minutes. Based on the results of these parametric runs and the computation, it was decided to use 25,000 runs for the Monte Carlo analysis as it offered a good trade-off between the accuracy (two decimal places) and computation time.

The following steps describe the Monte Carlo simulation carried out for each data set. Assume that there are 50 data points in the data set.

1. Generate 25,000 data sets, based on normal distribution, each comprising of 50 data points.
2. Develop regression model (curve fit) for each data set, based on the 10-coefficient polynomial. One model each is developed for power consumption and mass flow rate, as a function of Te and Tc.
3. Predict each point in the original dataset using the regression models. Thus, for each of the 50 points, we will have 25,000 predicted values for power consumption.
4. Compute the mean and the standard deviation of these 25,000 predicted values. The difference between this mean value and the measured value is termed as the Error in Mean. The ratio of the standard deviation and the mean is termed as the coefficient of variance (COV).
5. For each of those 25,000 predicted values, we can also compute the individual errors, i.e., difference between predicted power consumption at that point (i.e., [Te,Tc]) and the measured value. The maximum absolute percent error can then be computed for each of these 50 points.
6. The error in mean and the maximum absolute error can then be plotted on [Te,Tc] plot representing the compressor operating envelope. Thus for each compressor dataset, we can generate four plots (i.e., 2 each for mass flow rate and power consumption).

5.3.3 Results

This section presents the results for the Monte Carlo analysis. Instead of showing all 176 plots developed through the analysis, only a subset of the plots are shown here. The shading scale is maintained consistent across all the error plots for consistency and ease of interpretation.

The detailed error metrics, along with the number of available data points in each data set, are included in Table 6. The same information is also presented in Figures 21 and 22. The columns in Table 6 should be interpreted as follows:

- Max. Error in Mean – This is the maximum error over the entire operating envelope in the mean value of mass flow rate (or power).
- COV [%] – This is the Coefficient of Variance, and is the standard deviation expressed as a percentage of mean. Lower COV is better.
- MAPE – This is the maximum absolute percent error and indicates the worst case prediction error in mass flow rate (or power) over the entire operating envelop.

Based on the error metrics and the individual analysis of each of the 176 plots, the following general conclusions can be drawn:

1. The minimum absolute error in the predicted mean power is 0.2% and the maximum error in the predicted mean power is 5% (neglecting the R410A outlier, at 12%). The maximum COV is 1.7%.
2. The minimum absolute error in predicted mean mass flow rate is 0.4% and the maximum error in the predicted mean mass flow rate is 4.3%. The maximum COV is 3.5%.
3. The worst case maximum absolute error in predicted power is 9%.
4. The worst case maximum absolute error in predicted mass flow rate is 17%.
5. In general, the maximum (worst case) errors in mass flow rate prediction are much higher than those in power prediction.
6. For most compressors, the highest errors occur in Quadrant-3, i.e., low suction dew point and low discharge dew point region. These are the compressors that have "sufficient" number of data points distributed across the entire operating envelope.
7. Refrigerants R134a, R404A and R407C exhibit higher errors compared to R410A, but the corresponding datasets do not have 'sufficient' points to begin with. As such these errors could be due to insufficient data available for regression.
8. Larger compressors (i.e., high power and mass flow rate values) exhibit higher errors.

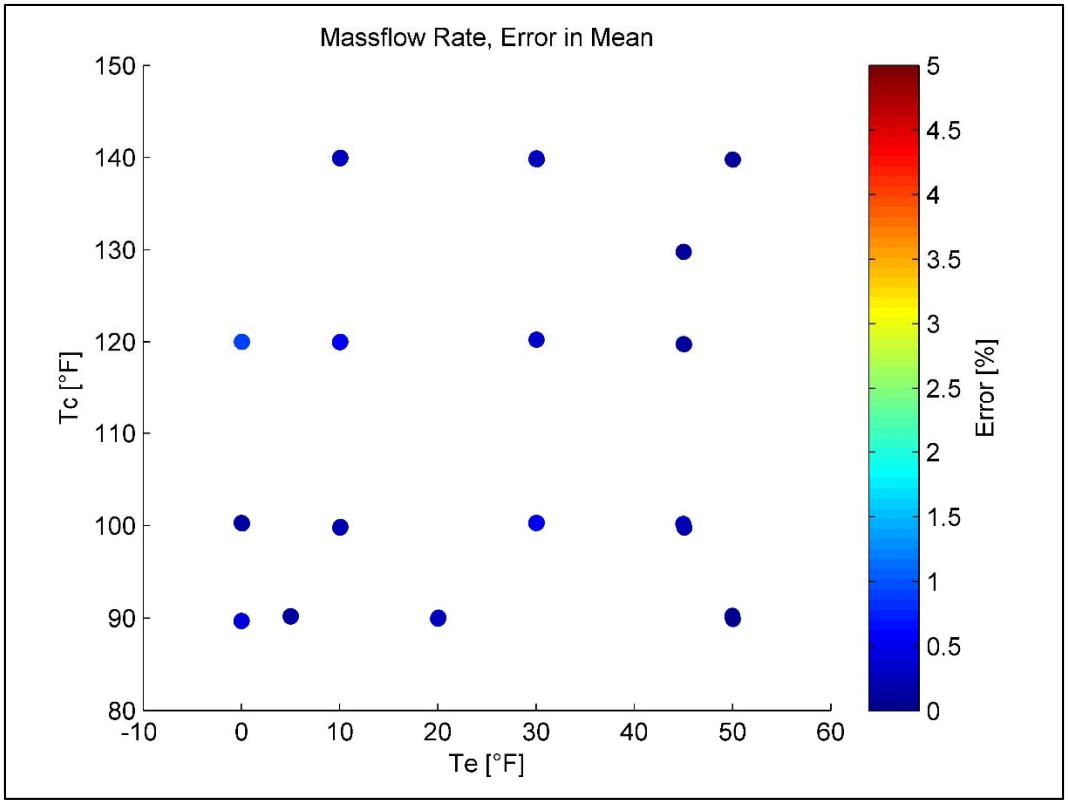

Figure 1: R22 Compressor, error in mean mass flow rate

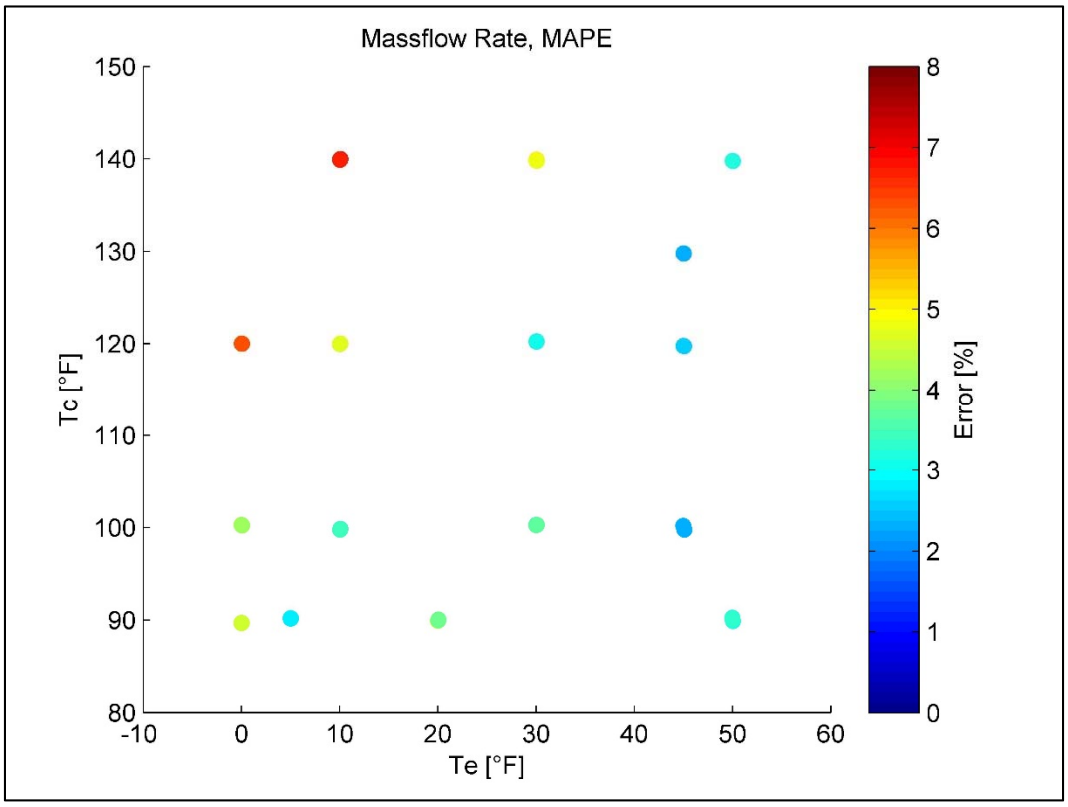

Figure 2: R22 Compressor, maximum absolute percent error in mass flow rate

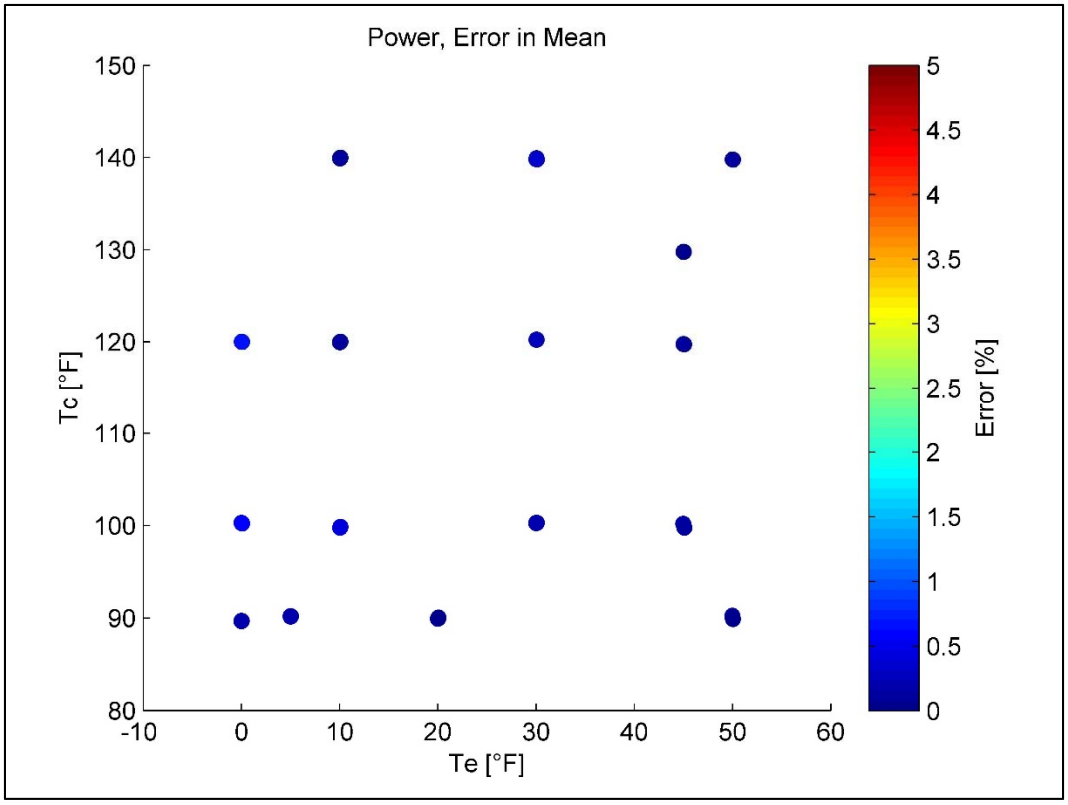

Figure 3: R22 Compressor, error in mean power

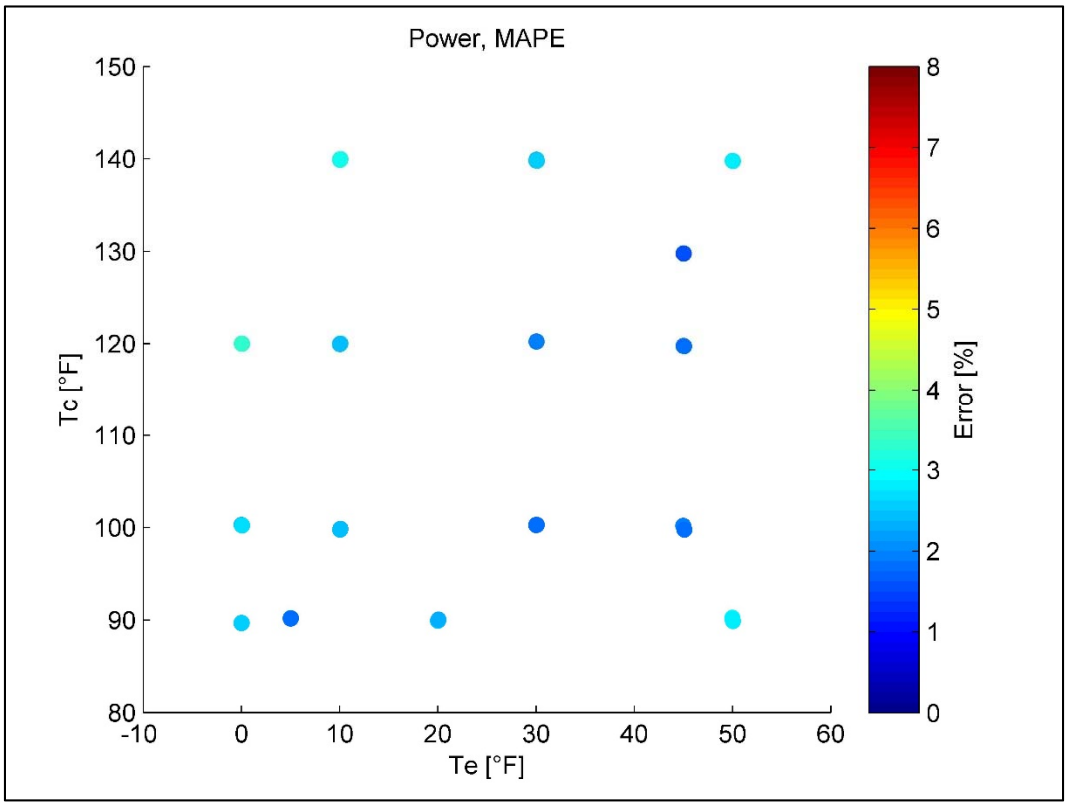

Figure 4: R22 Compressor, maximum absolute percent error in predicted power

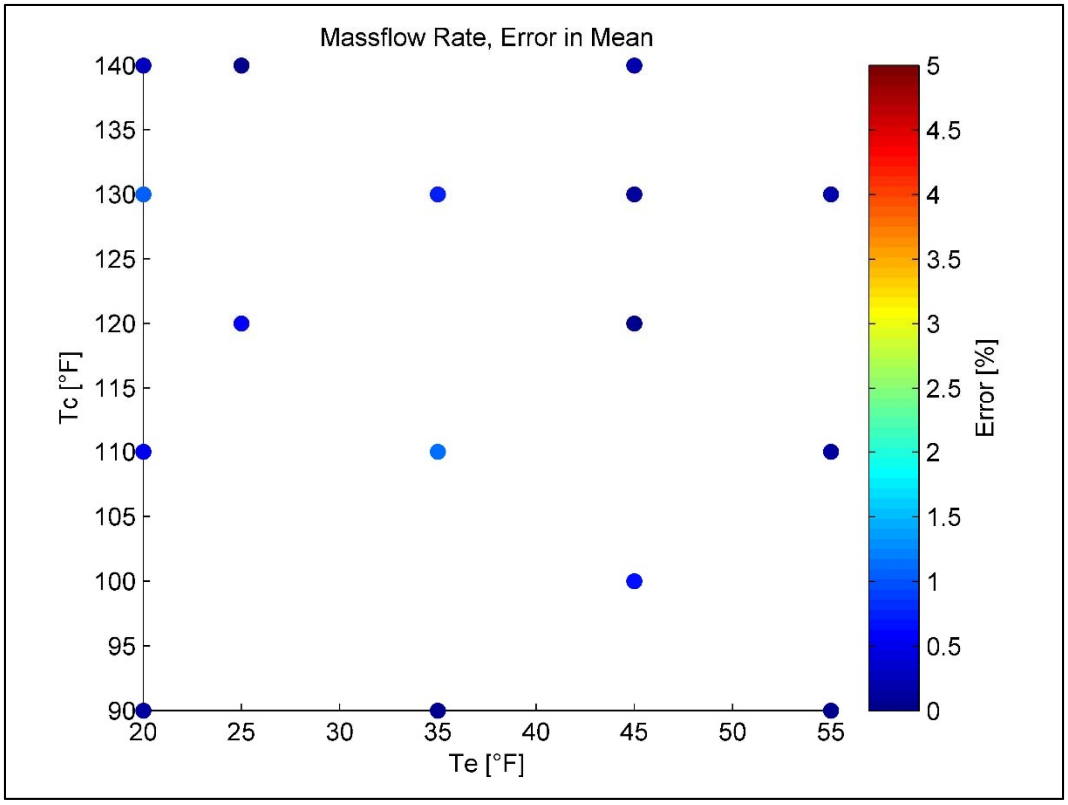

Figure 5: R134a Compressor, error in mean mass flow rate

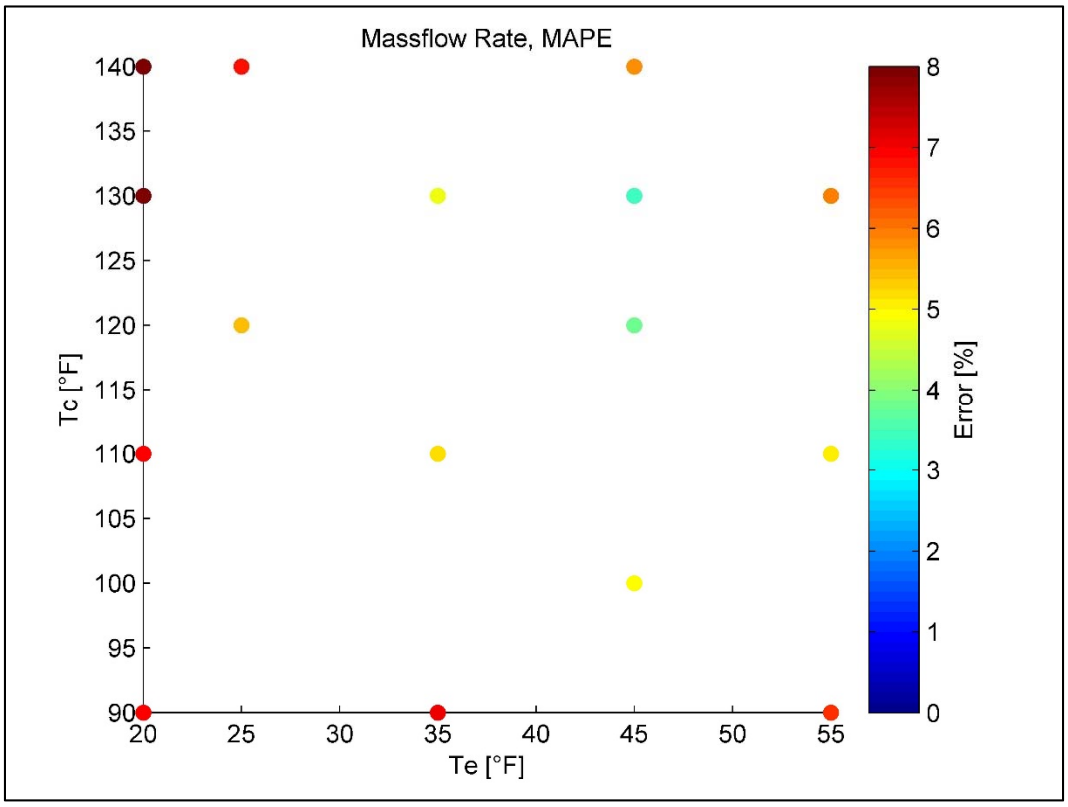

Figure 6: R134a Compressor, maximum absolute percent error in predicted mass flow rate

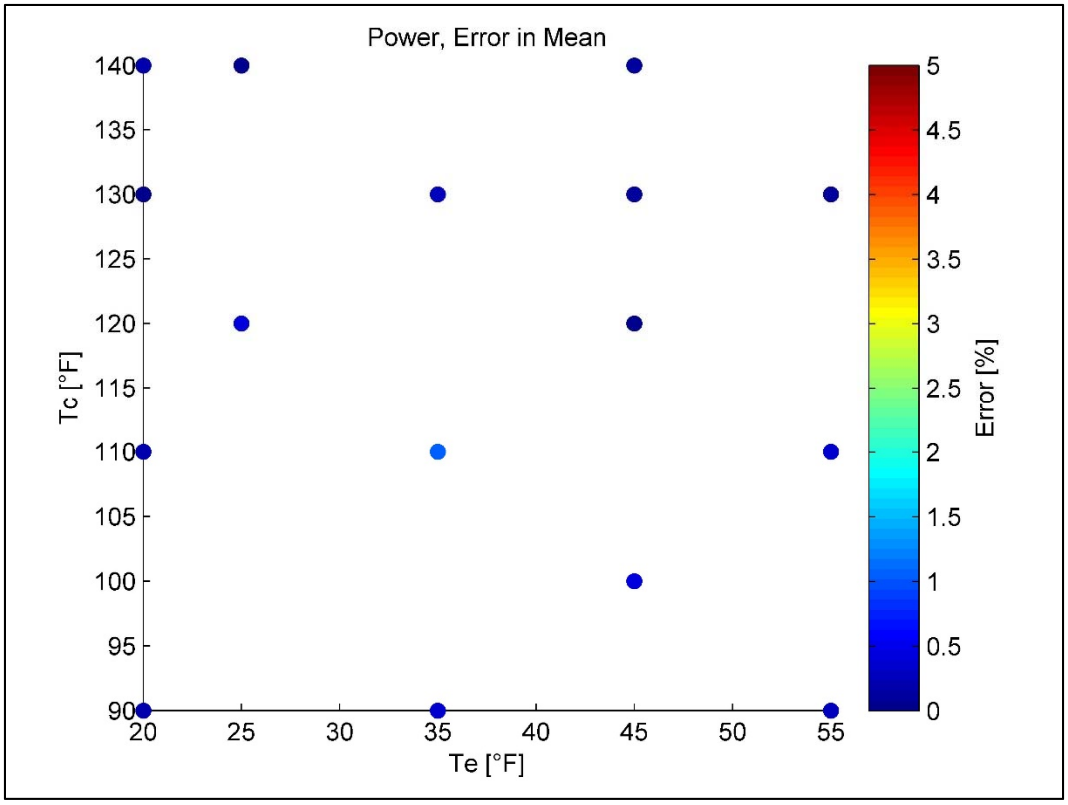

Figure 7: R134a Compressor, error in mean power

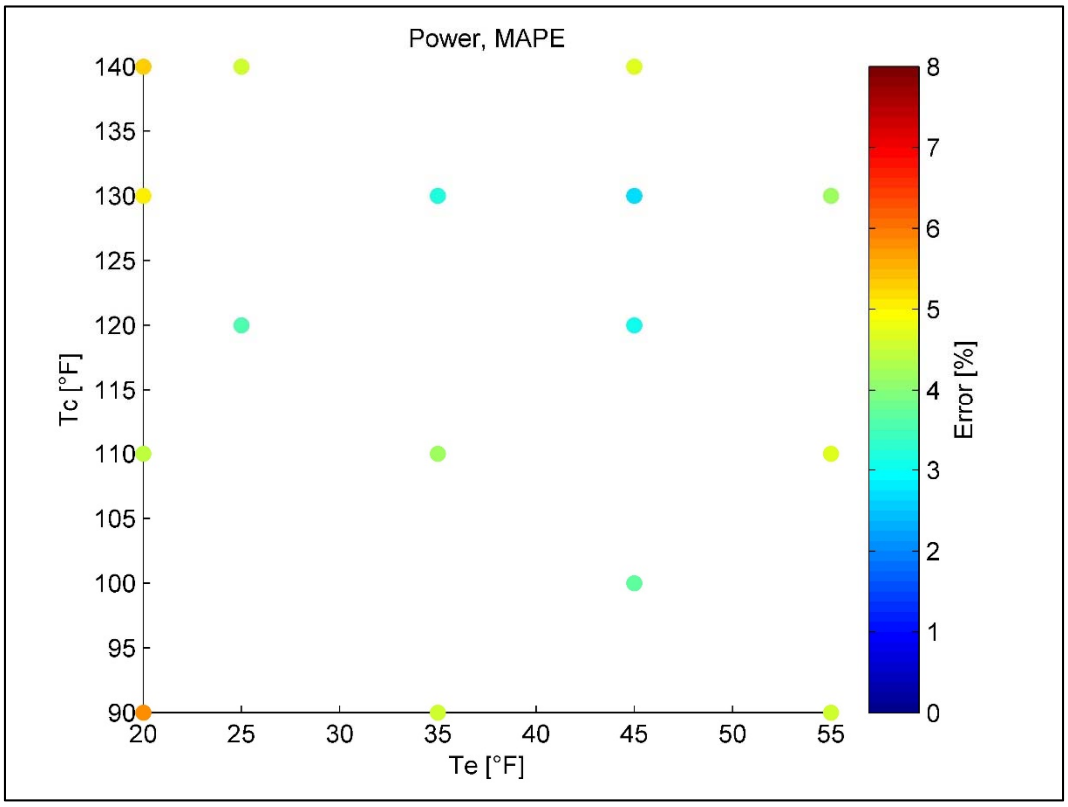

Figure 8: R134a Compressor, maximum absolute percent error in predicted power

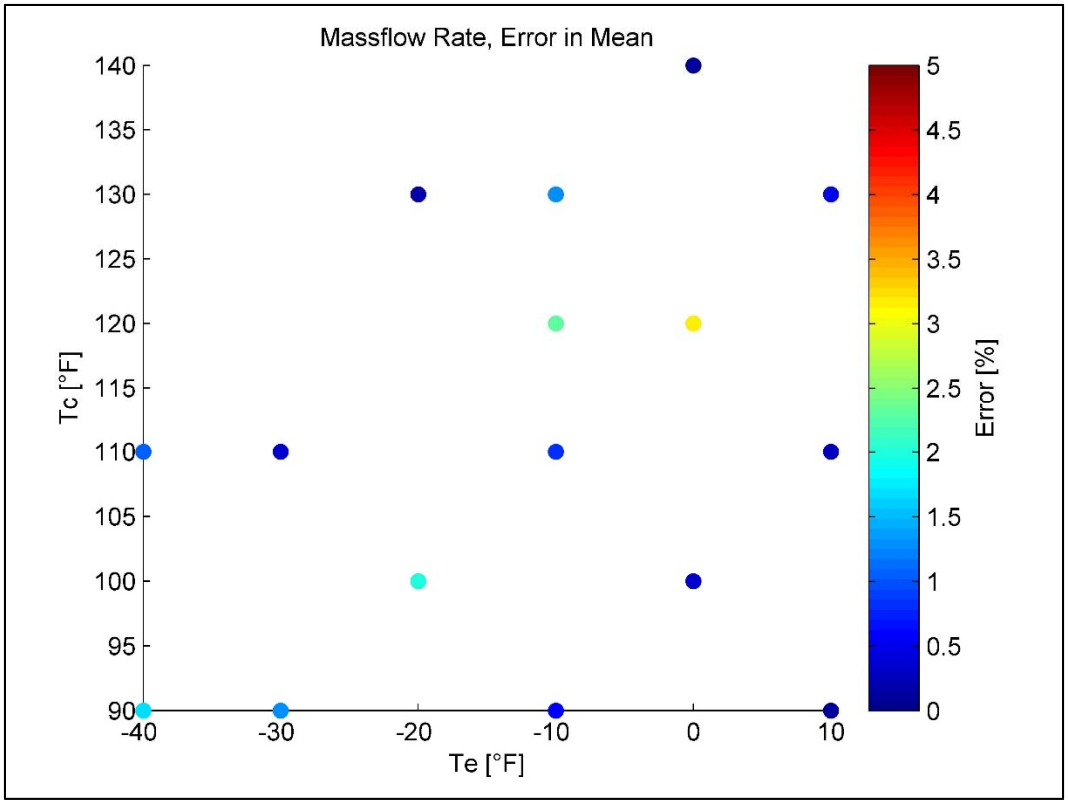

Figure 9: R404A Compressor, error in mean mass flow rate

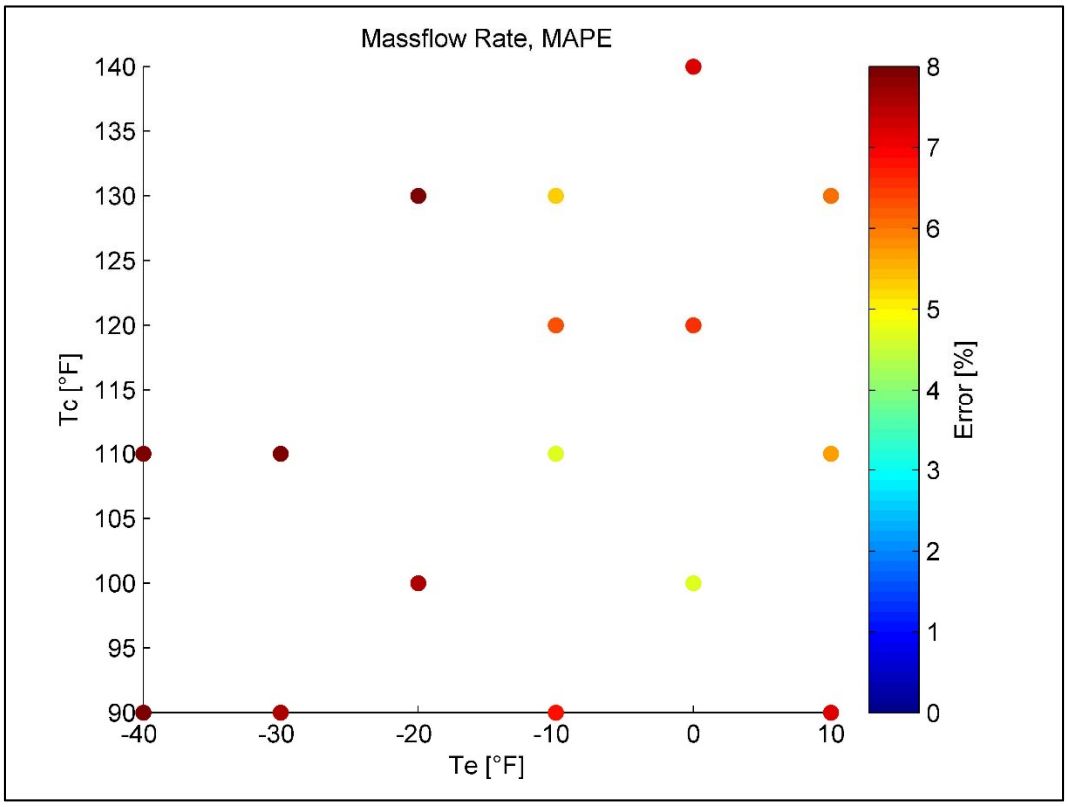

Figure 10: R404A Compressor, maximum absolute percent error in predicted mass flow rate

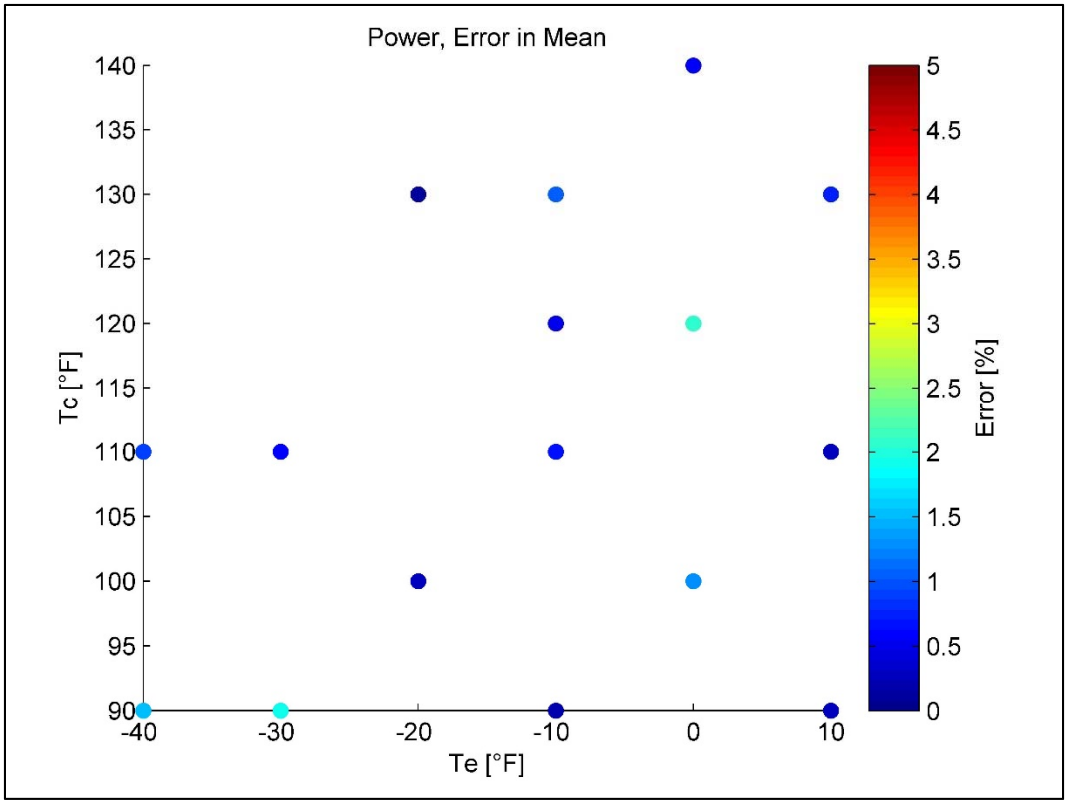

Figure 11: R404A Compressor, error in mean power

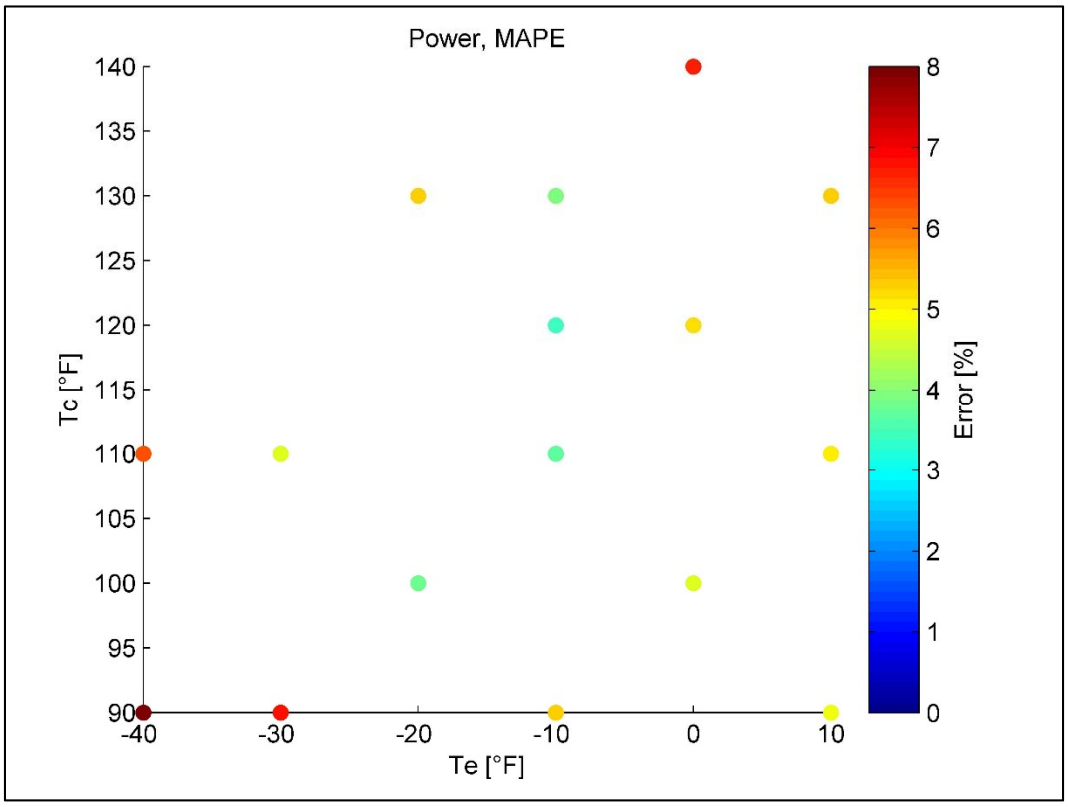

Figure 12: R404A Compressor, Maximum absolute percent error in predicted power

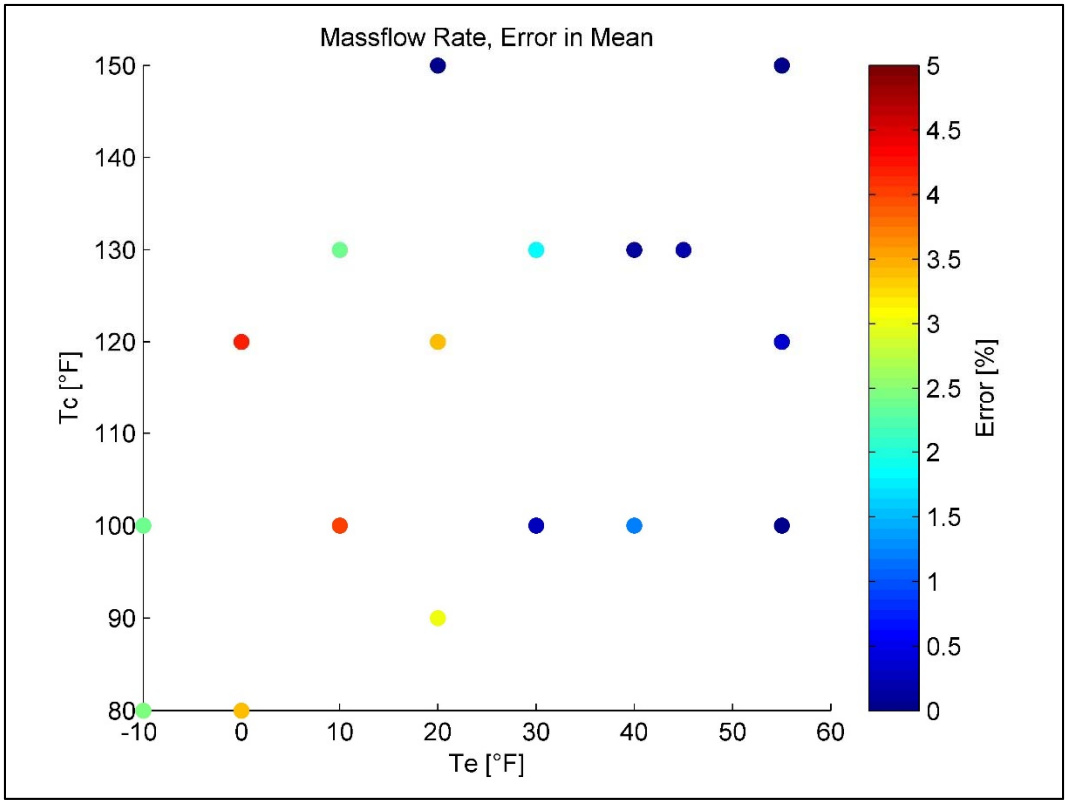

Figure 13: R407C Compressor, error in mean mass flow rate

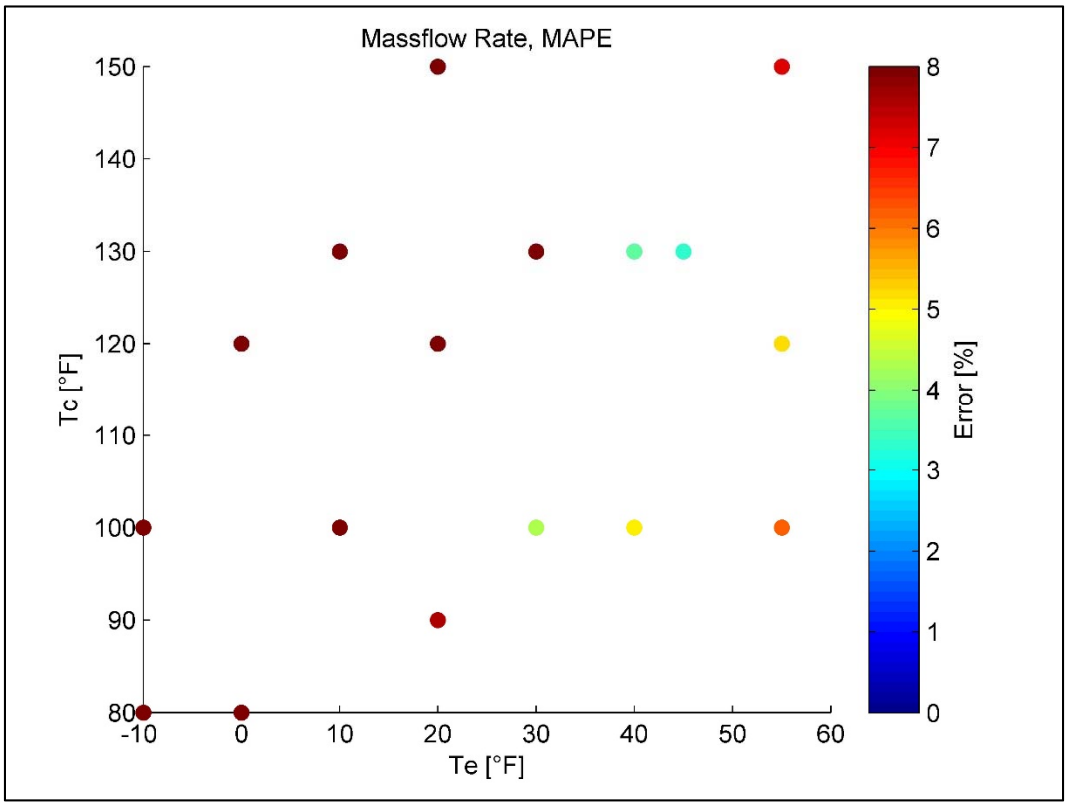

Figure 14: R407C Compressor, maximum absolute percent error in predicted mass flow rate

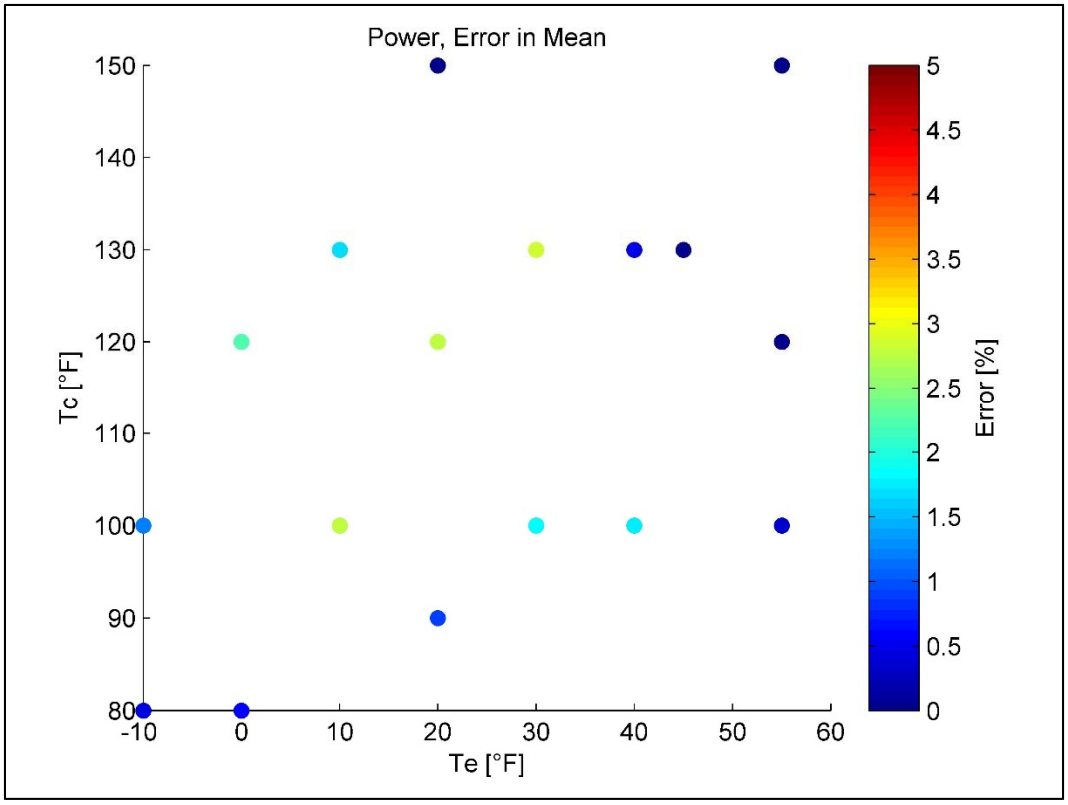

Figure 15: R407C Compressor, error in mean power

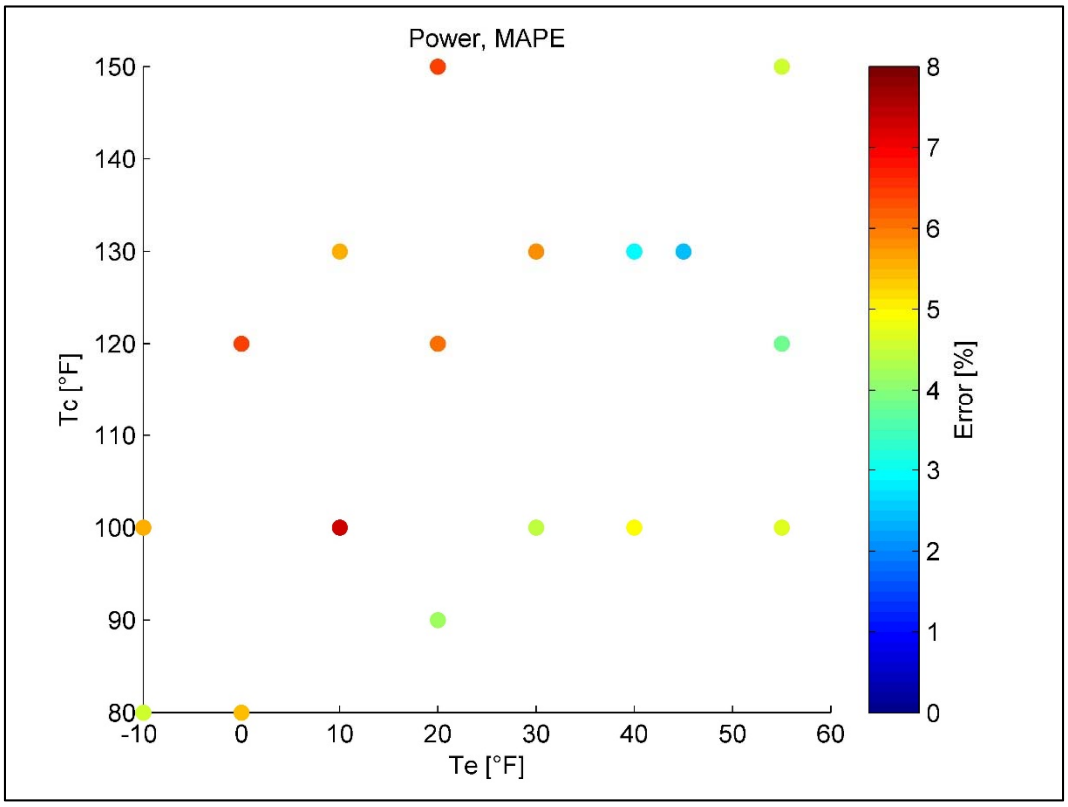

Figure 16: R407C Compressor, maximum absolute percent error in predicted power

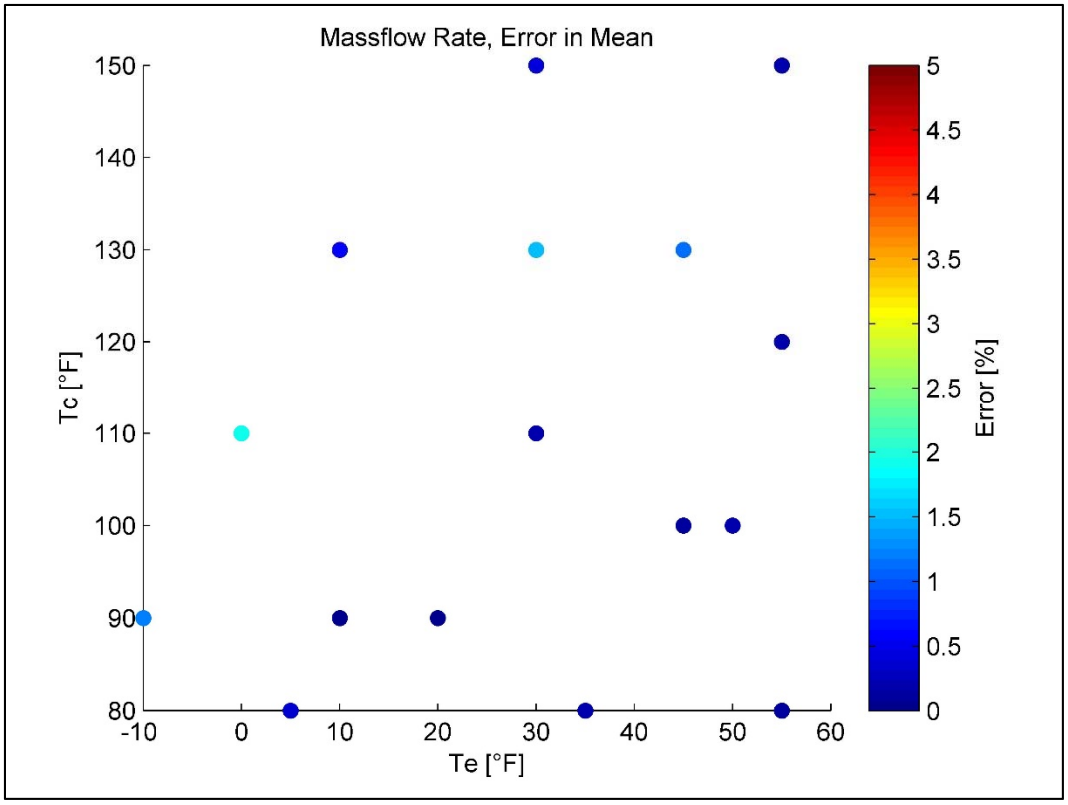

Figure 17: R410A Compressor, error in mean mass flow rate

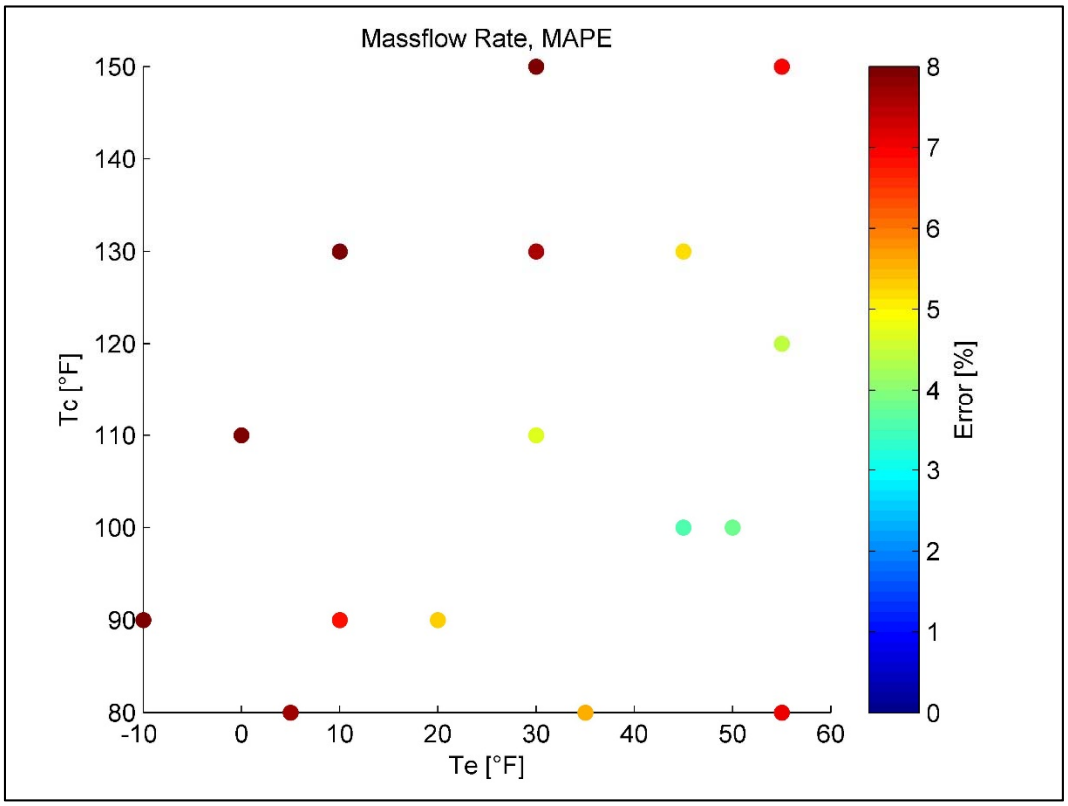

Figure 18: R410A Compressor, maximum absolute percent error in predicted mass flow rate

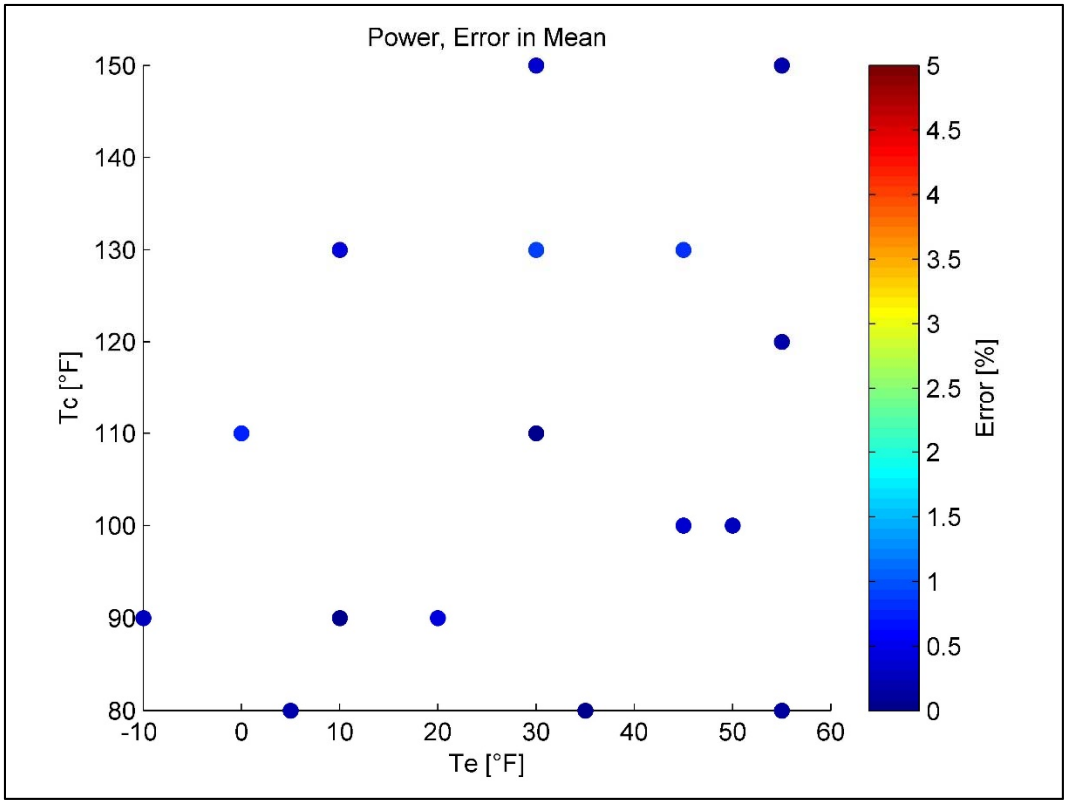

Figure 19: R410A Compressor, error in mean power

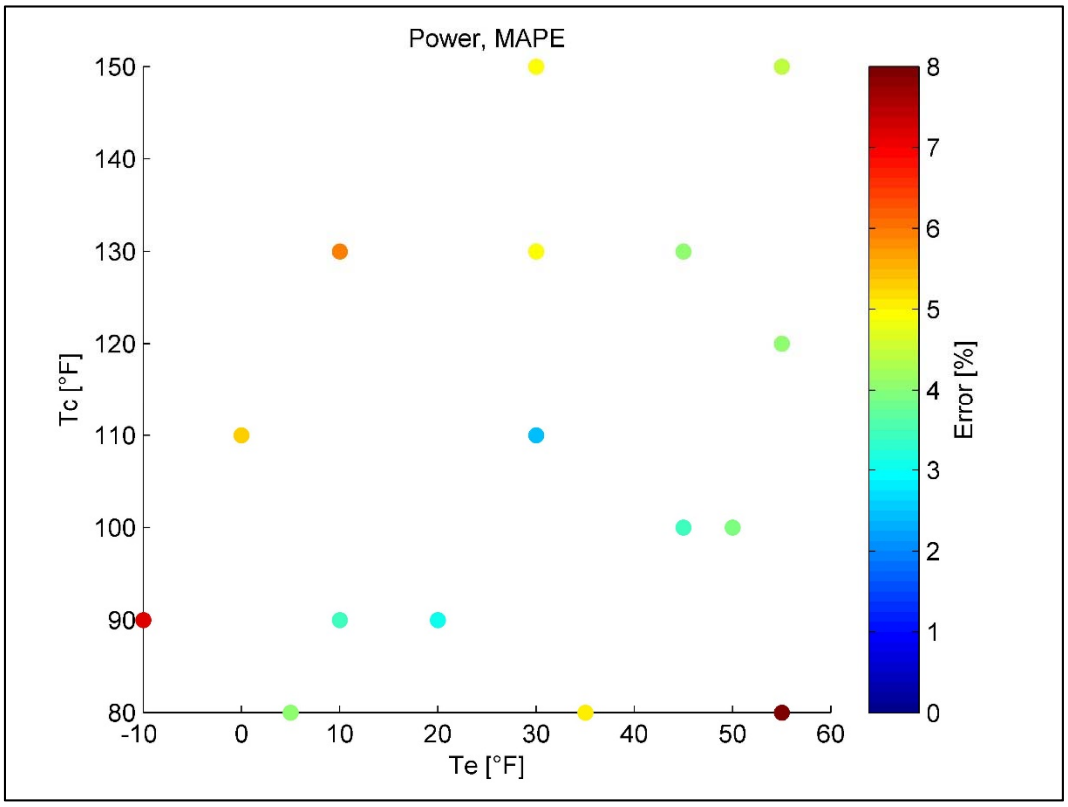

Figure 20: R410A Compressor, maximum absolute percent error in predicted power

Table 6: Monte Carlo simulation results

Fluid	Test Points	Power Max. Error in Mean [%]	Power COV [%]	Power MAPE [%]	Mass Flow Max. Error in Mean [%]	Mass flow COV [%]	Mass flow MAPE [%]
R134a	17	1.09	1.18	5.82	1.12	1.82	9.03
R134a	17	0.56	1.25	6.00	0.80	2.10	12.49
R134a	17	1.87	1.29	6.16	0.68	2.00	9.21
R22	48	0.63	0.77	3.31	0.96	1.39	6.87
R22	48	0.98	0.79	3.78	2.81	1.50	7.54
R22	49	0.64	0.76	3.73	1.40	1.44	7.15
R22	48	0.38	0.76	3.06	0.67	1.39	6.22
R22	49	0.56	0.75	3.57	0.75	1.28	6.22
R22	49	0.45	0.74	3.74	4.33	1.19	9.03
R404A	17	2.04	1.53	8.60	3.16	2.55	16.08
R404A	22	3.38	1.21	7.66	2.23	1.94	8.98
R404A	21	2.27	1.31	7.62	1.70	2.50	13.02
R407C	19	0.76	1.22	5.86	4.36	2.28	15.31
R407C	18	2.81	1.46	7.31	4.19	2.36	14.02
R410A	21	5.09	1.27	7.07	1.13	1.90	7.77
R410A	16	0.21	1.09	5.03	1.89	1.92	10.27
R410A	16	0.88	1.73	9.10	1.88	3.51	17.40
R410A	17	0.75	1.31	5.86	0.98	2.62	12.65
R410A	17	2.52	1.47	7.25	1.67	2.98	13.01
R410A	21	1.44	1.32	5.63	2.79	2.05	13.51
R410A	19	0.41	1.13	4.94	0.41	1.54	6.72
R410A	20	12.28	1.12	15.37	3.06	1.48	7.01
R410A	22	0.34	1.15	6.06	0.99	1.71	8.23
R410A	21	1.19	1.16	6.60	0.59	1.57	7.58
R410A	23	0.90	1.21	5.99	0.47	1.64	8.68
R410A	21	1.34	1.15	5.50	0.73	1.58	7.70
R410A	49	1.17	1.28	6.16	1.47	2.90	12.96
R410A	50	0.79	1.03	5.10	1.61	2.22	11.16
R410A	49	1.40	1.05	5.12	2.20	2.46	11.33
R410A	49	0.71	0.80	3.54	0.79	1.17	5.55
R410A	49	0.52	0.78	3.44	0.72	1.22	5.45
R410A	50	0.62	0.76	3.95	1.78	1.26	6.97
R410A	49	0.86	1.04	5.02	1.96	2.57	11.97
R410A	47	1.09	1.14	4.55	2.28	2.51	12.01
R410A	48	0.36	0.87	3.83	1.70	1.98	9.13
R410A	52	0.63	0.77	3.58	2.15	1.66	7.89
R410A	52	0.48	0.84	3.89	3.53	1.78	9.38
R410A	52	0.54	0.88	4.05	3.09	1.84	8.46
R410A	49	0.37	0.79	3.38	0.65	1.25	5.88
R410A	49	0.36	0.80	3.78	1.00	1.25	6.23
R410A	49	1.14	0.79	3.36	1.07	1.22	6.66
R410A	48	0.70	0.80	3.59	0.47	1.22	5.76
R410A	48	0.76	0.79	3.83	0.59	1.19	5.33
R410A	48	0.91	0.81	3.96	0.96	1.26	5.87

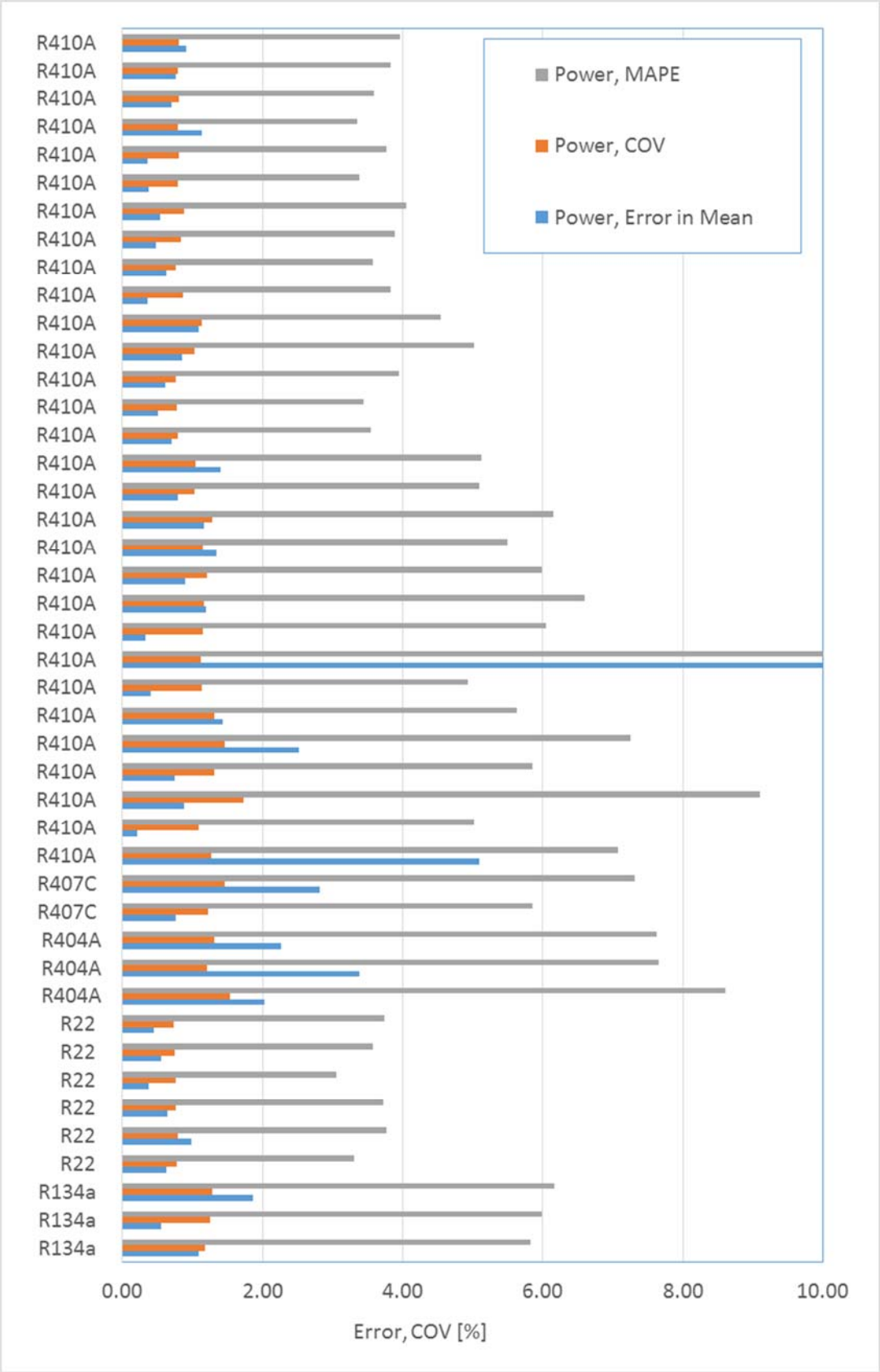

Figure 21: Monte Carlo results for power for different compressors

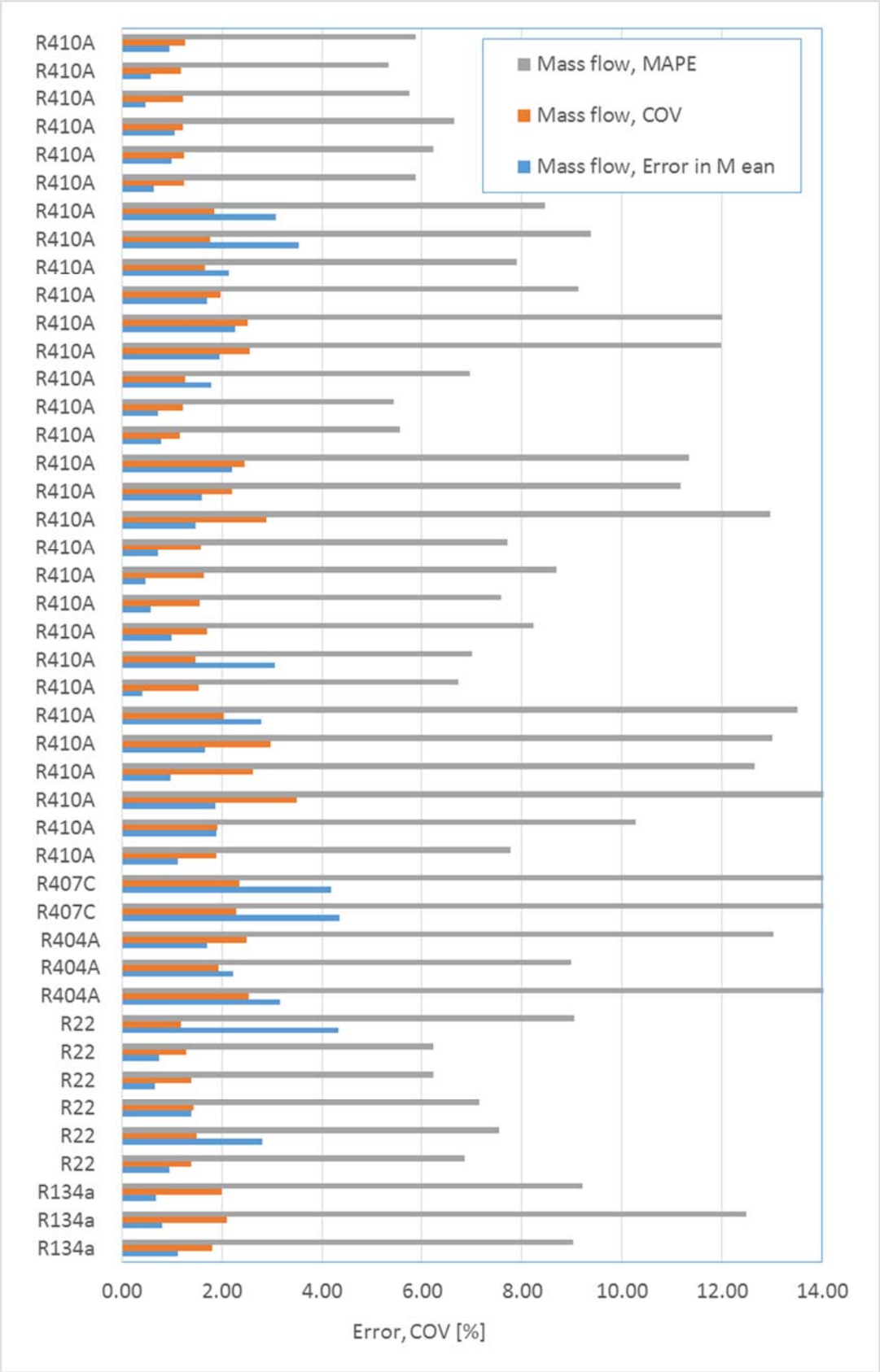

Figure 22: Monte Carlo simulation results for mass flow rate

5.4 Uncertainty Analysis Summary and Main Findings

A Monte Carlo analysis was carried out to estimate the uncertainty due to regression and instrument accuracies in the predicted compressor power and mass flow rate. The main findings are as follows:

1. The uncertainty due to regression and instrument accuracy in predicted power can be as high as 5%.
2. The uncertainty due to regression and instrument accuracy in predicted mass flow rate can be as high as 4.3%.
3. Large errors occur in the region of low suction dew point temperature and low discharge dew point temperature.
4. No conclusion can be drawn with regards to the refrigerants since the different data sets do not use the same number of test points.
5. The error in predicted power and mass flow rate is higher for large capacity compressors (i.e., high power and high mass flow rate).

6 Proposed Methods

In addition to understanding the sources of uncertainty in developing a compressor performance map, the major goal of the project is to determine the optimal method to represent performance data over the application envelope, while maximizing accuracy for a given number of test points. The following section outlines the need for an alternative method to the existing Standard 540, a background on other compressor models and data representation methods, and an overview of the analysis completed for the selected alternative methods evaluated for this project.

6.1 Literature Review

In general, compressor models can be categorized as map-based models, efficiency-based models and detailed or finite volume models:

1. Map-based models: Such models rely on manufacturer published data, such as the one used in AHRI Standard 540-2004. Extrapolation can result in significant prediction errors.
2. Efficiency-based models (Winkler, 2009): These models are based on first principles compression processes and may use varying isentropic and volumetric efficiencies. These models generally need to be tuned against measured data, but are capable of extrapolation, since they are physics-based.
3. Detailed / Finite Volume Models (Prakash and Singh): These models divide the compressor volume into distinct regions, which need accurate geometric description. The fluid conservation equations (continuity, momentum and energy) are then integrated over the entire compressor domain and an energy balance for the refrigerant inside the compressor is computed iteratively for every time step. These models are very comprehensive and accurate, but are time consuming are not generally suitable for performance characterization.

In order to identify alternative data representation methods, OTS conducted a comprehensive literature review of past research conducted for each of the above outlined models. Pertinent

findings and promising methods are summarized herein and are presented in chronological order. A summary of those methods selected for analysis and comparison against AHRI Standard 540 is presented in the following Section 7.3.

Prakash and Singh (1974) proposed a detailed mathematical model for reciprocating compressors that formulates the thermodynamic processes describing the successive states the refrigerant undergoes in three distinctly divided control volumes of the compressor: cylinder working space, suction manifold and associated piping, and discharge manifold and associated piping. First and second law analyses are performed that result in coupled partial differential equations, the solution of which may be obtained by the finite difference method. The inherent difficulty with this and other finite volume approaches (Chen et al.) is that a set of coupled partial differential equations need to be solved, which is computationally expensive and time intensive.

Staley et al. (1992) proposed an empirical model for R-12 positive displacement compressors, which predicts the data with which the coefficients were calculated within an error of 0.4% and with a standard deviation of 0.17%, for both mass flow rate and power outputs:

$$f(T_c, T_e) = (A + BT_e + CT_e^2) + (D + ET_e + FT_e^2)(T_c) + (G + HT_e + IT_e^2)(T_c^2) \quad 7.2.1$$

Jahnig et al. (1999) proposed a semi-empirical model to represent the performance of hermetic compressors used in domestic refrigeration applications. Their model proposes equations to calculate the mass flow rate and the power consumption with the assumption of a polytropic process, but uses parameters obtained from curve-fitting the data to achieve a relative error of approximately 1%. The equation for mass flow rate is:

$$\dot{m}_{calc} = \left\{1 - C\left[\left(\frac{p_{cond}}{p_{evap}(1 - \delta p)}\right)^{\frac{1}{k}} - 1\right]\right\} \cdot \frac{V.RPM}{\vartheta_{suction}.60} \quad 7.2.2$$

where C is the effective clearance volume ratio; p_{cond} is the condenser pressure, which is taken to be the same as the discharge pressure, neglecting discharge valve pressure losses; p_{evap} is the evaporator pressure; δp is a suction pressure drop parameter, introduced because the suction valve pressure drop has a significant detrimental effect on the mass flow rate; and *k* is the ratio of specific heats evaluated at the compressor suction. In the above equation, C and δp are obtained as curve fit parameters from the data. Since δp is calculated using a curve fit, it is expected that it captures the combined effect of suction pressure losses as well as internal heat transfer to the suction gas.

The equation for the power consumption is given as:

$$Power.\eta_{comb} = \dot{m} \cdot \frac{k}{k-1} \cdot p_{suction} \cdot \vartheta_{suction} \cdot \left[\left(\frac{p_{discharge}}{p_{suciton}}\right)^{\frac{k-1}{k}} - 1\right] \quad 7.2.3$$

where $p_{suction} = (1 - \delta p)p_{evap}$ and $p_{discharge} = p_{cond}$.

The only unknown term in the above equation is η_{comb}, which is obtained from a regression fit to an exponential equation as a function of the evaporator pressure:

$$\eta_{comb} = d + e.\exp(f.p_{evap}) \quad 7.2.4$$

with *d, e* and *f* being regression parameters.

The model was found to extrapolate to 10°C higher and lower evaporating and condensing temperatures, keeping the relative error to less than 5%.

Mackensen et al. (2002) attempted to extend Jahnig et al.'s model to larger scale reciprocating, scroll and screw compressors (semi-hermetic and open drive). With the assumption of a polytropic process, the model was found to predict the mass flow rate satisfactorily with mean weighted errors of 3.7% for reciprocating compressors, 2.3% for scroll compressors and 0.6% for screw compressors. Parameters estimated using data for one refrigerant were found to be useful in calculating the mass flow rate with another refrigerant, with a mean weighted error of around 3%.

Winandy et al. (2002) proposed a model for open-type reciprocating compressors (followed by one for hermetic scroll compressors), which assumes the presence of a fictitious wall that gains heat from the discharged gas and loses it to the suction gas and ambient, The model also accounts for electromechanical losses. The model was formulated along the lines of the ASHRAE toolkit for primary HVAC equipment, but was extended to include the influence of the ambient temperature. Winandy's team concluded that the clearance volume re-expansion and the throttling are the processes affect the mass flow rate the most. The clearance volume re-expansion affects the volumetric efficiency by heating up the suction gas; the throttling can be modeled as a fixed area model. As such, the equations require seven parameters to compute the mass flow rate and exhaust temperature:

$$\dot{m} = \left(\frac{\pi d_{su}^2}{4}\right).\sqrt{2\Delta P_{su}\rho_{su}} \quad 7.2.5$$

where d_{su} is a fictitious nozzle throat diameter where throttling occurs.

Heat transfer can be determined by a conventional steady state energy balance between the fictitious wall(t_w) and the suction gas$\left(\dot{Q}_{su},\ t_{su},\ AU_{su}\right)$, discharge gas$\left(\dot{Q}_{ex},\ t_{ex},\ AU_{ex}\right)$ and the ambient$\left(\dot{Q}_{amb},\ t_{amb},\ AU_{amb}\right)$, and heat due to electromechanical losses ($\dot{W}_{loss}$). The swept volume V_s and the clearance factor C_f are used to compute the effect of the clearance volume re-expansion on the volumetric efficiency:

$$\frac{\dot{m}\vartheta_{su2}}{N} = V_s - V_s C_f\left(\frac{\vartheta_{su2}}{\vartheta_{ex2}} - 1\right) \quad 7.2.6$$

With the compression process regarded as isentropic, the exhaust temperature can be computed as a function of the fluid properties and the temperatures:

$$t_{ex2} = t(fluid, p_{ex2}, p_{su2}, t_{su2}, s = s_{su2}) \quad 7.2.7$$

where *su2* and *ex2* represent the properties inside the compressor cylinder and *su* and *ex* represent the properties in the intake and exhaust manifolds. Two more parameters would be needed to predict the compressor shaft power requirement. The relative error for predicting the mass flow rate varied between -6% and 6% and between -7% and 3% for the shaft power. Despite the advantage that the model can easily be extended to other types of compressors (scroll, rotary, hermetic and open-type), the difficulty of collecting data for the parameters required for this model make it unfeasible for performance characterization.

Shao et al. (2004) proposed a black box model to calculate the refrigerant mass flow rate, compressor power input and the COP of variable speed compressors. The input parameters are the compressor motor power input and the refrigerant mass flow rate as functions of evaporation temperature for several condensation temperatures, obtained from the manufacturers. When operating at a certain frequency, the performance of an inverter compressor is similar to that of a constant speed compressor operating at the same frequency. Thus, the inverter compressor can be scattered as an infinite constant speed compressor for each of the different frequencies. Since the performance curves provided by compressor manufacturers represent the performance of an inverter compressor operating at different frequencies, a map based model of the inverter compressor can be obtained via an analysis of the performance and fitting of the performance curves. The compressor power input and mass flow rate at the map condition may be expressed as second order functions of the evaporation temperature and the condensation temperature:

$$M_0^* = a_1 T_c^2 + a_2 T_c + a_3 T_c T_e + a_4 T_e^2 + a_5 T_e + a_6 \quad 7.2.8$$

$$P_0^* = b_1 T_c^2 + b_2 T_c + b_3 T_c T_e + b_4 T_e^2 + b_5 T_e + b_6 \quad 7.2.9$$

where T_c and T_e are the condensation and the evaporation temperatures; $a_1 - a_6$ and $b_1 - b_6$ are constants depending on the compressors.

Assuming there are more than six data points (n≥6),

$$M_0^* = \left[M_{0,1}^*, M_{0,2}^*, M_{0,3}^*, \ldots M_{0,n}^*\right]^T \quad 7.2.10$$

$$a = [a_1, a_2, a_3, \ldots a_6]^T \quad 7.2.11$$

Then M_0^* can be expressed as $M_0^* = T.a$

$$\text{where T} = \begin{bmatrix} T_{c,1}^2 & T_{c,1} & T_{c,1}T_{e,1} & T_{e,1}^2 & T_{e,1} & 1 \\ \vdots & & \ddots & & & \vdots \\ T_{c,n}^2 & & \cdots & & & 1 \end{bmatrix}$$

Then the vector *a* can be calculated as

$$a = (T^T T)^{-1} T^T M_0^* \quad 7.2.12$$

A simulation model such as the one above may be set up at each frequency if experimental data is provided. However, since manufacturers provide data only at certain frequencies, a relationship between the performance and compressor frequency needs to be defined. It can be observed from the data that the ratio between the mass flow rate at a constant frequency to that at the basic frequency remain constant at different evaporation and condensation temperatures. Thus, the relationship between the ratio of mass flow rates and the compressor frequency may be expressed as a second order function of compressor frequencies:

$$K_M = \frac{M_0}{M_0^*} = c_1(f - f^*)^2 + c_2(f - f^*) + c_3 \quad 7.2.13$$

$$c = [c_1, c_2, c_3]^T \quad 7.2.14$$

$$K_M = [k_{M,1}, k_{M,2}, \ldots . k_{M,n}]^T \quad 7.2.15$$

Thus $k_M = F.c$

where $$F = \begin{bmatrix} (f_1 - f^*)^2 & (f_1 - f^*) & 1 \\ \vdots & \ddots & \vdots \\ (f_n - f^*)^2 & (f_n - f^*) & 1 \end{bmatrix}$$

Then the vector C can be calculated via

$$C = (F^T F)^{-1} F^T k_n \quad 7.2.16$$

A similar procedure can be followed for compressor power as well. Model validation suggests that the average relative errors are less than 2%, 3% and 4% for refrigerant mass flow rate, compressor power input and the COP, respectively.

Duprez et al. (2007) proposed an extension to Winandy's fictitious thermal wall model, using REFPROP to simplify the calculation procedure for reciprocating and scroll compressors for domestic heat pumps. The refrigerant mass flow rate is calculated from a knowledge of the operating conditions and four different parameters: the temperature of the fictitious wall (assumed constant), the overall heat transfer coefficient of the suction line, the diameter of the suction pipe and the clearance volume factor. A functional relationship between the product of the electrical and isentropic efficiencies ($\eta_{elec}\eta_{isen}$) and the compression ratio is proposed in the form of a 6th-degree equation, the coefficients of which are computed by least squares regression of compressor data (a minimum of 7 points) provided by manufacturers. The model for scroll compressors is similar. Mean errors for the mass flow rate calculations were 1.1% and 2.42% and 1.69% and 1.04% for electrical power calculations, for reciprocating and scroll compressors, respectively.

Navarro et al. (2007) proposes a 10 parameter model representing the main sources of losses in the compressor to predict the volumetric and compressor efficiency. The compression process is assumed to be isentropic and least square correlation methods for fitting are replaced with Monte Carlo techniques, which are better for non-linear system simulation but computationally

inefficient. The model is a phenomena oriented model where the main sources of loss include vapor heating due to motor cooling, mechanical loss dissipation and leakages from the discharge, isenthalpic pressure loss at the suction valve, isentropic compression, isenthalpic leakages at the discharge, and vapor cooling due to heat transfer to the suction side. The main drawback of the developed model is that the equations for volumetric and compressor efficiencies are presented as a system of implicit equations, which require time consuming computations. Another drawback is that, although the model can predict the efficiencies with an error of less than 3%, it was proposed specifically for reciprocating compressors and is quite difficult to adapt to other compressor types.

Castaing-Lasvignottes et al. (2009) contend that the volumetric and isentropic efficiencies are the most efficient way to simulate compressor behavior and propose a model that studies the influence of the clearance volume ratio on the volumetric efficiency and friction factor on the isentropic efficiency. The mass flow rate, shaft power, discharge enthalpy and heat exchanged can also be calculated. Thus, this model, from thermodynamic conditions and geometric design of the compressor, allows determination of the three macroscopic efficiencies that are needed for a global refrigeration system simulation.

Aprea and Renno (2009) extended Shao's model to include the cooling capacity Q:

$$Q_0^* = c_1 T_c^2 + c_2 T_c + c_3 T_c T_e + c_4 T_e^2 + c_5 T_e + c_6 \qquad 7.2.17$$

The same procedure as presented by Shao is followed. Aprea and Renno conclude that these equations allow to determine the optimum frequency for each working condition, once the evaporation and condensation temperatures and the cooling load are fixed.

Zhao et al. (2009) constructed a polynomial artificial neural network (ANN) model to simulate an economized, gas injected, screw compressor. A three layer perceptron network was used with the Levenberg-Marquardt algorithm used for training. A third order polynomial function and a pure linear function were used as transfer functions in keeping with the third order polynomial equation in AHRI Standard 540. The results of the screw compressor modeling show that almost all the points for un-economized system performance lie in the 5% error band and for economized performance, 93% of points fall in the 10% error band.

C.P. Arora (2009) proposes equations that can be used to calculate the volumetric efficiency and power consumption of a reciprocating compressor directly, although the equations are general enough to extend to other compressor types. Specifically, volumetric efficiency is calculated using equation 7.2.18.

$$\eta_{vol} = (1 + C)\left(\frac{p_s}{p_1}\right)^{\frac{1}{n}} - C\left(\frac{p_d}{p_1}\right)^{\frac{1}{m}} - 0.015\left(\frac{p_2}{p_1}\right) \qquad 7.2.18$$

where clearance volume factor $C = \frac{V_c}{V_p}$

In the above formulae, V_c is the clearance volume in the compressor cylinder and V_p is the piston swept volume. p_1 and p_2 refer to the pressures in the suction and discharge manifolds

respectively, and p_s and p_d are the in-cylinder pressures at the end of the suction and discharge strokes, respectively. n and m are the polytropic exponents of the compression and the re-expansion process, respectively. The power input to the compressor is calculated from

$$\dot{W} = \eta_{vol} \frac{\dot{V_p}}{\nu_1} \left(\frac{h_2 - h_1}{\eta_{mech} \eta_{\imath sen}} \right) \qquad 7.2.19$$

where $\dot{V_p}$ is the volumetric flow rate, ϑ_1 is the specific volume at suction, and h_1 and h_2 are the enthalpies of the refrigerant in the suction and discharge manifolds.

Zhao et al. (2010) also proposed a loss efficiency model for representation of compressor performance. A neural network loss efficiency model was developed to simulate the performance of positive displacement compressors such as screw, reciprocating and scroll compressors. A three layer perceptron network with a second order polynomial transfer function is used for the volumetric efficiency model, whereas a third order polynomial transfer function is used for the isentropic efficiency model. The compression ratio and condensation temperature are the inputs for the volumetric efficiency model and the condensation and evaporation temperatures are the input parameters for the isentropic efficiency model. The selection of input parameters of neural networks was found to be critical to network prediction accuracy. A pure linear transfer function was used in the output layer of both the models. The proposed neural networks gives less than 0.4% standard deviation and 1.3% maximum deviation against manufacturer's data.

Regression analysis is a method used to understand the effect a particular variable has on other dependent variables. Regression based models include both parametric methods, such as linear regression and ordinary least squares, and non-parametric models where the independent variable is constructed from information gathered from the data. Lee et al. (2012) performed a study in which the performance prediction ability of eleven regression based empirical models for water chillers were evaluated using over 2,000 data sets in which they identified bi-quadratic, multivariate polynomial, simpler multivariate polynomial and the modified design of experiments (DOE-2) models as having the best predictive capability, with the coefficient of variation of the root mean square error for all being less than 1%. However, it should be emphasized that this analysis was a system level performance audit and not specific to compressors.

Qiao et al. (2014) proposed a semi-empirical model for a variable speed compressor in which the volumetric efficiency is calculated as a regression function of the suction pressure, discharge pressure and the compressor operating frequency:

$$\eta_{vol} = c_0 + c_1\varphi + c_2\varphi^2 + c_3\varphi^3 + c_4(p_{dis} - p_{suc})(1 + c_5 p_{suc}) \qquad 7.2.20$$

$$\begin{aligned} c_0 &= a_1 + a_2\emptyset + a_3\emptyset^2 \\ c_1 &= a_4 + a_5\emptyset + a_6\emptyset^2 \\ c_2 &= a_7 + a_8\emptyset + a_9\emptyset^2 \\ c_3 &= a_{10} + a_{11}\emptyset + a_{12}\emptyset^2 \end{aligned} \qquad 7.2.21$$

$$c_4 = a_{13} + a_{14}\emptyset + a_{15}\emptyset^2$$
$$c_5 = a_{16} + a_{17}\emptyset + a_{18}\emptyset^2$$

$$\varphi = \frac{p_{dis}}{p_{suc}} \quad 7.2.22$$

$$\emptyset = \frac{f}{f_{nominal}} \quad 7.2.23$$

The power input to the compressor can be determined as a function of the suction pressure, the compressor operating frequency and the volumetric flow rate at suction:

$$\dot{W_{comp}} = z_1 p_{suc} \dot{V_{suc}} (\varphi^{z_2} - 1) + z_3 \quad 7.2.24$$

$$z_1 = b_1 + b_2\emptyset + b_3\emptyset^2$$
$$z_2 = b_4 + b_5\emptyset + b_6\emptyset^2 \quad 7.2.25$$
$$z_3 = b_7 + b_8\emptyset + b_9\emptyset^2$$

Compressor performance was not specifically analyzed as part of this work since the focus was on control investigation of multi-evaporator air conditioning systems. As shown in the follow section, however, this method was selected for analysis as it provides an approach for variable speed compressors while keeping the number of test iterations required to a minimum. This model is also simpler than the earlier method presented by Shao et al. (2004) model.

This review summarizes those papers that were identified as having the most potential to usefully be adapted for the purpose of this project. The major factors considered in the choice of publications to review were accuracy, ease of computation, number of tests required and general applicability.

6.2 Identified Alternative Methods and Variations

Based on the literature review outlined above, several alternative methods were identified for further analysis and comparison against Standard 540. These are summarized in Table 7.

Table 7: Compressor performance map data representation methods evaluated for AHRI Project 8013

Reference (Model Identifier)	Equations	Parameters Required	Number of Data Points Required	Superheat Correction Required
AHRI Standard 540 (AHRI)	$X = C1 + C2(S) + C3(D) + C4(S^2) + C5(S.D) + C6(D^2) + C7(S^3) + C8(S^2.D) + C9(S.D^2) + C10(D^3)$ $S = Tsuc: Suction\ dew\ point\ temperature$ $D = Tdis: Discharge\ dew\ point\ temperature$ $X: Performance\ metric$ $C1 - C10: Coefficients\ determined\ by\ linear\ regression$	T_{suc} T_{dis}	11	Yes
Qiao, et al. (QIAO)	$\eta_{vol} = c_0 + c_1\varphi + c_2\varphi^2 + c_3\varphi^3 + c_4(p_{dis} - p_{suc})(1 + c_5 p_{suc})$ $c_0 = a_1 + a_2\emptyset + a_3\emptyset^2$ $c_1 = a_4 + a_5\emptyset + a_6\emptyset^2$ $c_2 = a_7 + a_8\emptyset + a_9\emptyset^2$ $c_3 = a_{10} + a_{11}\emptyset + a_{12}\emptyset^2$ $c_4 = a_{13} + a_{14}\emptyset + a_{15}\emptyset^2$ $c_5 = a_{16} + a_{17}\emptyset + a_{18}\emptyset^2$ $\dot{W}_{comp} = z_1 p_{suc} \dot{V}_{suc}(\varphi^{z_2} - 1) + z_3$ $z_1 = b_1 + b_2\emptyset + b_3\emptyset^2$ $z_2 = b_4 + b_5\emptyset + b_6\emptyset^2$ $z_3 = b_7 + b_8\emptyset + b_9\emptyset^2$ $\varphi = \frac{p_{dis}}{p_{suc}} \qquad \emptyset = \frac{f}{f_{nominal}}$	p_{suc} p_{dis} f	10	Yes

Jahnig, et al. (KLEIN)	$\dot{m}_{calc} = \left\{1 - C\left[\left(\frac{p_{cond}}{p_{evap}(1-\delta p)}\right)^{\frac{1}{k}} - 1\right]\right\} \cdot \frac{V.RPM}{\vartheta_{suction}.60}$ $Power.\eta_{comb} = \dot{m}.\frac{k}{k-1}.p_{suction}.\vartheta_{suction}.\left[\left(\frac{p_{discharge}}{p_{suction}}\right)^{\frac{k-1}{k}} - 1\right]$ $p_{suction} = (1-\delta p)p_{evap}$ $p_{discharge} = p_{cond}$ $\eta_{comb} = d + e.\exp(f.p_{evap})$	p_{evap} p_{cond} V RPM T_{evap}	6	Yes
Winandy, et al. (Winandy)	$\dot{m} = \left(\frac{\pi d_{su}^2}{4}\right).\sqrt{2\Delta P_{su}\rho_{su}}$ $\frac{\dot{m}\vartheta_{su2}}{N} = V_s - V_s C_f\left(\frac{\vartheta_{su2}}{\vartheta_{ex2}} - 1\right)$ $\dot{W_{sh}} = \dot{W_{in}} + \dot{W_{loss}}$ $\dot{W_{loss}} = \alpha\dot{W_{in}} + \dot{W_{loss0}}\left(\frac{N}{N_0}\right)^2$ $\dot{W_{in}} = \dot{M}(h_{ex2} - h_{su2})$	V_s C_f δ_{su} AU_{su} AU_{ex} AU_{amb} ΔP_{ex} $\dot{W_{loss0}}$ α	10	No
Arora, C.P. (Arora)	$\eta_{vol} = (1+C)\left(\frac{p_s}{p_1}\right)^{\frac{1}{n}} - C\left(\frac{p_d}{p_1}\right)^{\frac{1}{m}} - 0.015\left(\frac{p_2}{p_1}\right)$ $\dot{W} = \eta_{vol}\frac{V_p}{\nu_1}\left(\frac{h_2 - h_1}{\eta_{mech}\eta_{isen}}\right)$	p_1 p_2 p_s p_d m n	7	No
MPOLY	$r = \frac{p_{dis}}{p_{suc}}$ $Volumetric\ Efficiency\ (or\ Power) = C0 + C1r + C2Ps + C3rPs + C4r^2 + C5Ps^2 + C6rPs^2 + C7r^2Ps + C8r^3 + C9Ps^3$	p_{suc} p_{dis}	11	Yes

6.3 Analysis and Comparison of Current Method

6.3.1 Analysis of AHRI-540 Method with Black Box Models

As a first step, the 10-coefficient AHRI-50 method was compared against various other black-box curve fit models from a commercially available curve-fitting software package. The models investigated included traditional polynomials, rational polynomials, Chebychev polynomials and sigmoid functions. For polynomial-like functions varying degrees were also investigated. It was found that the current 10-coefficient map still provided the best prediction and surface shape. The map is also computationally cheaper to implement and evaluate at 24 floating point operations. The other polynomial forms such as Chebychev polynomials had a much better goodness of fit (r^2 and Fit standard error) measures, but did not represent the underlying physics.

6.3.2 Analysis of AHRI-540 Method with Comprehensive Data Sets

Comprehensive data sets, with finer increments in suction and discharge dew point temperatures were made available by AHRI. The data sets for these three were used to conduct detailed analysis of the current representation method.

For each compressor, two data sets were made available. The first data set (16 points), referred to as the "map data" or the "source data", is the set of points typically used to generate the 10 coefficients. The second data set, referred to as the "verification data" or the "comprehensive data" was the comprehensive performance map (600+ points) measured over the entire operating envelope, but at finer increments than the map data. Figure 23 shows the map data and the verification data for the first test data set.

In this analysis, the first data set, referred to as the "map data" is used to fit the 10-coefficient polynomial. This polynomial is then used to predict the original map data as well as the comprehensive verification data.

Table 8 below shows the regression metrics for the map data set. The various metrics are defined as follows:

AAPE: Average Absolute Percent Error
MAPE: Maximum Absolute Percent Error
RRMSE: Relative Root Mean Square Error (RMSE, but normalized with actual value)

The AHRI-540 regression developed based on the map data was then used to predict the performance for the points in comprehensive data set. The corresponding errors along with the respective operating envelope are shown in Figure 24 through 31.

Based on this analysis, the following conclusions can be drawn:

1. The AHRI-540 map predicts source data for both power and mass flow rate within ±0.5%.
2. Comparison against verification data shows that the highest errors are concentrated in the third-quadrant, i.e., low suction and discharge dew point temperatures. This region is also outside the original map data and requires extrapolation.

3. Within the operating envelop for which map data is available, there are certain regions that exhibit errors of more than 1% in mass flow rate and power, as shown in Figure 29 and Figure 31 respectively. These regions can be correlated to corresponding regions in Figure 23, where-in there aren't sufficient measured data points. For example, the region bounded by Te < 30°F and Tc > 100°F. This error information can be used in developing a sampling plan for testing.

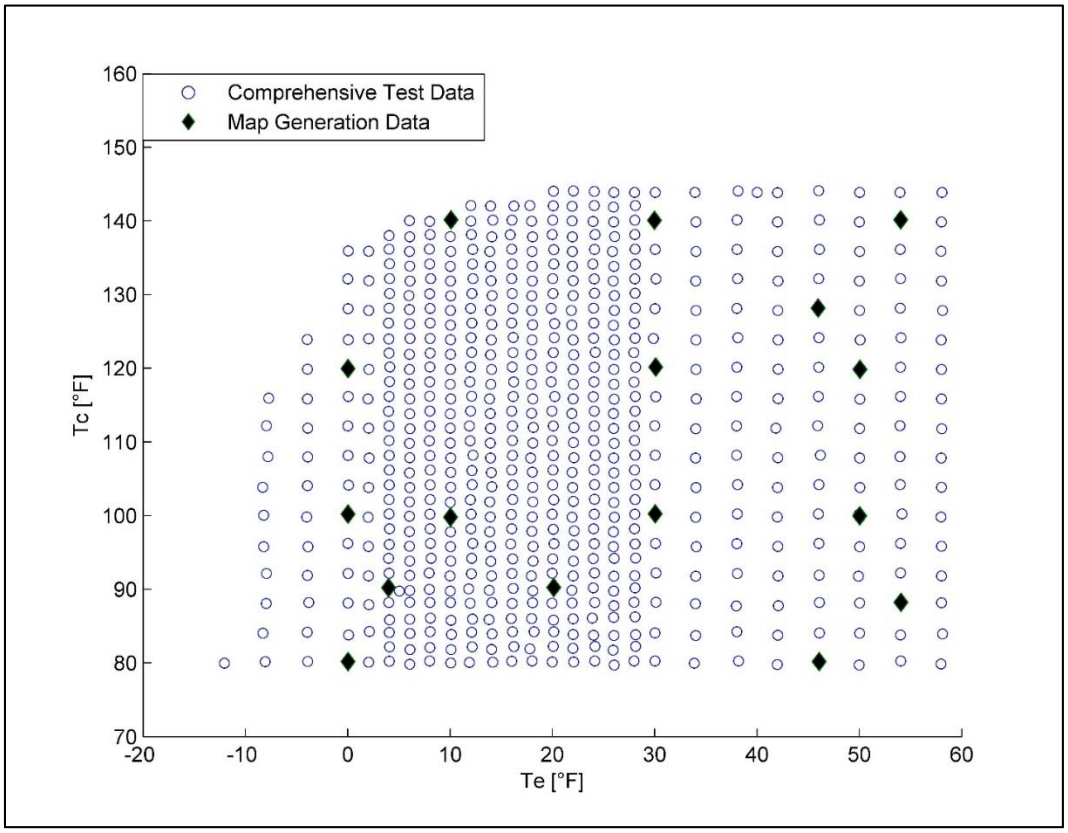

Figure 23: Sample comprehensive test data, points used for map generation and comprehensive testing

Table 8: Comparison against comprehensive test data

	Map Generation Data	Verification Test Data
Points	16	611
Power AAPE	0.153791	0.684785
Power MAPE	0.492499	9.068185
Power RRMSE	0.001938	0.011601
Mass flow AAPE	0.312222	0.595986
Mass flow MAPE	0.677742	7.81275
Mass flow RRMSE	0.0035	0.009424

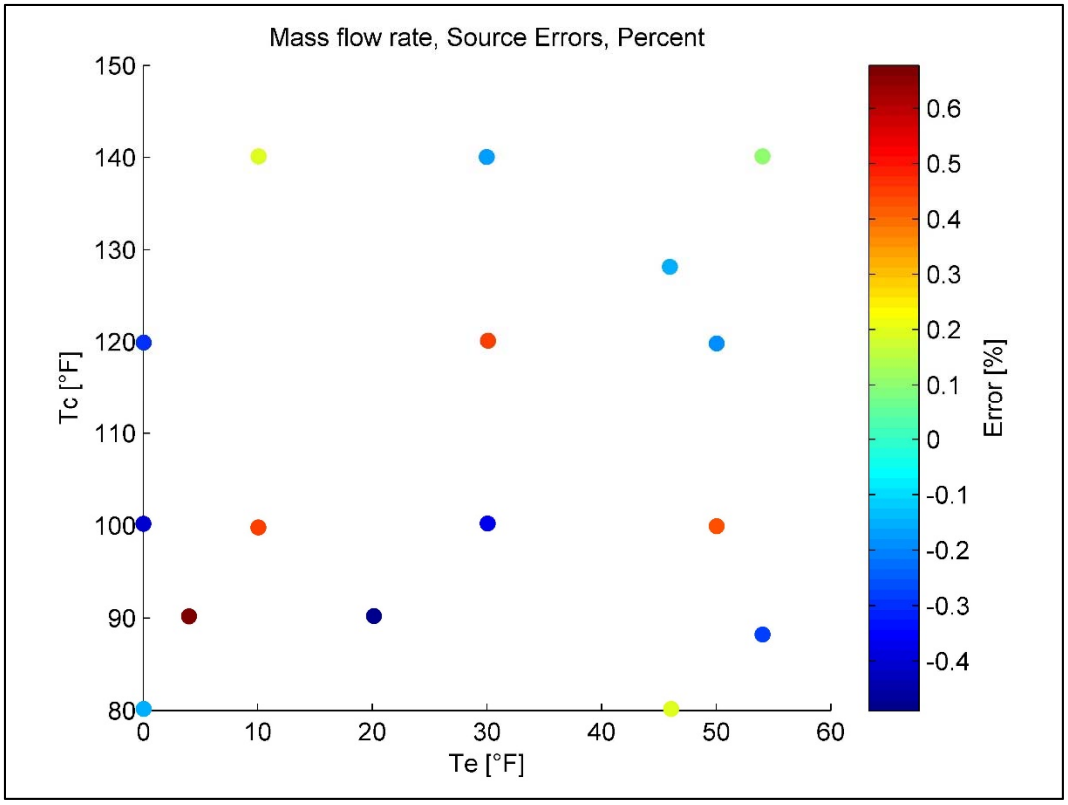

Figure 24: Comprehensive Set-1, errors in mass flow rate, based on source data

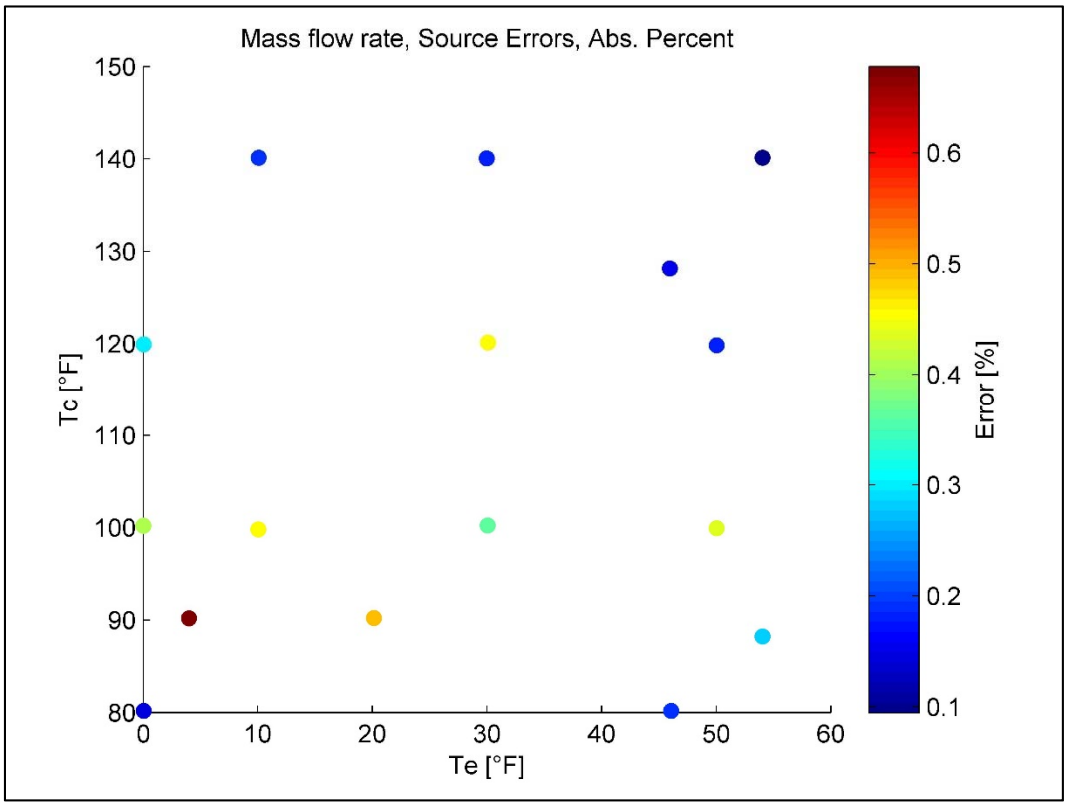

Figure 25: Comprehensive Set-1, absolute errors in mass flow rate, based on source data

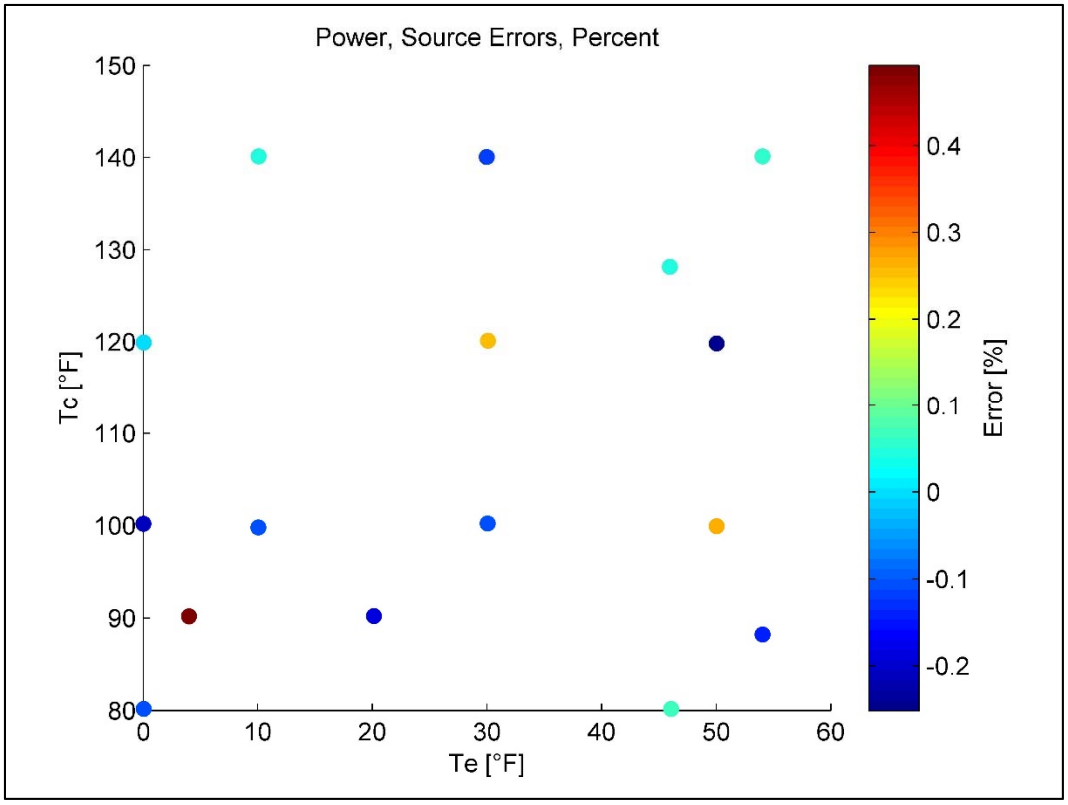

Figure 26: Comprehensive Set-1, errors in power, based on source data

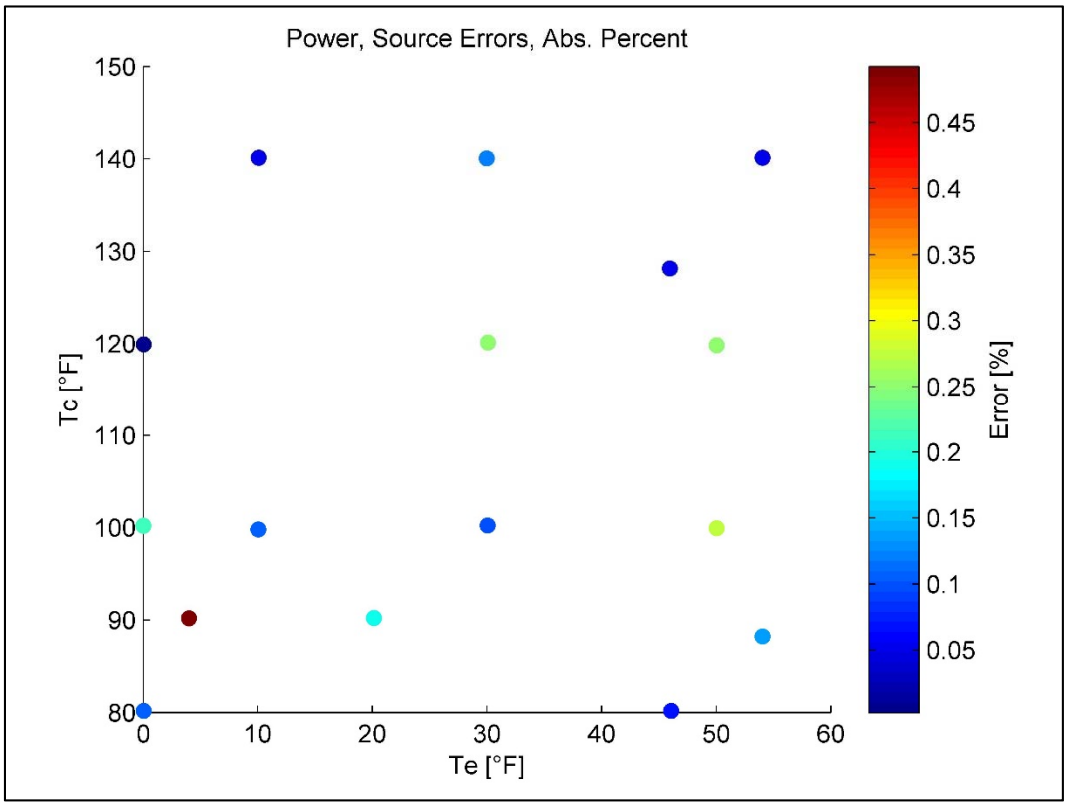

Figure 27: Comprehensive Set-1, absolute errors in power, based on source data

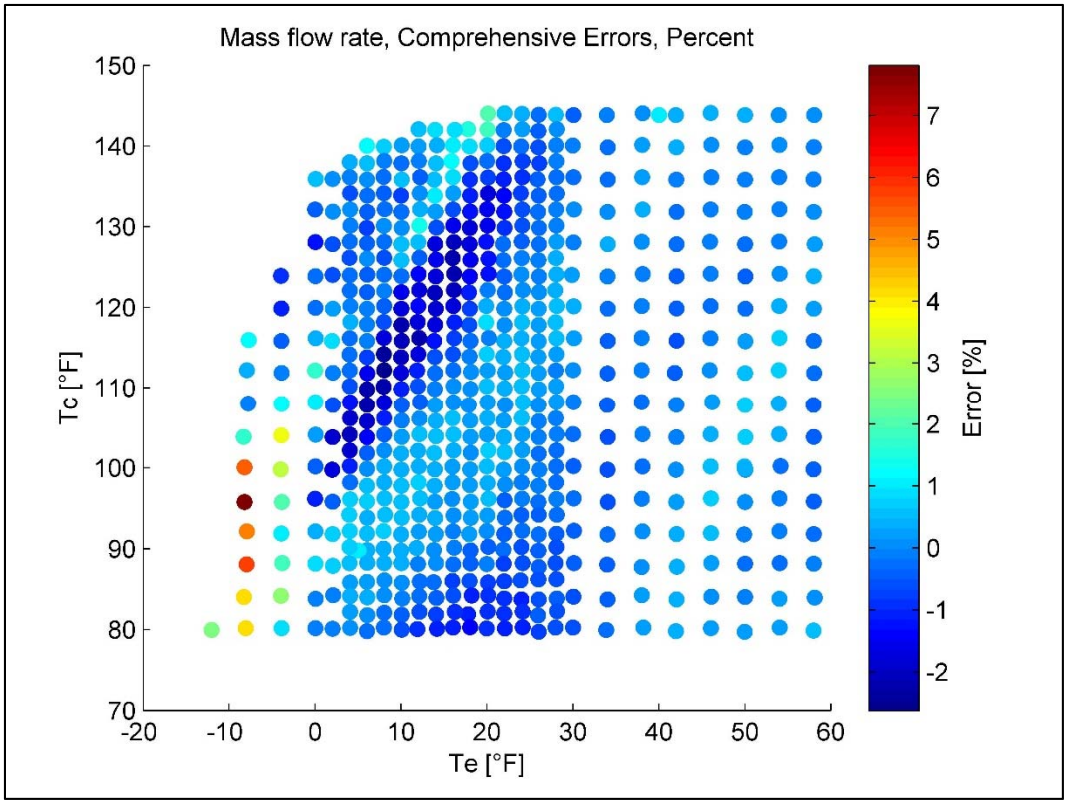

Figure 28: Comprehensive Set-1, errors in mass flow rate, based on verification data

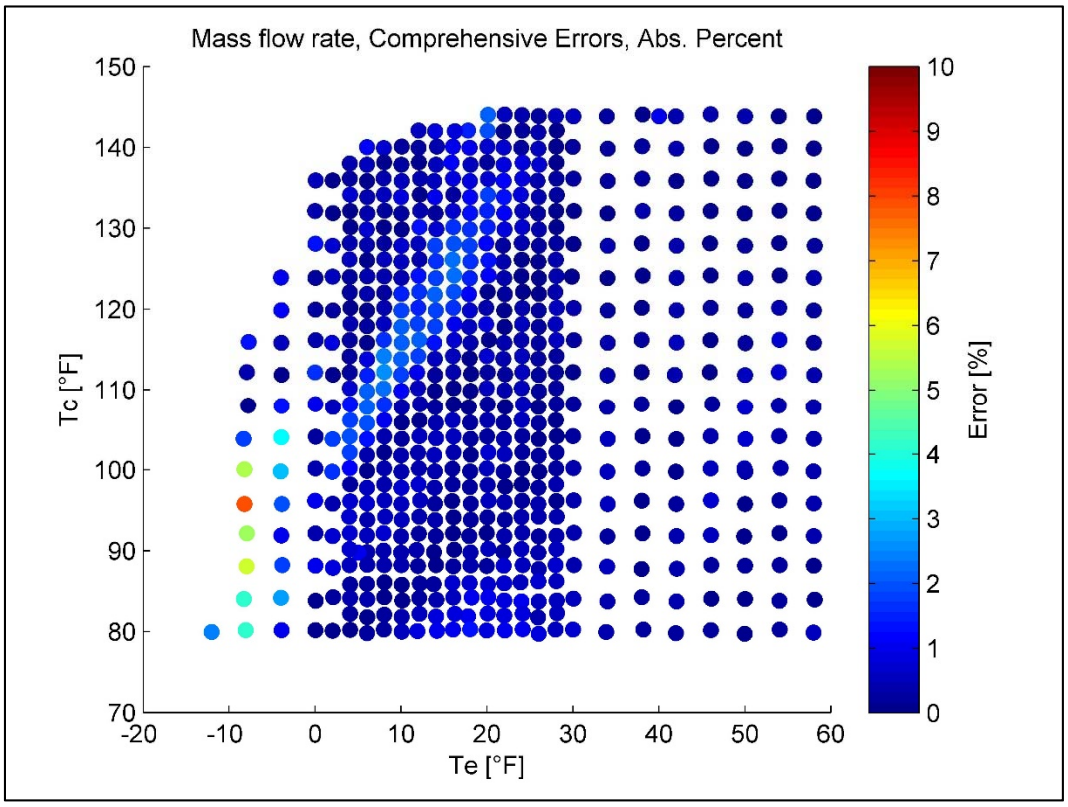

Figure 29: Comprehensive Set-1, absolute errors in mass flow rate, based on verification data

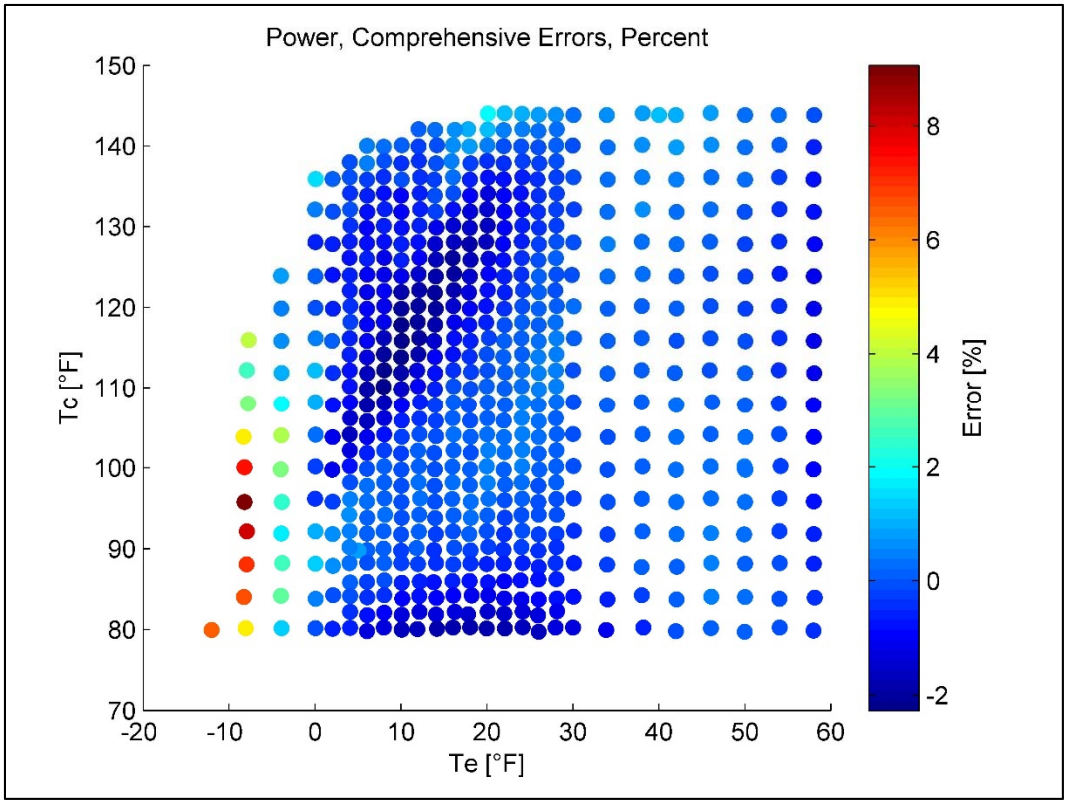

Figure 30: Comprehensive Set-1, errors in power, based on verification data

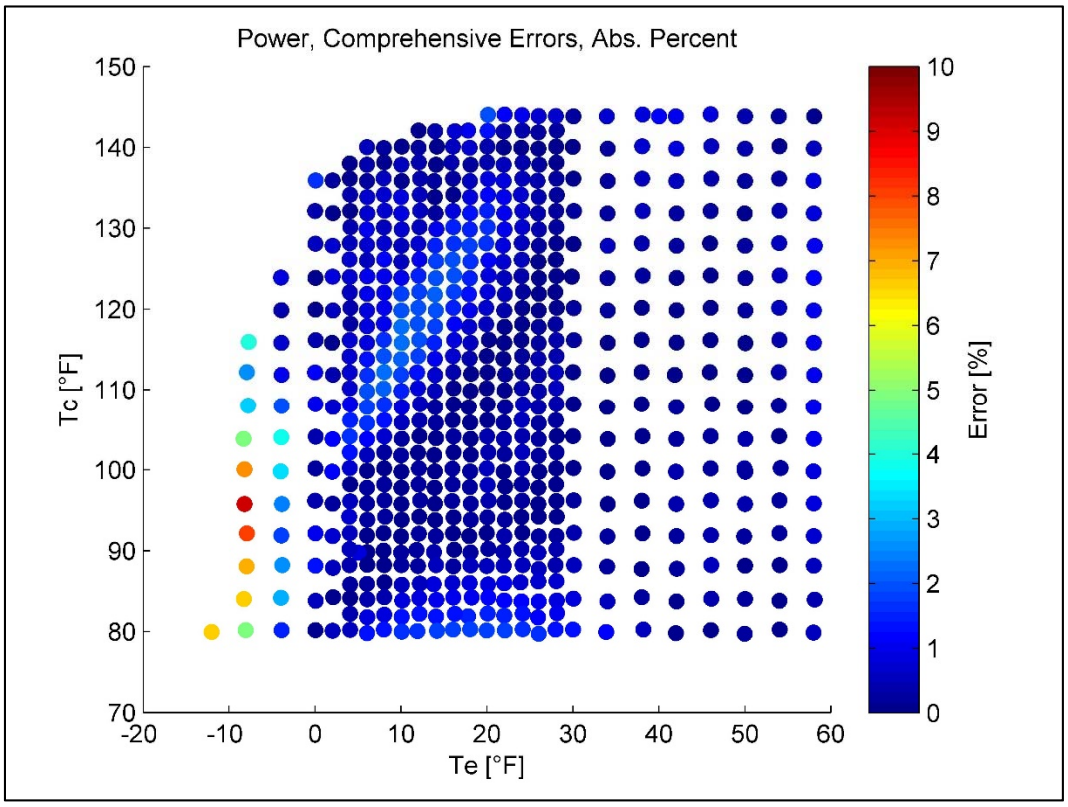

Figure 31: Comprehensive Set-1, absolute errors in power, based on verification data

6.4 Comparison of Current Method and Methods from Literature

The current AHRI-540 method is compared against four other methods from the literature. The candidate methods presented in Table 7 were selected before the complete data sets were available for present analysis. In light of available data sets and the numerical issues that resulted during model fitting for some of these equations, it was decide to choose a modified set of candidate methods. These methods and the nomenclature used are summarized in Table 9 below.

Table 9: Summary of performance representation methods

Model/Method	Required # of Data Points	Regression Type	Comments
AHRI540 (baseline)	11	Linear	Easy to solve, no guess values
MPOLY	11	Linear	Variation of the AHRI-540 method; easy to solve, no guess values required.
QIAO (Qiao et al.)	7	Mixed	Requires guess values; capable of handling variable speed, with 19 points
KLEIN (Jahnig et al.)	6	Non-linear	Most comprehensive and popular model from literature; requires guess values
EMILIO (Emilio Navarro et al., 2007)	6	Non-linear	Can handle superheat; requires guess values

During analysis, the nonlinear models were found to be numerically highly unstable for several data sets. For such cases, a multi-start non-linear least squares fitting method was used.
As a first test, all the models were fitted based on the source data and were used to predict the source data itself. It is expected that a regression model should be able to predict its source data with reasonable accuracy. There were 43 different data sets as described previously. The models were fitted for all these data sets and the various error metrics were computed. For the sake of brevity, the average values are reported here. For example, consider the metric of Average Absolute Percent Error (AAPE). This metric was evaluated for each model for each data set. Then, the AAPE values were averaged across different compressor types. Similar averaging was carried out for other metrics of Maximum Absolute Error Percent (MAEP) and Relative Root Mean Square Error (RRMSE).

The average errors in mass flow rate prediction for different models are shown in Figure 32 and those for the power prediction are shown in Figure 33. It can be seen that in general, the AHRI540 model has very good prediction capabilities. One of the reasons is that the underlying regression does not require starting guess values and with the use of linear regression, it is possible to achieve near perfect fit. The models EMILIO and KLEIN exhibit the worst errors. This is in part because of the highly non-linear nature of the equations and the numerical challenges encountered during data fitting. It is also observed from Figure 33 that the AHRI540, QIAO and the MPOLY models are more suited for rotary and reciprocating compressors as compared to scroll compressors.

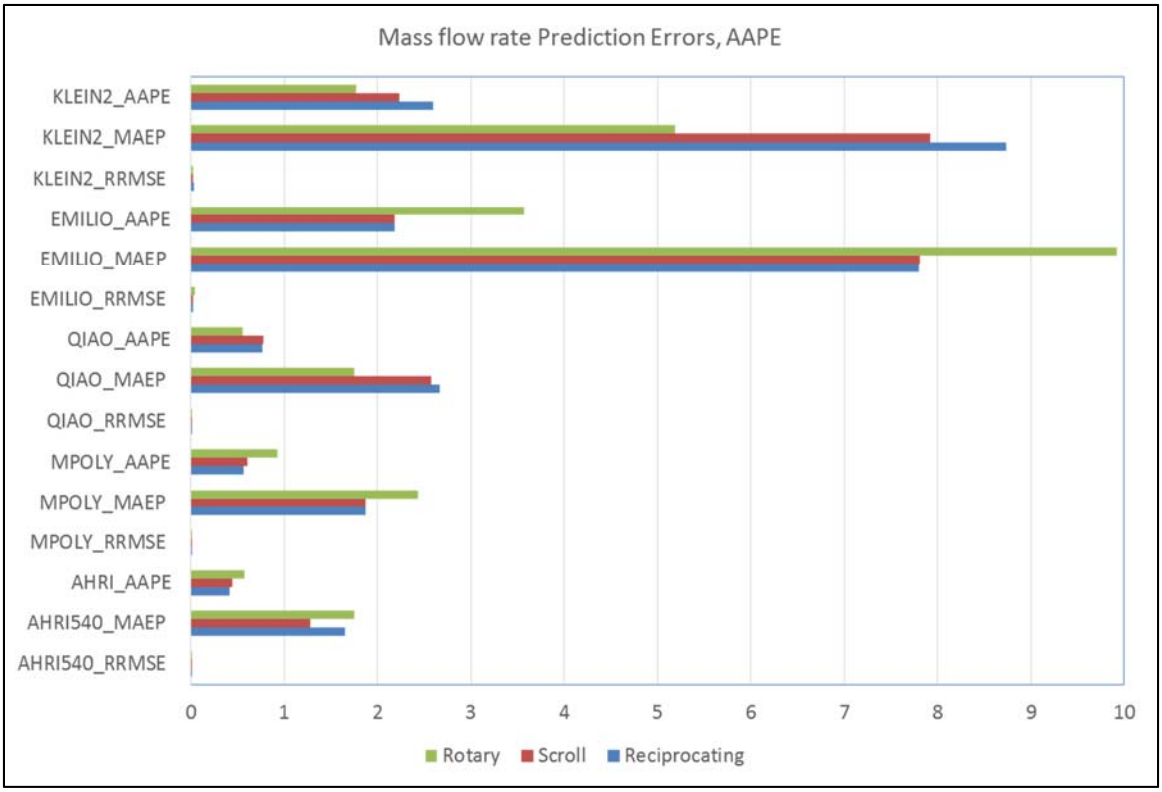

Figure 32: Average errors in mass flow rate prediction

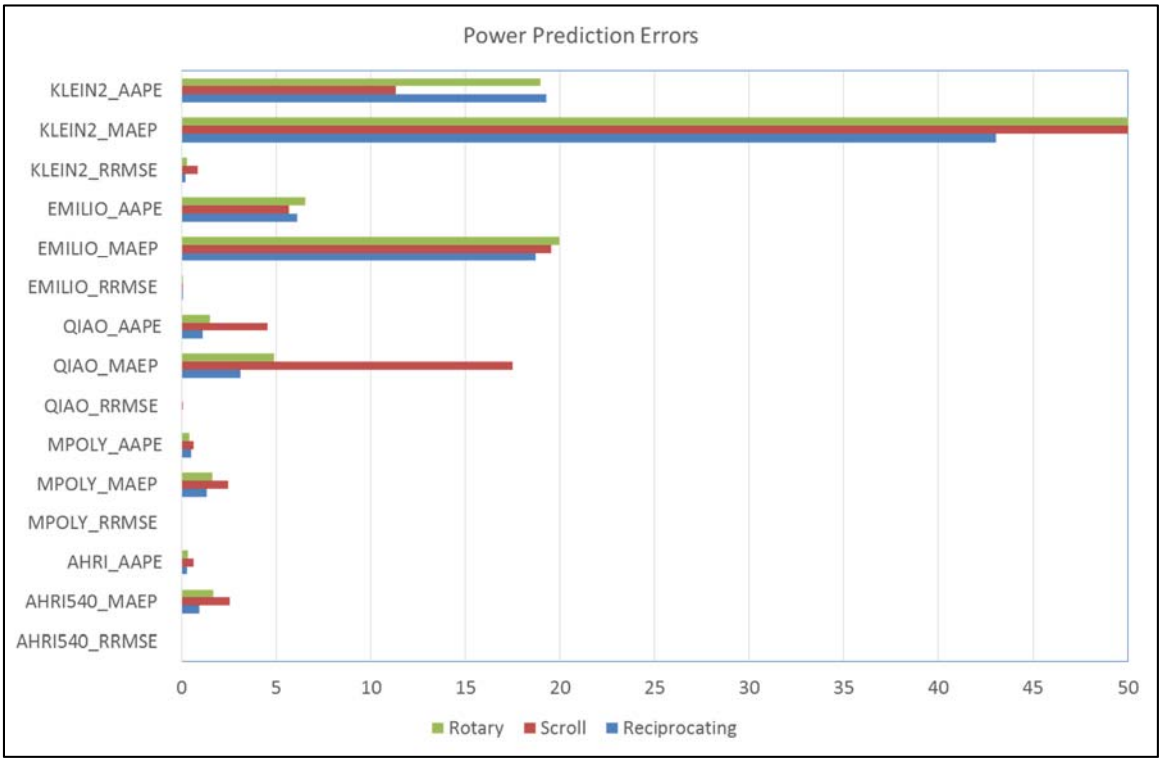

Figure 33: Average errors in power prediction

6.5 Effect of Superheat

The conventional AHRI-540 standard requires that the compressor performance be rated as a fixed 20°F suction superheat. As such, any model based on such data is valid for 20°F suction superheat only. Some of the physics-based models can be used for other superheat values without additional corrections.

In the literature, one of the most popular method of superheat correction for the AHRI-540 performance map is the one proposed by Dabiri and Rice (1981). Their proposed mass flow rate correction is a multiplier that is based on the ratio of actual suction density and the suction density corresponding to 20°F.

In this section, the various models are evaluated for their prediction capabilities with different superheat values. Data sets are available for four different compressors, each at a superheat of 20°F and 40°F. The number of points and the actual values for the two cases are not necessarily the same. A summary of this data set is provided in Table 10.

Table 10: Summary of data available for superheat analysis

Model Code	Compressor Type	Refrigerant	Points at 20°F superheat	Points at 40°F superheat
R32-S-OX	Scroll	R32	59	52
R404A-S-OX	Scroll	R404A	63	64
R410A-S-OX1	Scroll	R410A	66	64
R410A-S-OX2	Scroll	R410A	66	64

6.5.1 Model Analysis

For the purposes of comparison, 20°F data was used to fit all models and then these models were used to predict the data for the 40°F superheat cases. For the sake of completeness, the 20°F model fitting results are also included here.

Figures 34 and 35 show the baseline model prediction errors for the different compressors and prediction models at 20°F superheat. The average error in mass flow rate prediction is less than 1%. This is expected since the source data used to develop the model are used to predict performance. The maximum error in mass flow rate prediction for each case is less than 3%, which is consistent with that observed in the previous sections. It should be noted that the KLEIN and the EMILIO models work surprisingly well in this case.

In the case of power prediction, the average absolute errors for the AHRI540 model are less than 5%, whereas for the QIAO model, they are less than 15%. The KLEIN and EMILIO models have the worst predictions. As highlighted previously, this is mainly attributed to the numerical challenges encountered during non-linear regression.

The mass flow rate prediction errors for the case of 40°F are shown in Figure 36. The first observation is that the AHRI540 map predictions show errors greater than 5% for all of the compressor data sets. The AHRI540-C model shown in Figures 36 and 37 refers to the corrected model. The corrections proposed by Dabiri and Rice (1981) were utilized. The predictions from the QIAO and the KLEIN models exhibit errors less than 3%, with average errors for the QIAO

model being less than 1.5%. This is expected, since both of these models correlate the volumetric efficiency and use it along with suction density to calculate the mass flow rate. The EMILIO model still exhibits significant errors. For the AHRI540-C case (AHRI540 with superheat correction), the errors are less than 1%. This shows that the Dabiri and Rice (1981) superheat correction works very well for the mass flow rate.

In the case of power, the AHRI540 model exhibits the best performance, i.e., the lowest errors. The QIAO model also has average errors less than 3%, but there are some regions in the map wherein the prediction error is more than 5%. This is indicated by the Maximum Absolute error (MAEP).

In order to better understand the sources of the errors and to investigate if these errors are correlated with any input or operating parameters, additional data visualization was carried out. For each case (compressor data set and model), three plots were generated. The first plot shows the data points on the operating envelope (i.e., [Te,Tc]) chart with errors indicated by shading. The second plot shows the errors vs. ratio of suction density and saturated suction density with pressure ratio (Pr) indicated by shading. The third plot shows the errors vs. ratio of suction density vs. the map suction density (i.e., 20°F superheat) with pressure ratio indicated by the shading. Figure 38 shows such plots for mass flow rate errors corresponding to an R32 compressor using the AHRI540 model. Figure 39 shows the corresponding plot for errors in power prediction.

In order to improve readability of the report, only a subset of the plots are shown here. Figures 40 and 41 show a particular cases where a strong correlation between the mass flow rate errors and the ratio of suction densities are observed for the AHRI540 model. This explains why the Dabiri and Rice (1981) correction (linear in ratio of suction densities) works so well. Same behavior was observed for the other compressors in this data set.

As seen from Figures 42 and 43, the errors in mass flow rate prediction from the EMILIO and KLEIN models show an approximate linear correlation with the ratio of suction densities. Thus, it is possible to develop a corresponding correction for these models as well.

For the QIAO model, however, no strong correlation between mass flow rate errors and any other parameters was observed. One reason is that the model already predicts most data within 3%. In the case of power prediction, as shown in Figure 44, there was no obvious correlation between prediction errors and any of the parameters. Further investigation is recommended to fully evaluate this behavior.

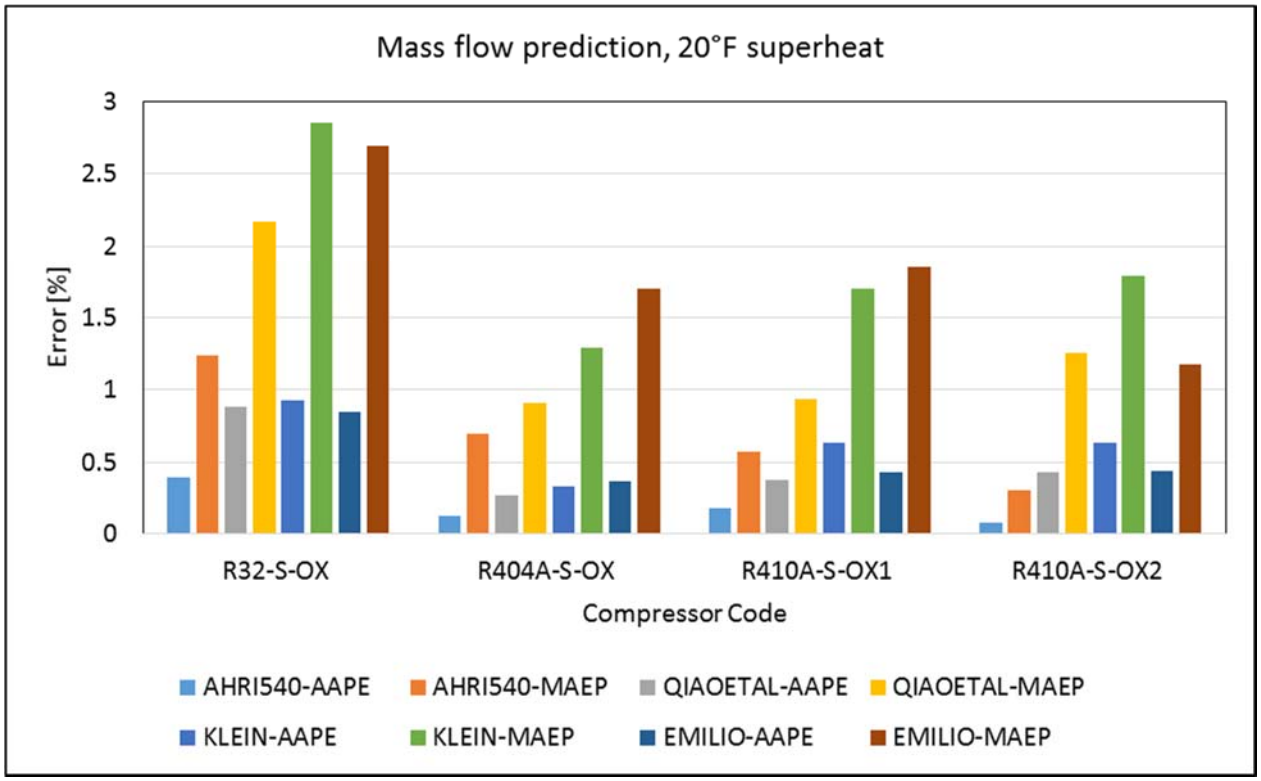

Figure 34: Baseline comparison for mass flow prediction, at 20°F superheat

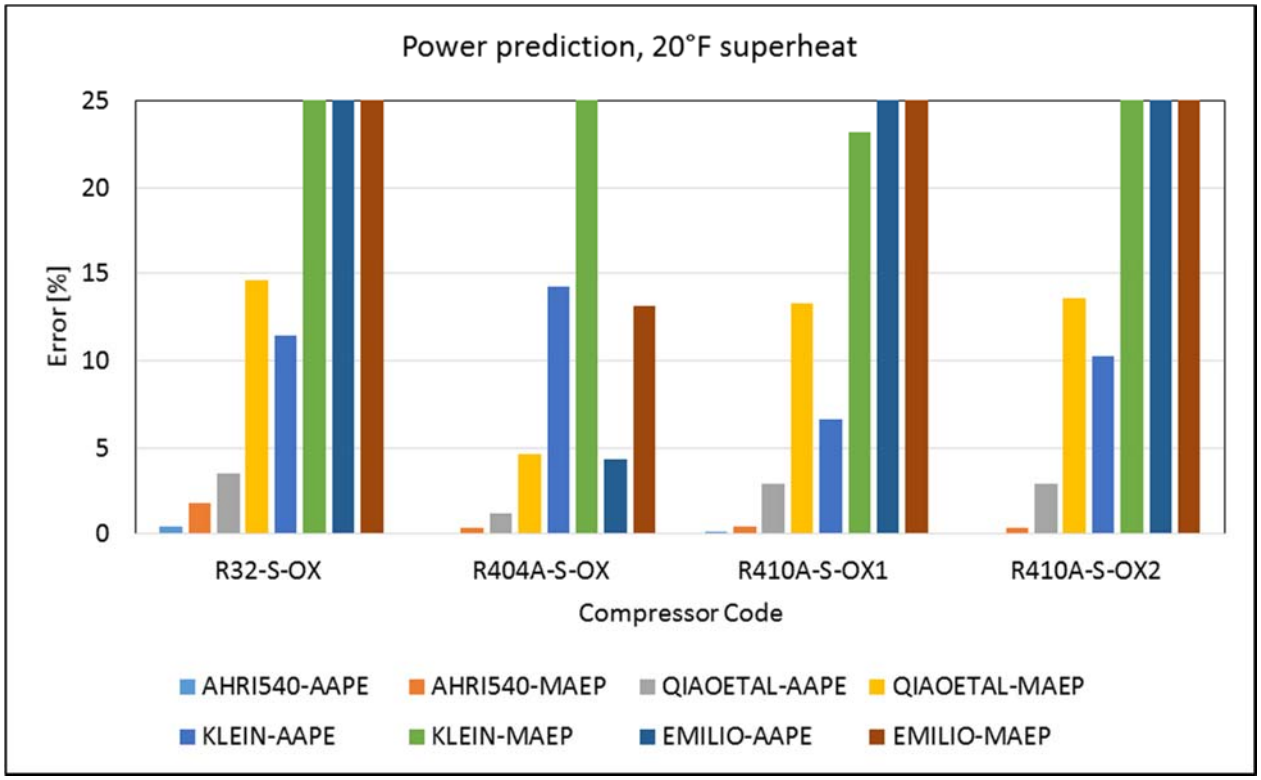

Figure 35: Baseline comparison for power prediction, at 20°F superheat

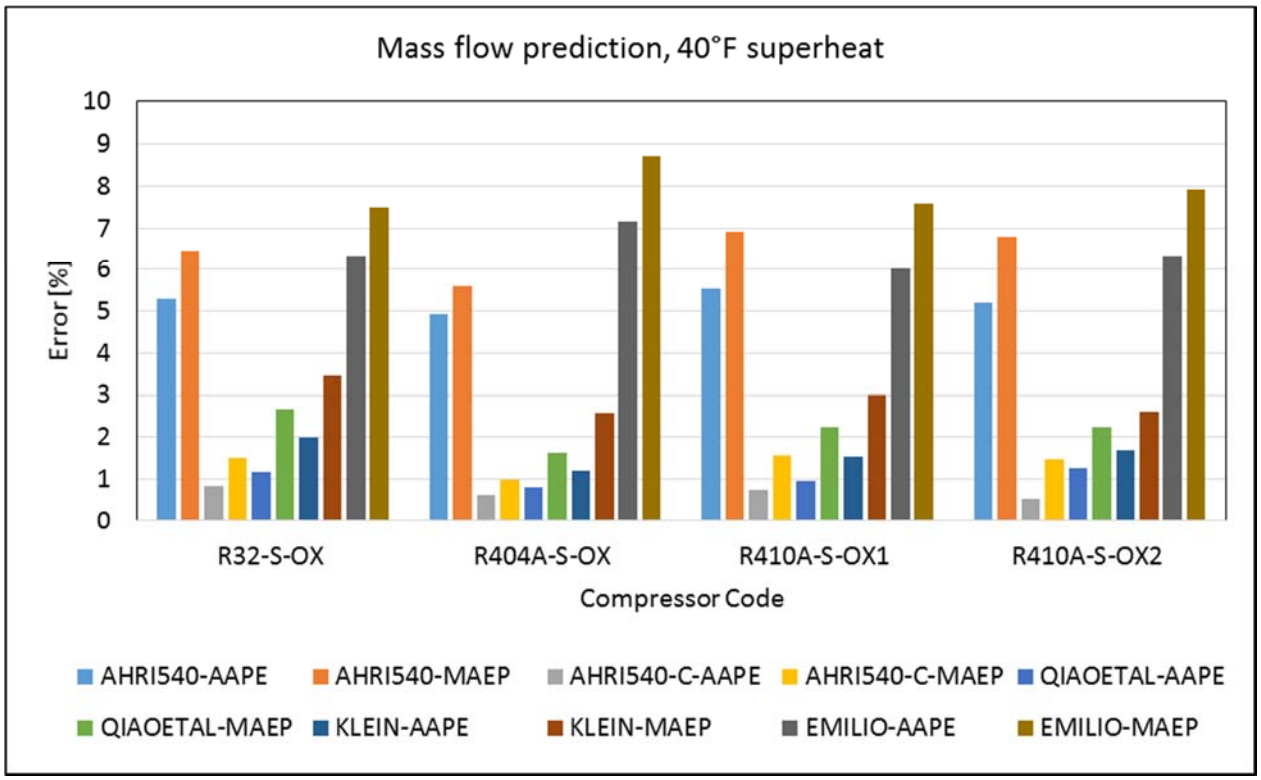

Figure 36: Comparison for mass flow prediction, at 40°F superheat

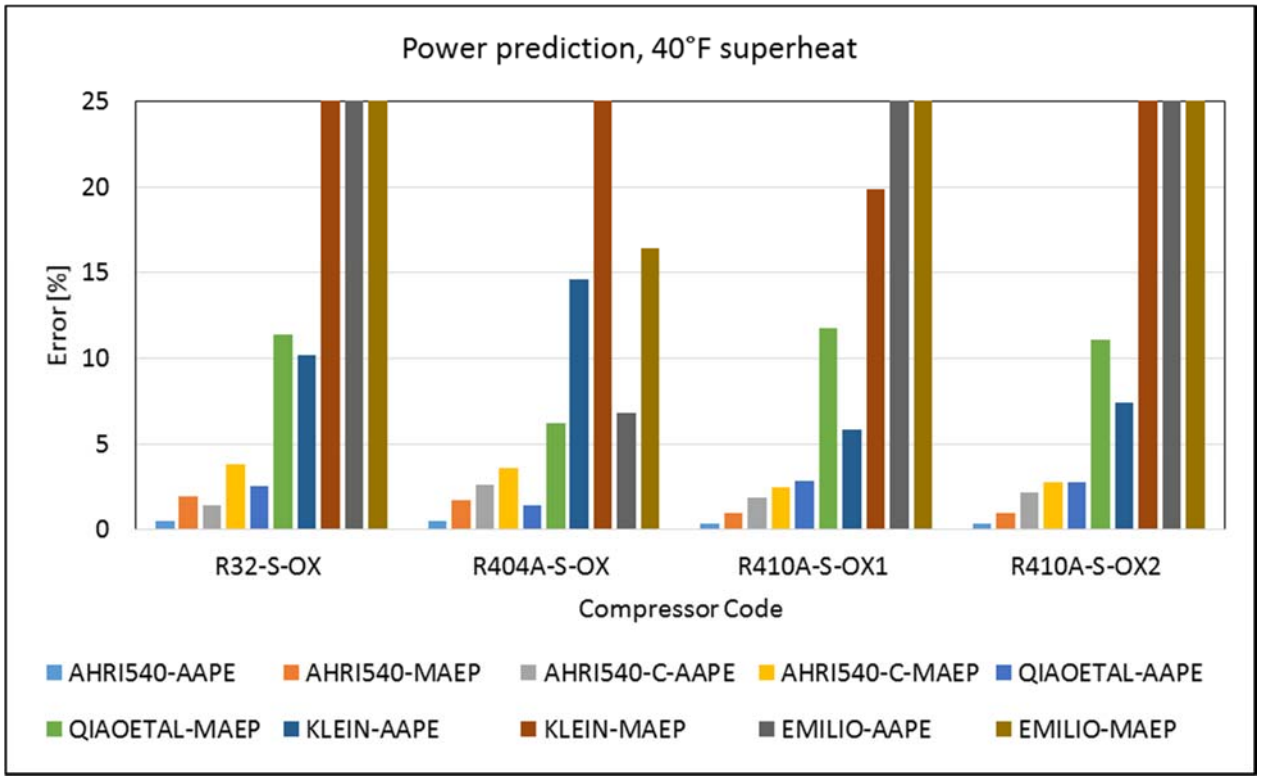

Figure 37: Comparison for power prediction, at 40°F superheat

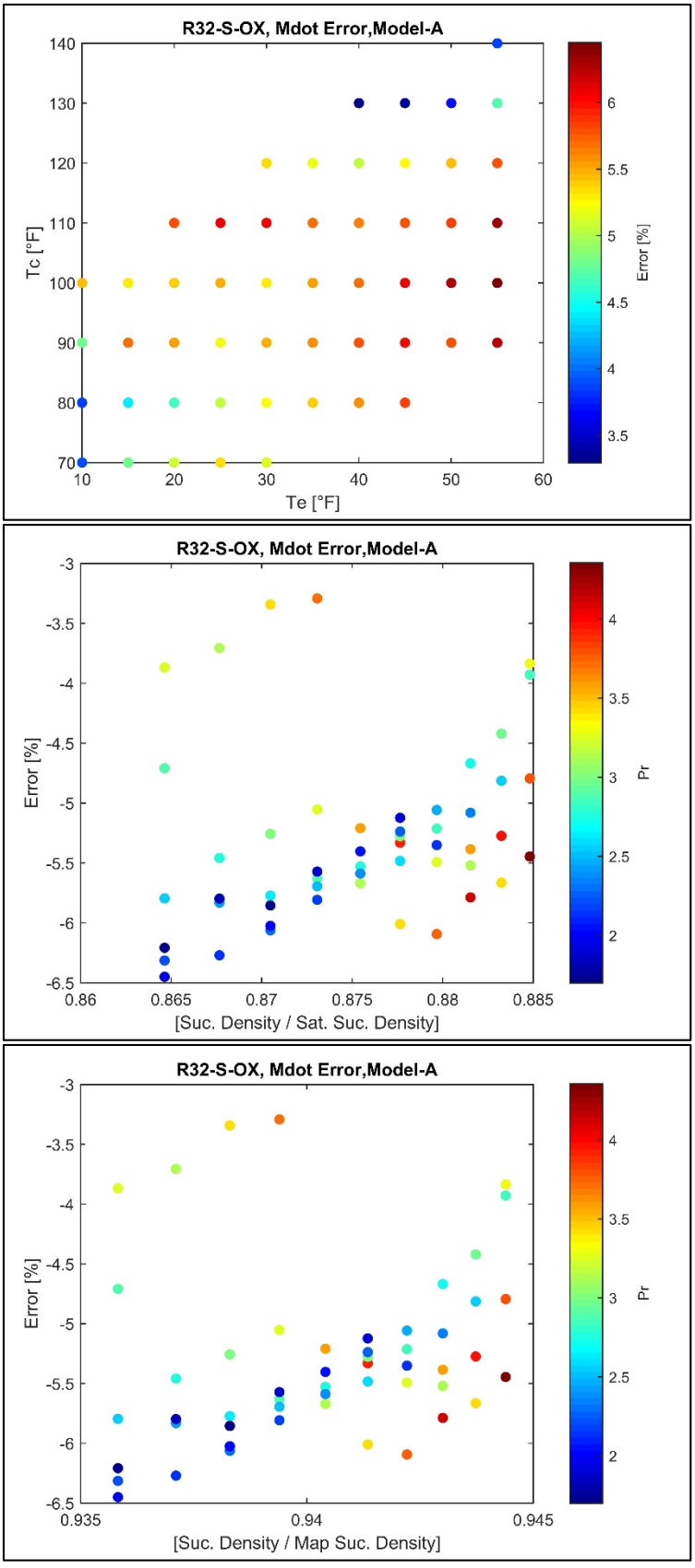

Figure 38: Errors in mass flow rate, R32 scroll compressor, at 40°F superheat

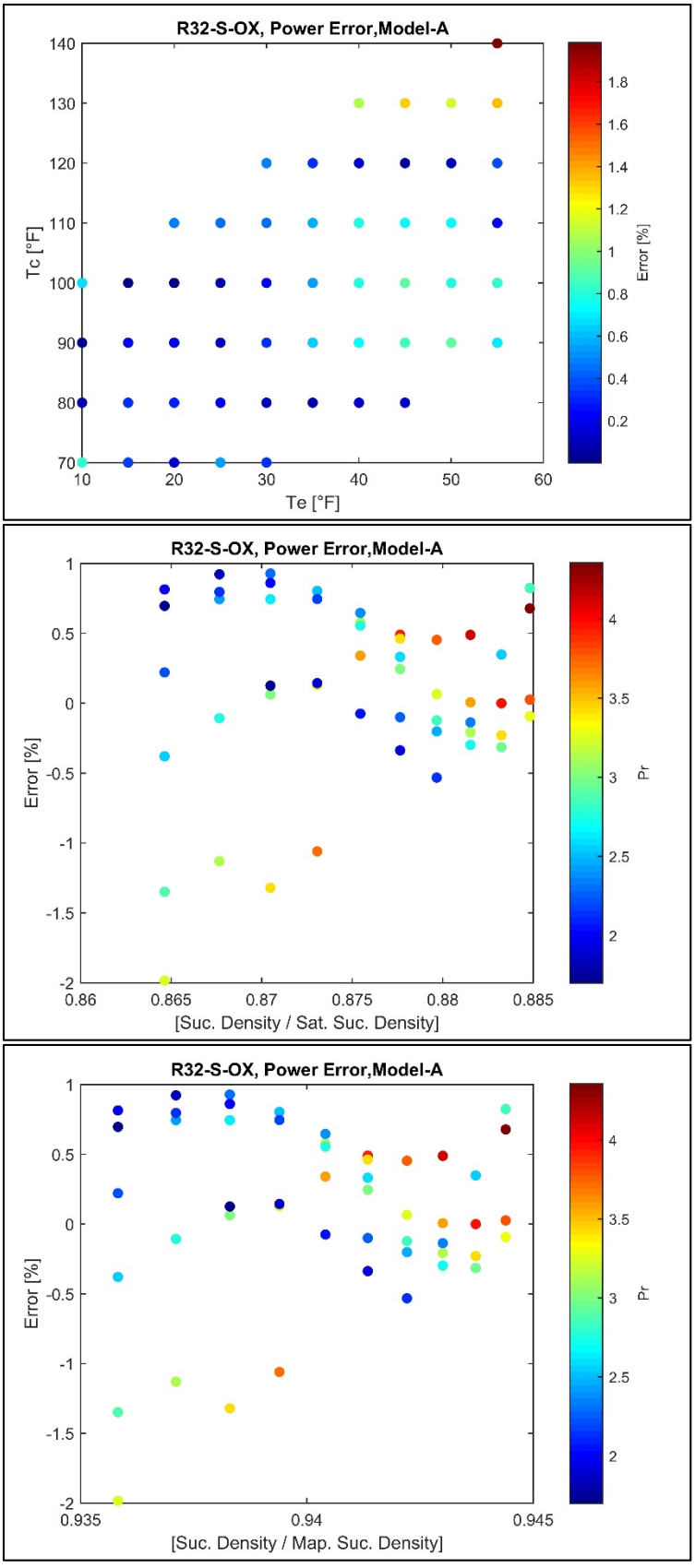

Figure 39: Errors in power, R32 scroll compressor, at 40°F superheat

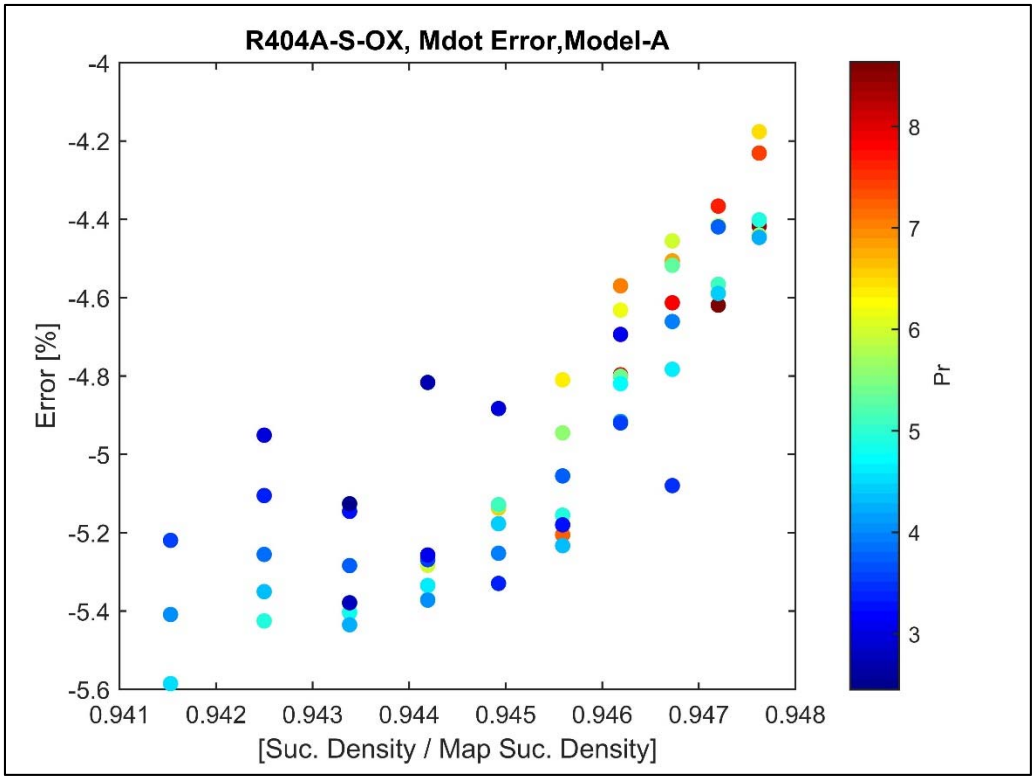

Figure 40: Strong linear correlation between mass flow rate errors from AHRI540 model and ratio of suction densities for R404A scroll compressor

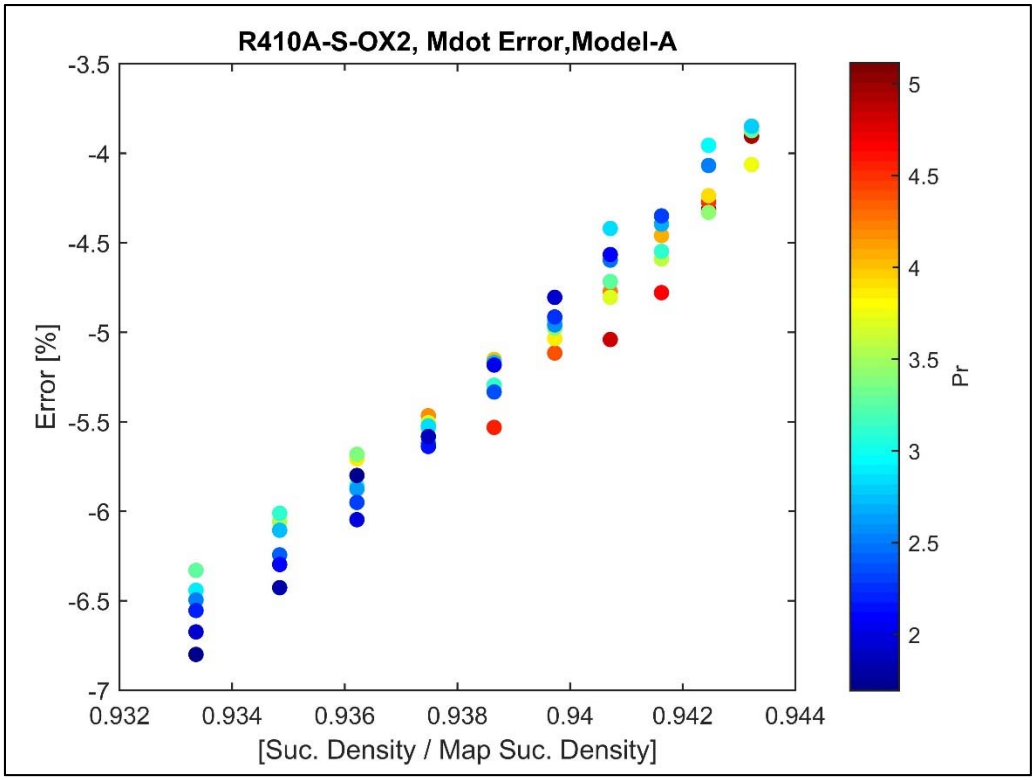

Figure 41: Strong linear correlation between mass flow rate errors from AHRI540 model and ratio of suction densities for R$10A scroll compressor

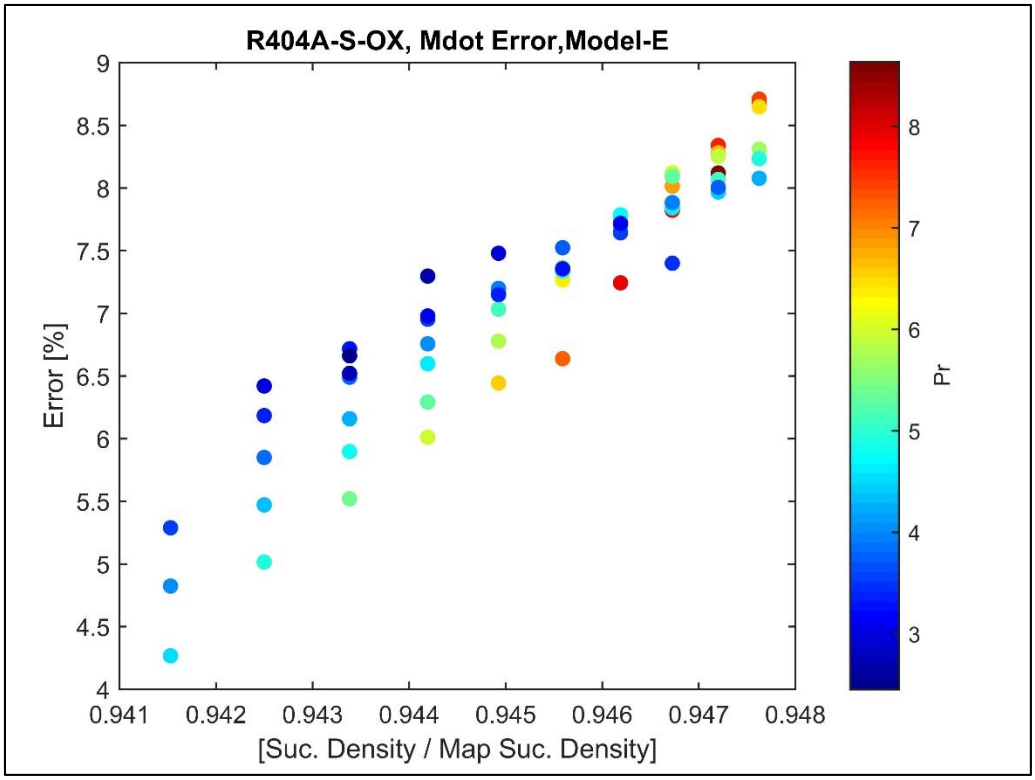

Figure 42: Strong linear correlation between mass flow rate errors from EMILIO model and ratio of suction densities for R404A scroll compressor

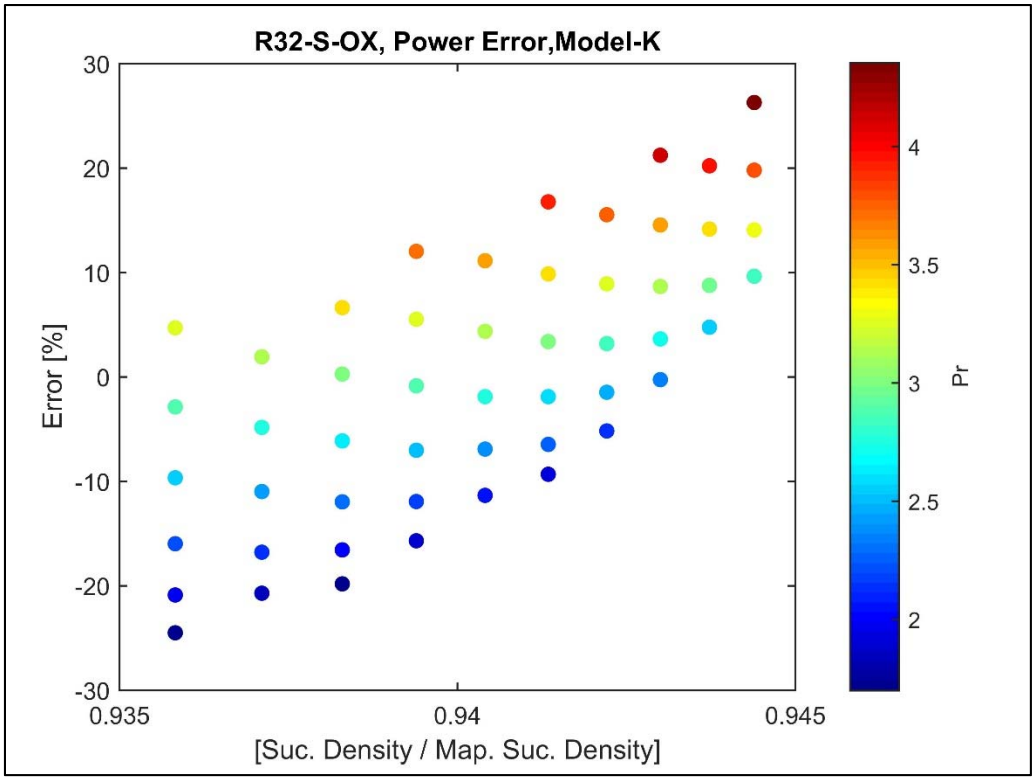

Figure 43: Correlation between power errors from KLEIN model and ratio of suction densities for R32 scroll compressor

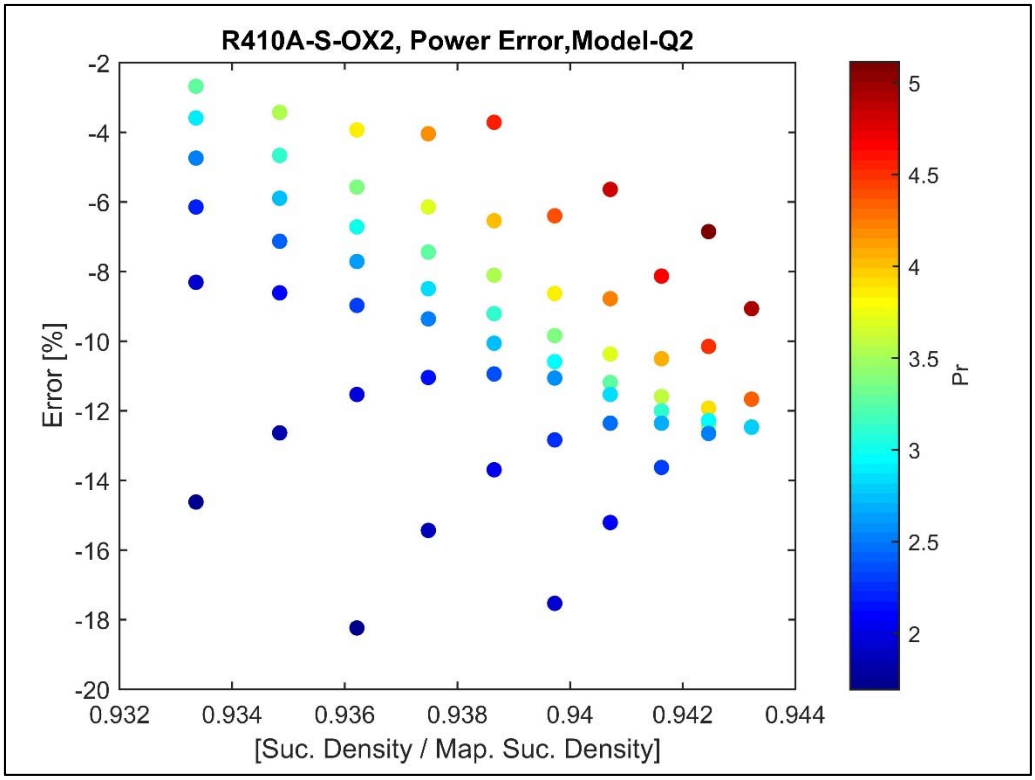

Figure 44: Correlation between power errors from QIAO model and ratio of suction densities for R410A scroll compressor

6.5.2 Summary of Superheat Analysis

Based on the analysis presented in the previous section, the following general conclusions can be drawn:

1. The error in predicted mass flow rate for superheat values different than the map superheat has a strong correlation with the ratio of suction densities. The same is true for errors in power prediction, except for the QIAO model.
2. The Dabiri and Rice (1981) correction for superheat works well for the AHRI540 map.
3. The QIAO and the KLEIN models have good predicted capabilities at superheat values different than the source (map) data superheat. Most errors were within 3%.
4. The AHRI540 maps gives the best predictions in power for the 40°F superheat case, even better than the corrected model. The QIAO model shows good average prediction, but very high maximum errors. All of the other models exhibit significantly high errors making them unusable for any prediction task.
5. Based on the error analyses, it is possible to develop a power correction equation for the QIAO and KLEIN models.
6. In the present analysis, all of the source data was based on 20°F superheat with only five compressor data sets. It would be interesting to see how the predictions change when mixed superheat data is used for model development. This is particularly important for the QIAO, KLEIN and EMILIO models, since they are physics-based.

7 Sampling Based on Conventional Methods

This section studies the influence of different sampling methods. Based on the manufacturer survey, there is no well-established methodology used in selecting the sample points for developing the 10-coefficient map.

7.1 Methodology

The map data sets and the comprehensive verification data sets described in Section 6.3 are used here. The general approach is as follows:

1. Use the map data to develop a 10-coefficient polynomial model for mass flow rate and power consumption and verify these models against the comprehensive data set.
2. Using the comprehensive verification dataset, develop a regression surface using the Kriging metamodel. The Kriging metamodel does not require a functional form and is capable of exactly reproducing the source data.
3. Choose different sampling methods (e.g., LHS – Latin Hypercube Design). For each sampling method, select a specified number of points from the operating envelope.
4. Compute the mass flow rate and power consumption using the Kriging metamodel for the sampled points.
5. Develop a 10-coefficient polynomial model based on the data from Step-4.
6. Verify the model from Step-5 against the comprehensive data set.

7.2 Results

7.2.1 Results for Comprehensive Test Set-1

The map data set contains a total of 16 points. For the present analysis, a Latin Hypercube (LHS) design comprising of 15 points is chosen. A comparison of the LHS sample points and the map data points is shown in the Figure 45 below.

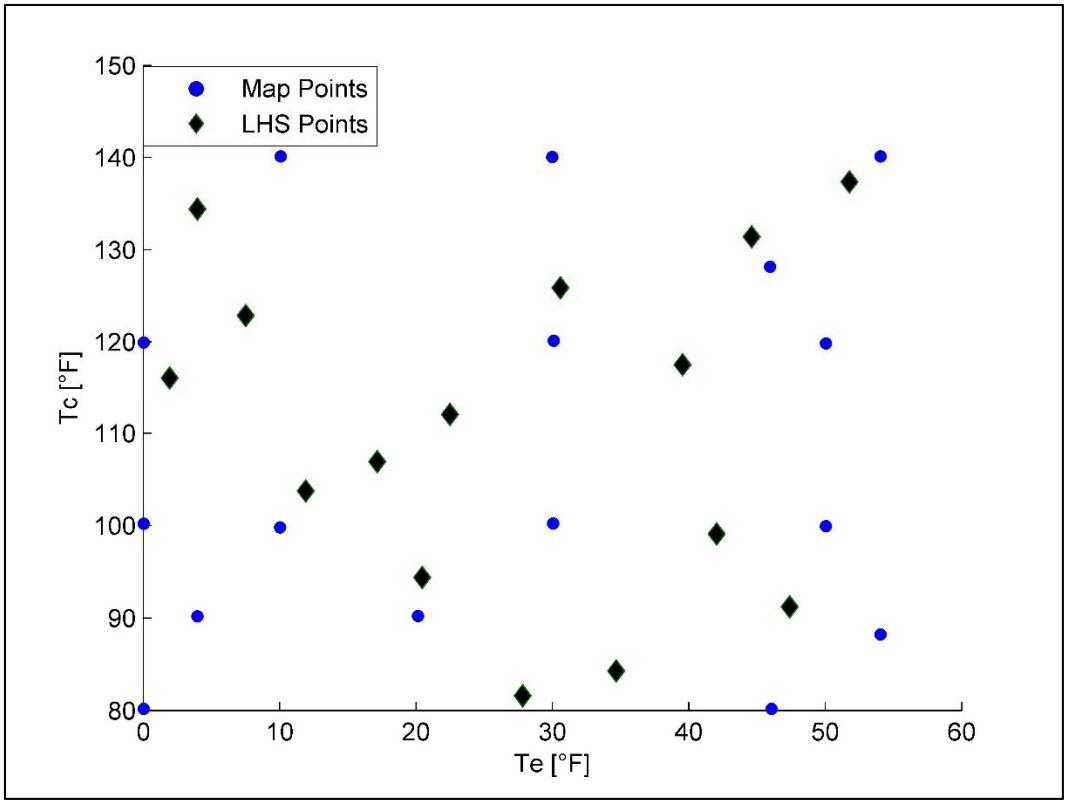

Figure 45: Map data points vs. LHS sample points

In the following figures, the errors in predicted mass flow rate and power are shown for comparison.

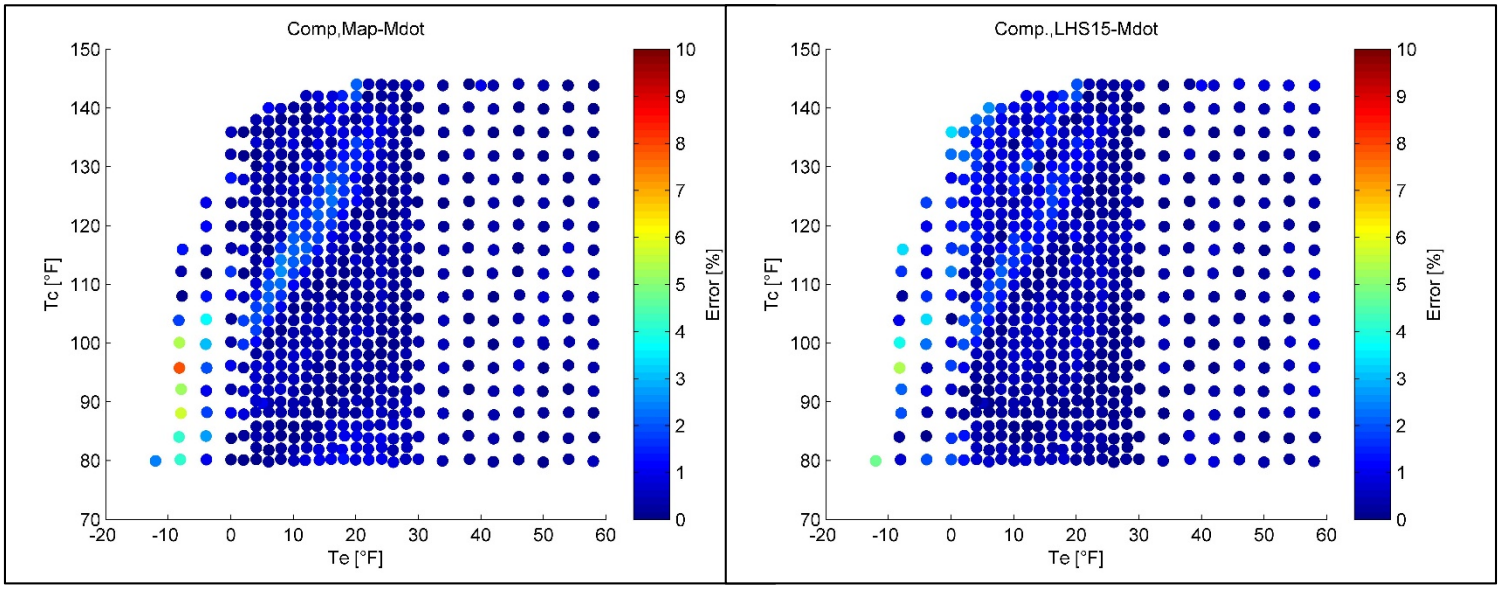

Figure 46: Comparison of errors in predicted mass flow rate for map data vs. LHS samples

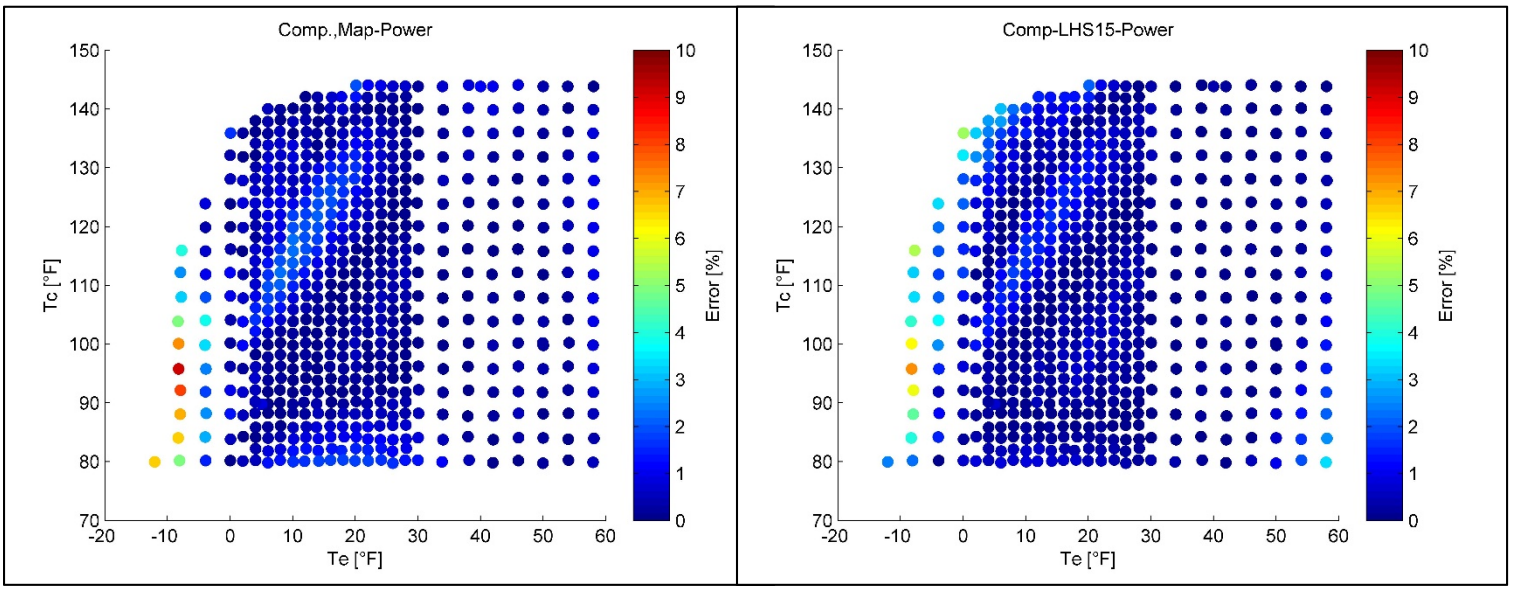

Figure 47: Comparison of errors in predicted power for map data vs. LHS samples

As observed from Figures 46 and 47, the 10-coefficient polynomial obtained using the LHS samples is more accurate (lower errors) in terms of both mass flow rate and the power consumption over the entire operating envelope, including some extrapolation.

Based on this preliminary analysis, the LHS sampling may be better suited for use with the 10-coefficient map. The challenge with LHS sampling is that it is based on random number generator and as such the samples can change from run to run and the accuracy may not be reproducible. Additional analysis in terms of deterministic methods and sensitivity to the number of samples points is required.

7.3 Summary

Conventional sampling techniques are designed to work with square or rectangular domains. In the analysis presented in the previous section, due to availability of over 600 data points encompassing the entire operating envelope, it was possible to use the LHS method for sampling for use with the AHRI-540 model.

8 Sampling Based on Non-Rectangular Domains

8.1 Overview of Sampling Technique

As mentioned in the previous section, the compressor operating envelope is non-rectangular, and hence, conventional sampling techniques are not directly applicable for selecting test points. A mathematically sound approach is required to handle non-rectangular domains.

A quick literature review reveals that very minimal work has been done in the area of design of experiments for non-rectangular domains. This is because, for most engineering problems, the design variables are always bounded and can be always be mapped onto the [0, 1] interval.

Furthermore, any non-rectangular domains are handled via linear constraints on the design variable during the optimization process. This approach works since optimization is generally carried out on models and not on the basis of physical experiments.

There are two main methods published in the literature on space-filling designs for non-rectangular domains. The first method is by Draguljic et al. (2012) and the second is by Lekivetz and Jones (2014). There is no open-source implementation available for either of the two methods, and hence, the method by Lekivetz and Jones (2014) was implemented with some simplifications as a part of this project.

8.1.1 Example of Sampling for Non-Rectangular Domains

This section describes the sampling approach implementation with easy to understand visuals. Consider a non-rectangular 2-D domain such as a compressor operating envelope represented on a [Te,Tc] plot. Assume it is desired to sample *n* points inside this domain. The steps in the approach are as follows:

1. Start with the non-rectangular domain as shown in Figure 48.
2. Generate a large number of candidate sample points, either randomly or based on a uniform grid. These candidate sample points are superimposed on the design domain as shown in Figure 49. Using the conventional methods, such points are generated on a rectangular domain, hence these points will span beyond the operating envelope (or domain).
3. Filter the candidate sample points that are outside the operating domain.
4. Use a clustering algorithm to generate *n* clusters based on a Euclidean distance metric. These clusters are shown in Figure 51.
5. Compute the convex hull for each of these clusters. These convex hulls are shown in Figure 52. Note that some of the polygons corresponding to the convex hulls overlap. This is due to the way the clustering technique works.
6. Use the convex hull information to find the centroids of these clusters. These are show in Figure 52. The centroids are marked with a star (*).
7. The *n* centroids represented as the (*x*,*y*) coordinates are the desired sample points.

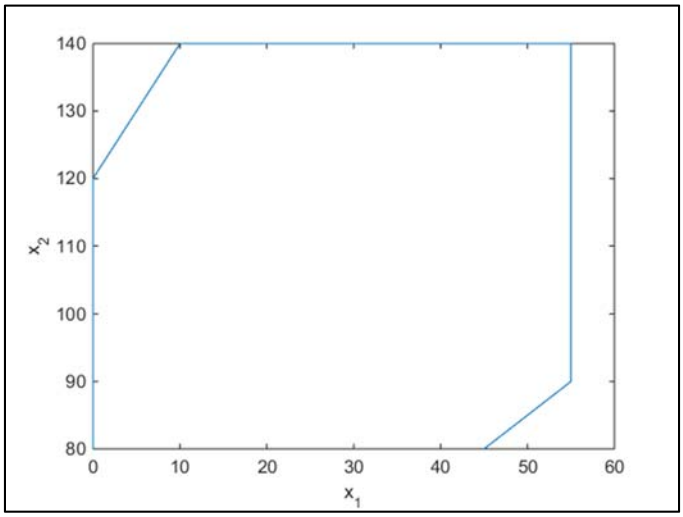

Figure 48: Example of a non-rectangular domain

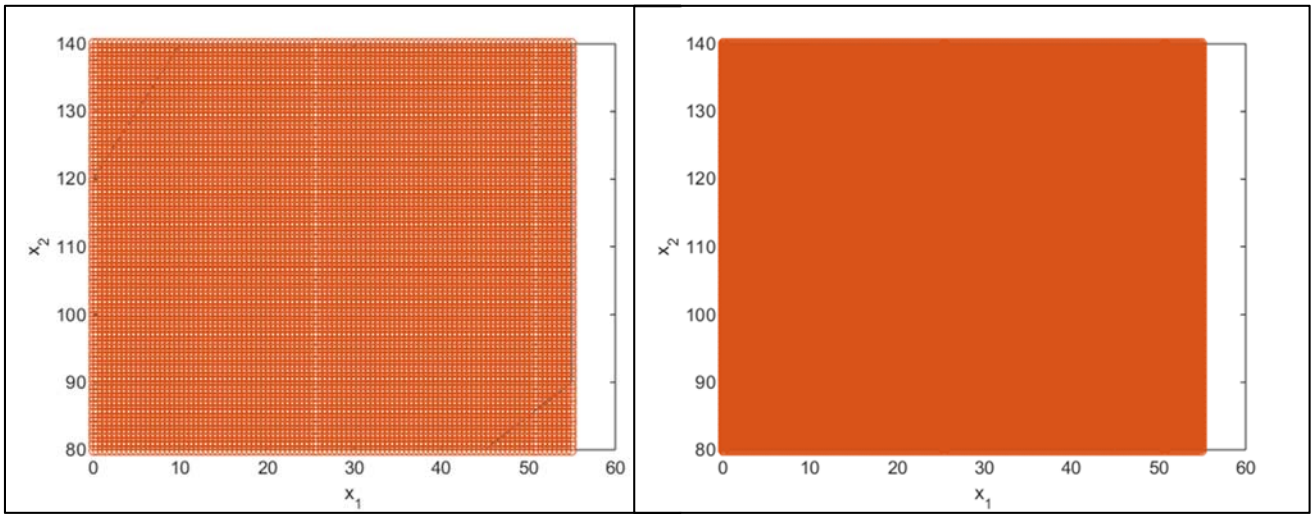

(a) (b)

Figure 49: Candidate sample points, (a) 10,000 samples, (b) 40,000 samples

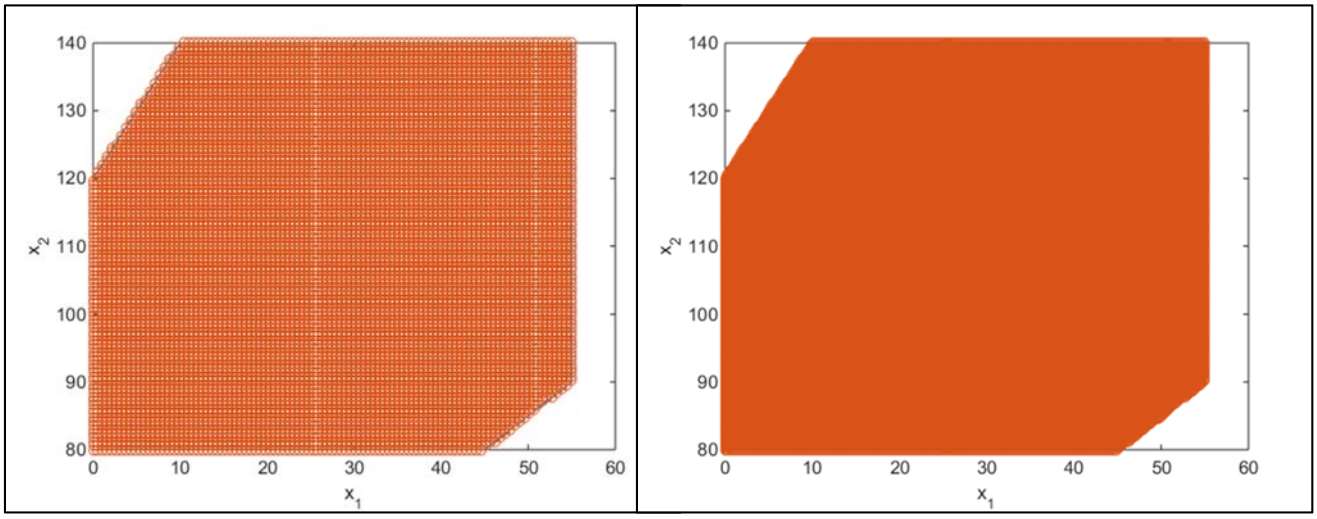

Figure 50: Candidate sample points, filtered based on the given domain

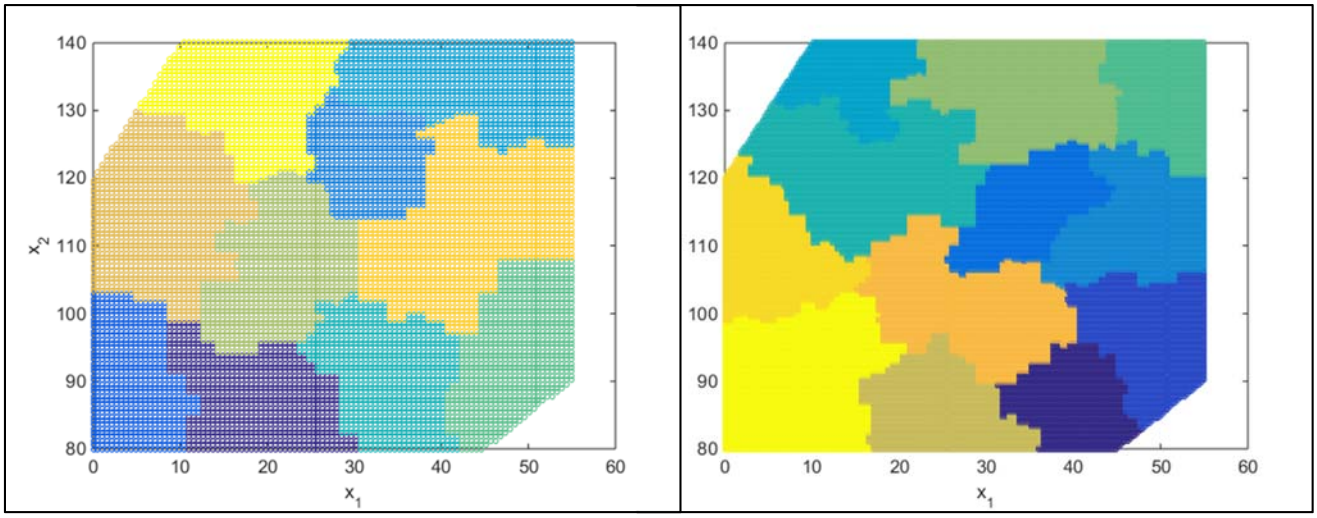

(a) (b)

Figure 51: Clustering of samples, (a) 10 clusters, 10,000 samples, (b) 12 clusters, 40,000 samples

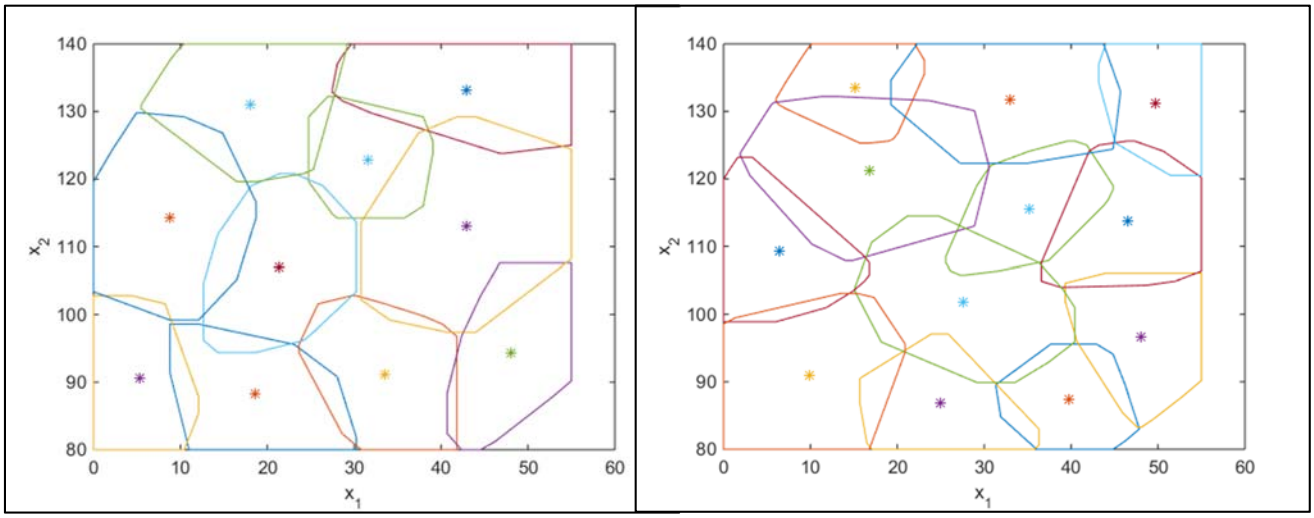

(a) (b)

Figure 52: Cluster centroids, (a) 10 clusters, 10,000 points, (b) 12 clusters, 40,000 points

The candidate sample points generated in Step-2 can be generated randomly, or out of a distribution or based on a uniform grid. In this study, a uniform grid was chosen to maintain reproducibility of results from one simulation to another for the same compressor data set. The clustering operation in Step-4 is the most computationally expensive part of this approach and depends on the number of candidate sample points used. Several numerical experiments were carried out to assess the quality of the final samples (i.e., how much they differ based on different grid resolution). A grid increment of 0.005 (total of 200 points in each dimension) was found to provide a good compromise between speed and sample distribution.

While the above method is an approximate implementation, it has several advantages as follows:

1. It retains the space-filling properties;
2. The computational cost is very low compared to a true implementation that would require one to solve successive optimization problems for each set of samples;
3. The use of the clustering followed by choosing centroid points guarantees that the samples are 'inside' the domain and sufficiently away from each of the vertices; and,
4. Reproducibility.

8.1.2 Proposed Sampling Approach (PDOE Method)

For the purposes of the current study, the following sampling strategy is implemented, assuming that the compressor operating envelope is given and *n* total samples are desired.

1. Initialize empty sample set *D*.
2. Start with the compressor operating envelope represented as a polygon with *k* vertices.
3. Add these *k* vertices to *D*.
4. Sample the remaining (*n*-*k*) points using the non-rectangular sampling method described in the previous section.

This method is referred to as the Polygon Design of Experiments (PDOE) method for brevity. The data representation methods being studied are meant to be used for interpolation purposes. As such, adding the *k* initial vertices is the simplest and the logical starting point.

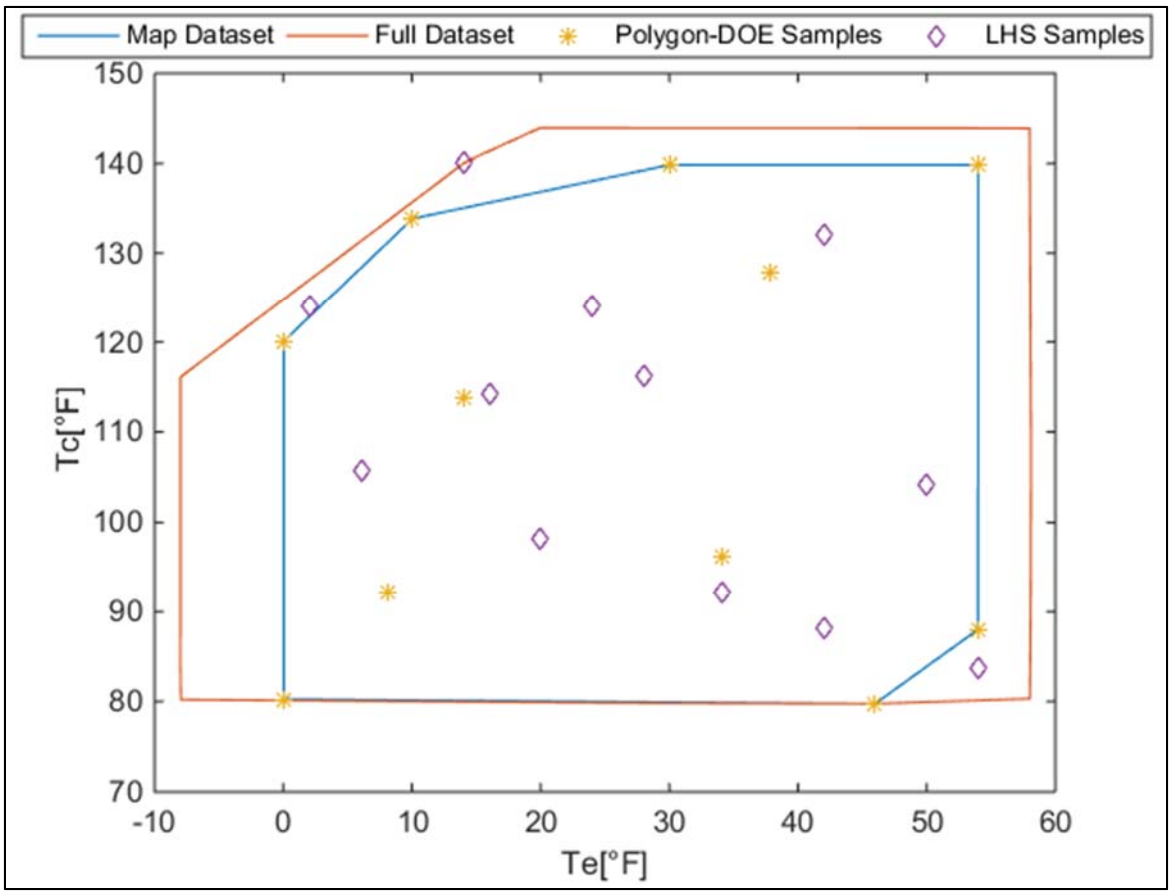

Figure 53: Comparison of samples generated using PDOE and LHS methods

Figure 53 shows a comparison of the samples generated using the PDOE method and the LHS method. The compressor operating envelope is shown along with the comprehensive data set envelope. Notice that the samples generated using the PDOE fall on or within the map dataset boundaries, whereas some of the samples generated using the LHS method fall outside the map dataset boundaries. This illustrates the challenge that conventional DOE methods were designed to operate on rectangular domains and are not suitable for non-rectangular domains.

Figure 54 shows the comparison of the samples generated using the PDOE method and the LHS method from a different run for the same data set. Notice that the PDOE samples are the same whereas the LHS samples are located in different regions. This is due to the fact that LHS method is based on a random starting point and as such each run of LHS design yields a different set of samples. This illustrates another challenge with the LHS method for the current application as reproducibility is important.

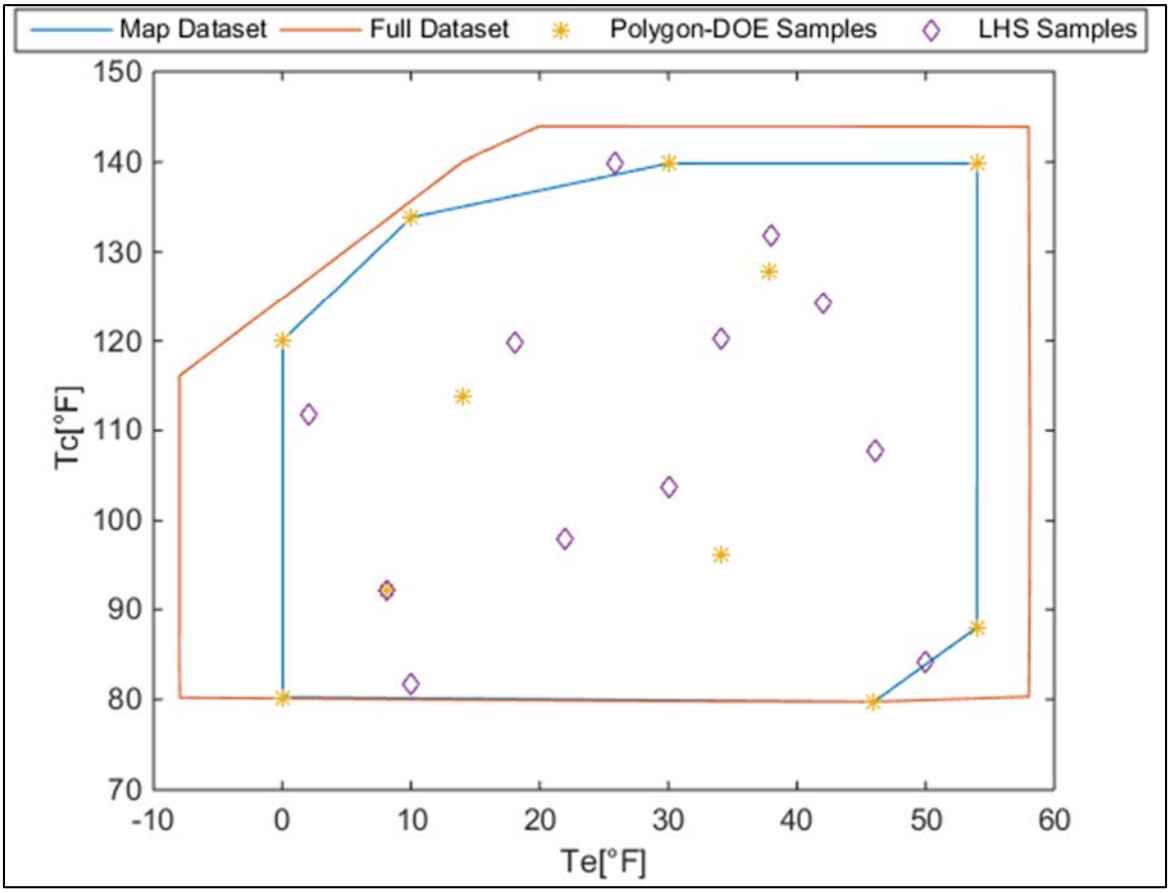

Figure 54: Comparison of samples generated using PDOE and LHS methods from a subsequent run

8.2 Analysis of Different Methods

The four data representation methods discussed in previous sections were analyzed with regards to the number of samples used in generating the performance map. The number of samples that were tried were [8, 10, 12, 14, 16]. Appropriate models were chosen for the different number of samples. For example, the AHRI-540 model requires a minimum of 11 points and so it cannot be used with 8 and 10 samples. Furthermore, comprehensive data sets were available for three

separate compressors. These datasets were analyzed separately from the normal (limited) data sets.

8.2.1 Analysis of Comprehensive Data Sets

This section presents the comparison of model performance for a different number of sample points. Three comprehensive data sets are available. The plots shown in this section are for a R410A scroll compressor. The verification data points were selected such that they all were inside the operating envelope for the compressor performance map for this compressor model. The total number of verification points was 478.

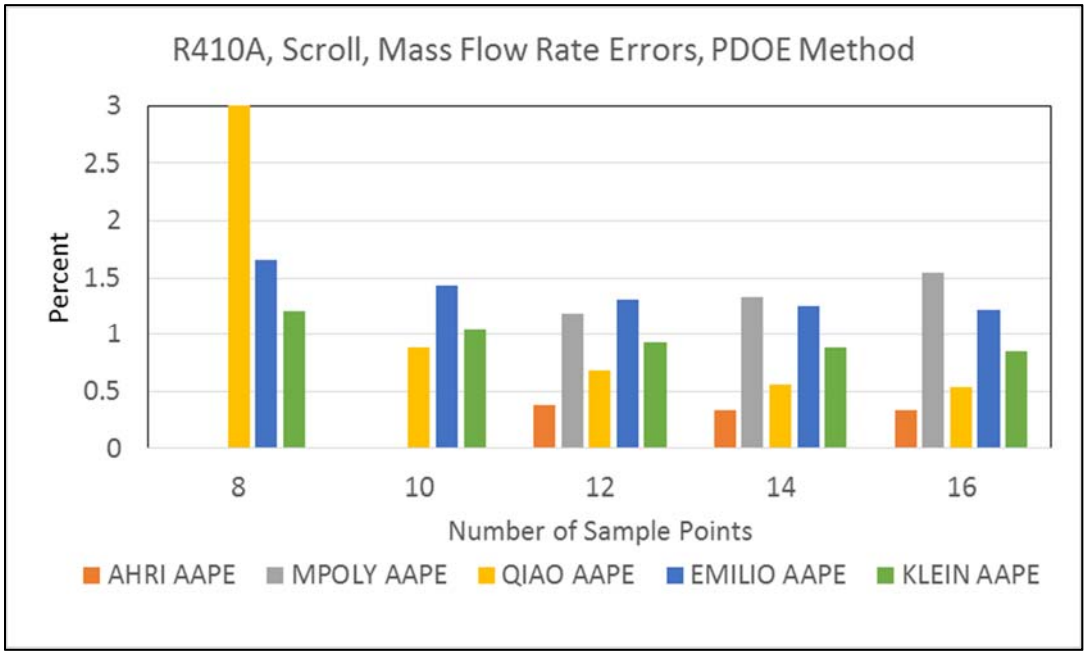

Figure 55: Effect of number of PDOE samples on mass flow rate errors

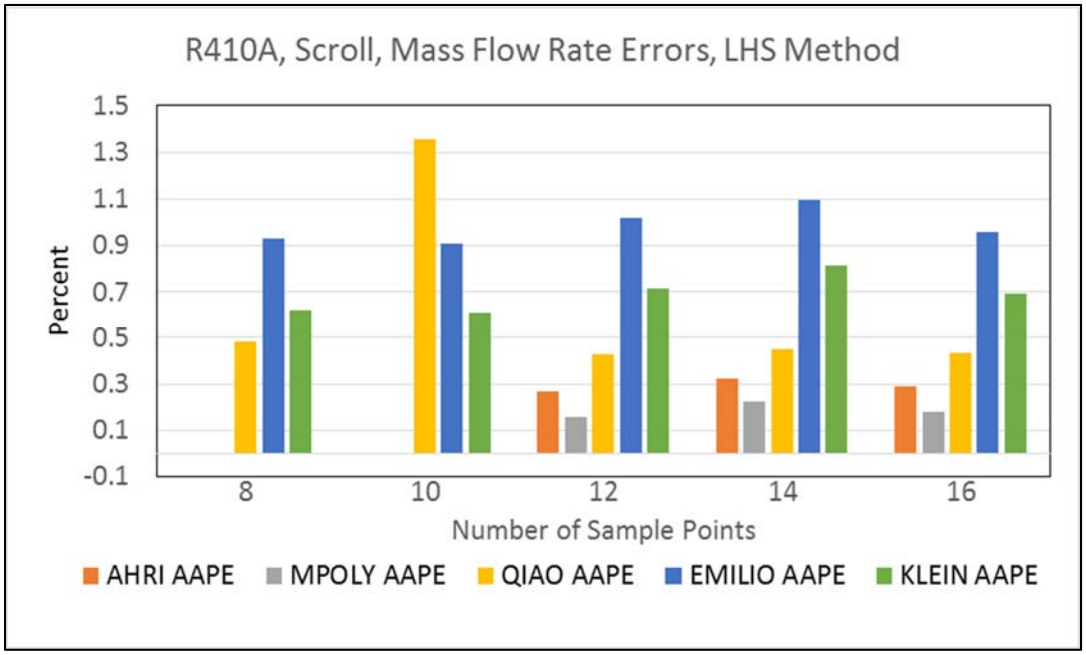

Figure 56: Effect of number of LHS samples on mass flow rate errors

Figures 55 and 56 show the average absolute percent errors in predicted mass flow rate as a function of the different number of samples for different models using the PDOE and the LHS methods. Based on this comparison, it appears that the LHS method provides a much better average prediction performance for a given number of samples. It is very much possible that this performance may change for a different run of the LHS design.

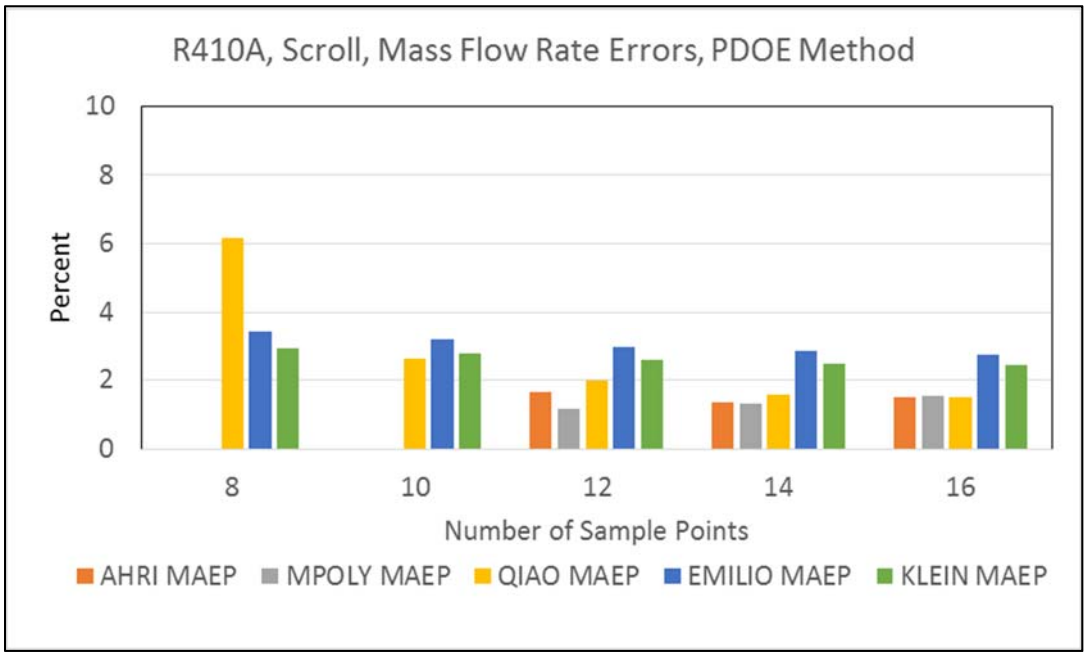

Figure 57: Effect of number of PDOE samples of maximum errors in mass flow rate

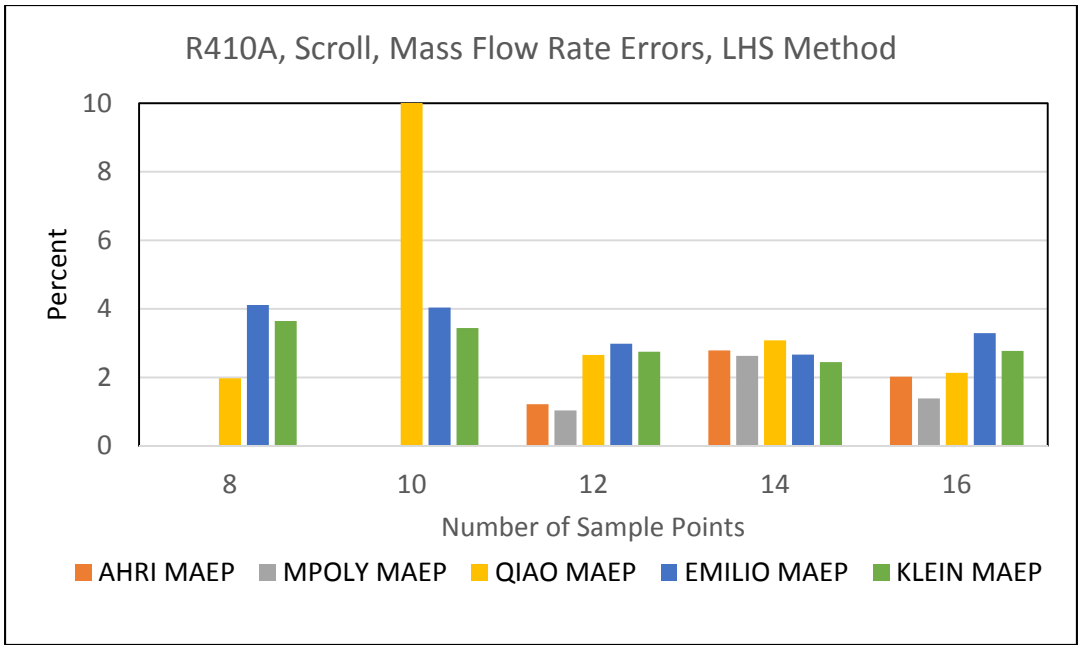

Figure 58: Effect of number of LHS samples on maximum errors in mass flow rate

Figures 57 and 58 show the corresponding results for the maximum absolute percent error in mass flow rate. The error in the QIAO model using 10 samples is more than 20%, but is truncated at 10% in Figure 58. This is also possible due to the random nature of LHS scheme. This shows that while the overall prediction at 10 sample points using the LHS design is better, there are areas within the map where in the local errors are unacceptably high.

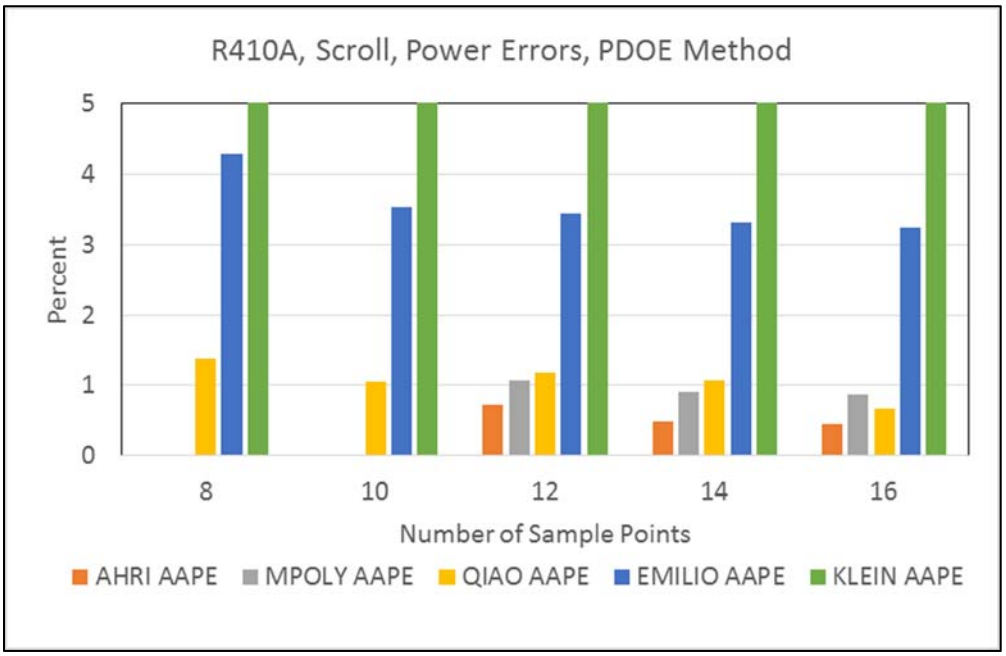

Figure 59: Effect of number of PDOE samples on average error in power

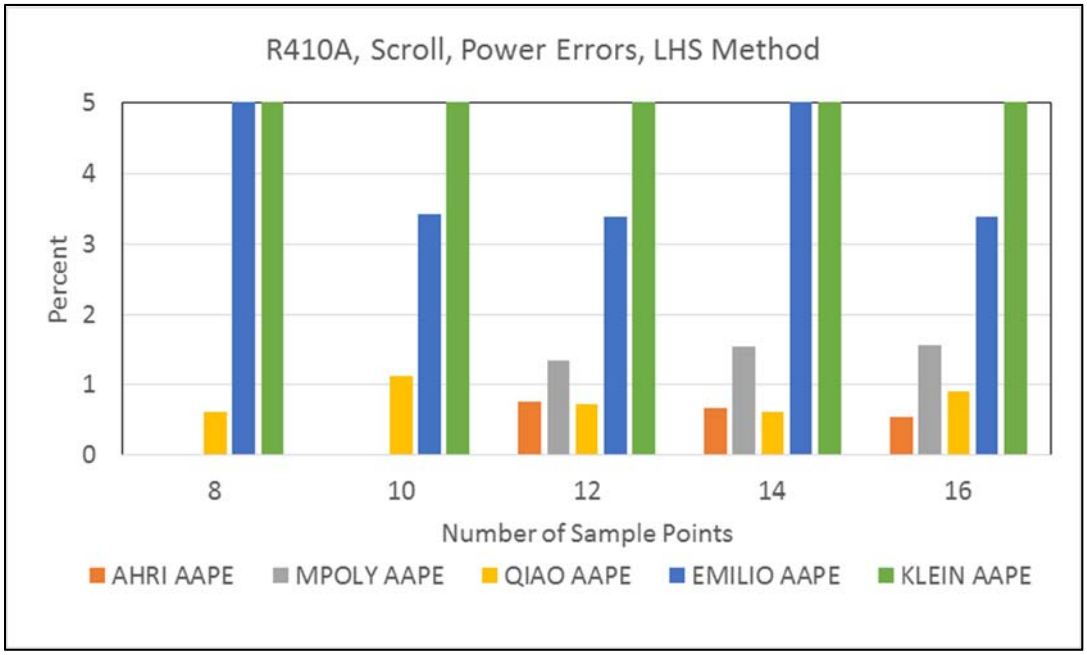

Figure 60: Effect of number of LHS samples on average errors in power

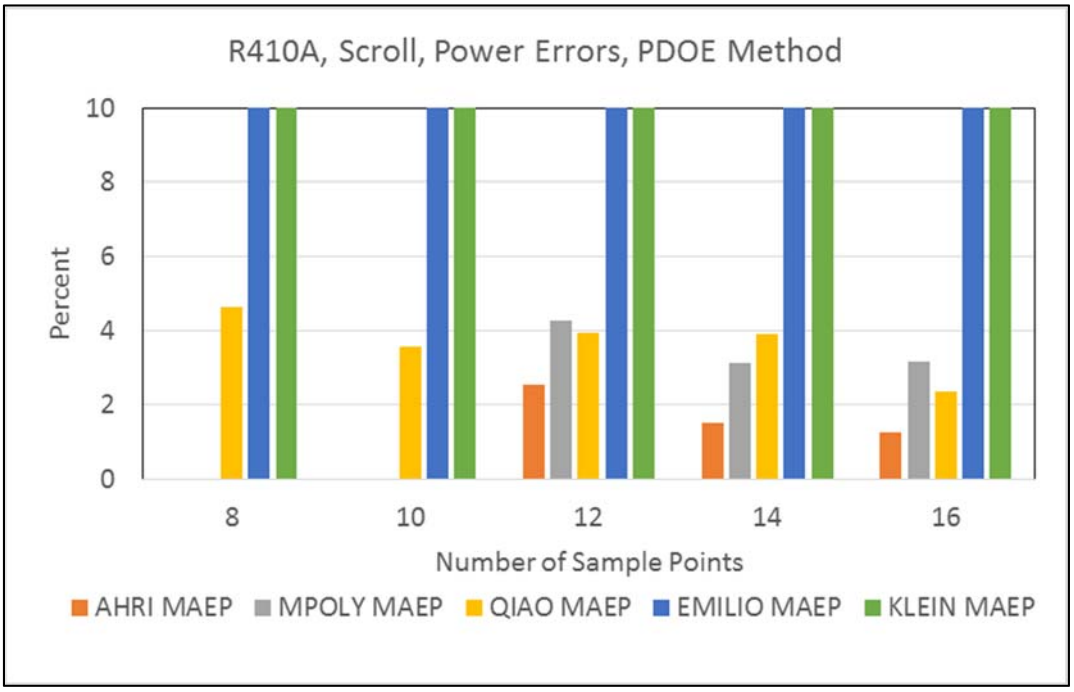

Figure 61: Effect of number of PDOE samples on maximum error in power

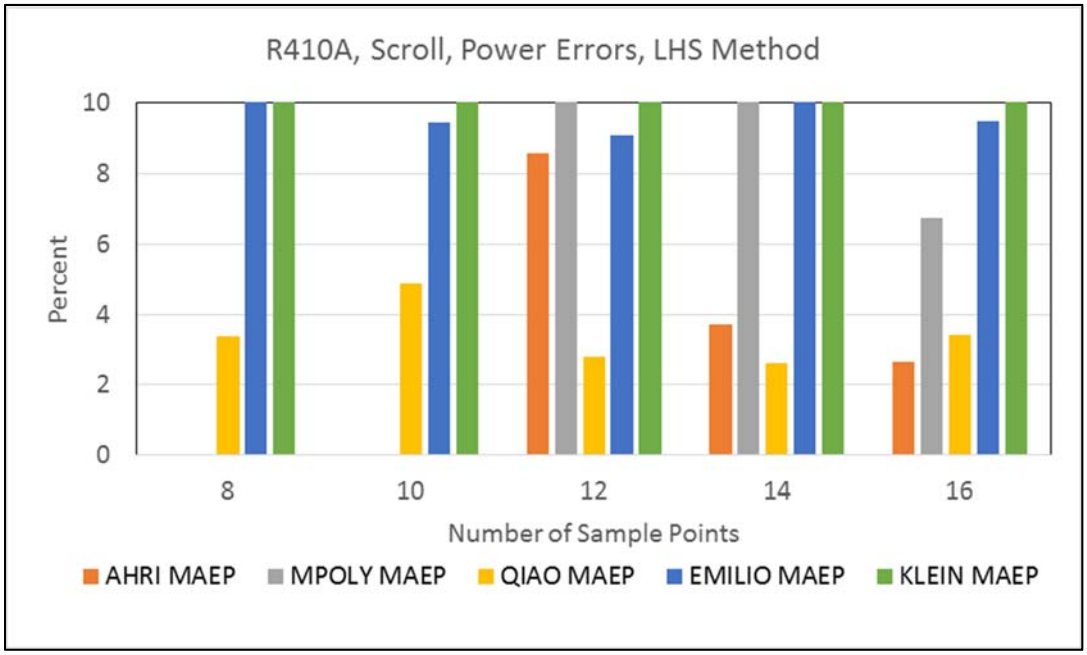

Figure 62: Effect of number of LHS samples on maximum error in power

Figures 59-62 show the corresponding errors in predicted power consumption. The average errors and the maximum absolute errors for the EMILIO and KLEIN models are significantly higher than all of the other models. The scale in the plots is truncated to improve readability. Irrespective of the sampling method, the AHRI540 and QIAO models show average errors below 1%. The maximum absolute errors, on the other hand, are relatively higher. Irrespective of the number of samples and the sampling method, the MAEP in predicted power is less than 5% for the AHRI540, QIAO and the MPOLY model. For the EMILIO and KLEIN models, the maximum absolute errors are more than 30% and, in some cases, more than 100%.

It is important to note here that the AHRI540 and the MPOLY models use independent regression for mass flow rate and power prediction, whereas all the other models use the predicted mass flow rate in the calculation of power consumption. As such, the errors in predicted mass flow rate are indirectly propagated into the power calculation leading to higher errors in predicted power.

In order to put these findings into perspective, the verification errors for the AHRI-540 model based on the default data set are compared to those using the PDOE sampling method with a varying number of points. These errors are shown in Figures 63 and 64. The previously shown results correspond to compressor-B. For this analysis, the AHRI-540 model was fitted with data points that the manufacturer would typically use to develop the performance map and the comprehensive data set was used for verification. Note that only the points within the valid operating envelope were used for verification. It is observed that for the same number of source points as the default data set, there is marginal improvement (less than 0.5 percent points) when systematic sampling is used. But for lower number of samples (e.g. 12, 14), comparable (though still within 0.25 percent points) prediction accuracy in terms of average absolute errors can be achieved by using systematic sampling method with the AHRI-540 model. This true for both mass flow rate and power prediction.

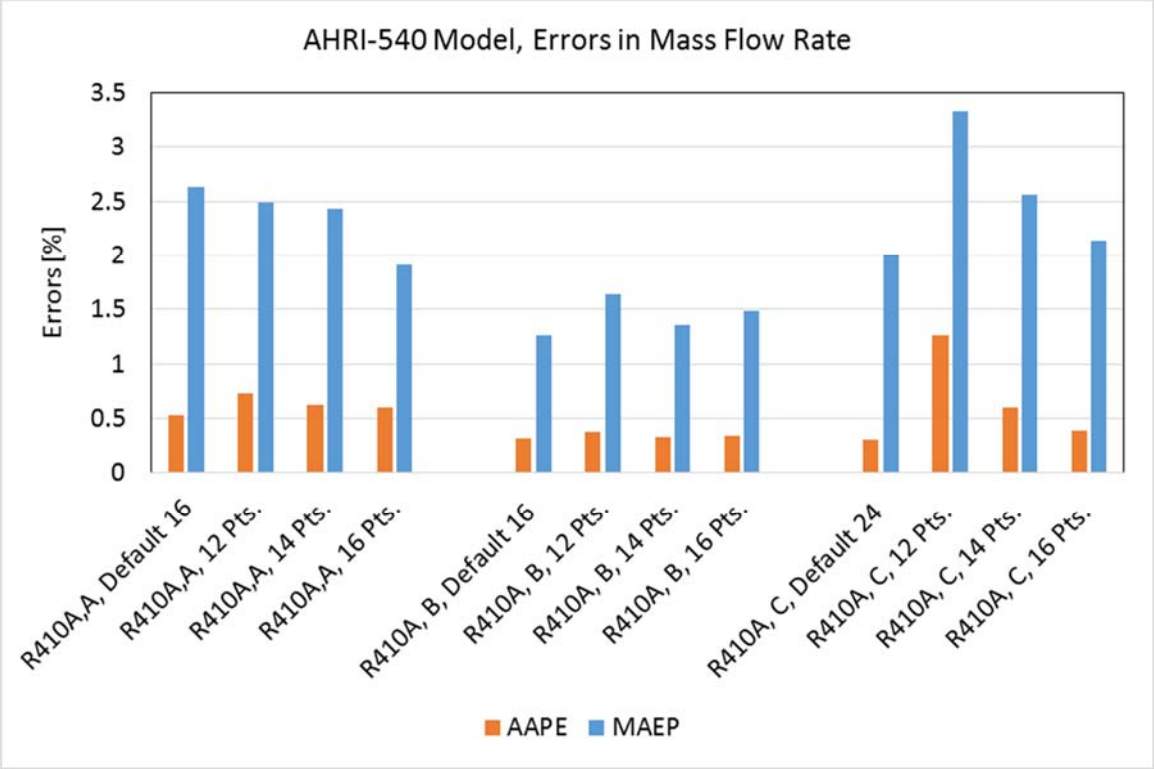

Figure 63: AHRI-540 Model, Errors in mass flow rate prediction with default data set and PDOE sampling

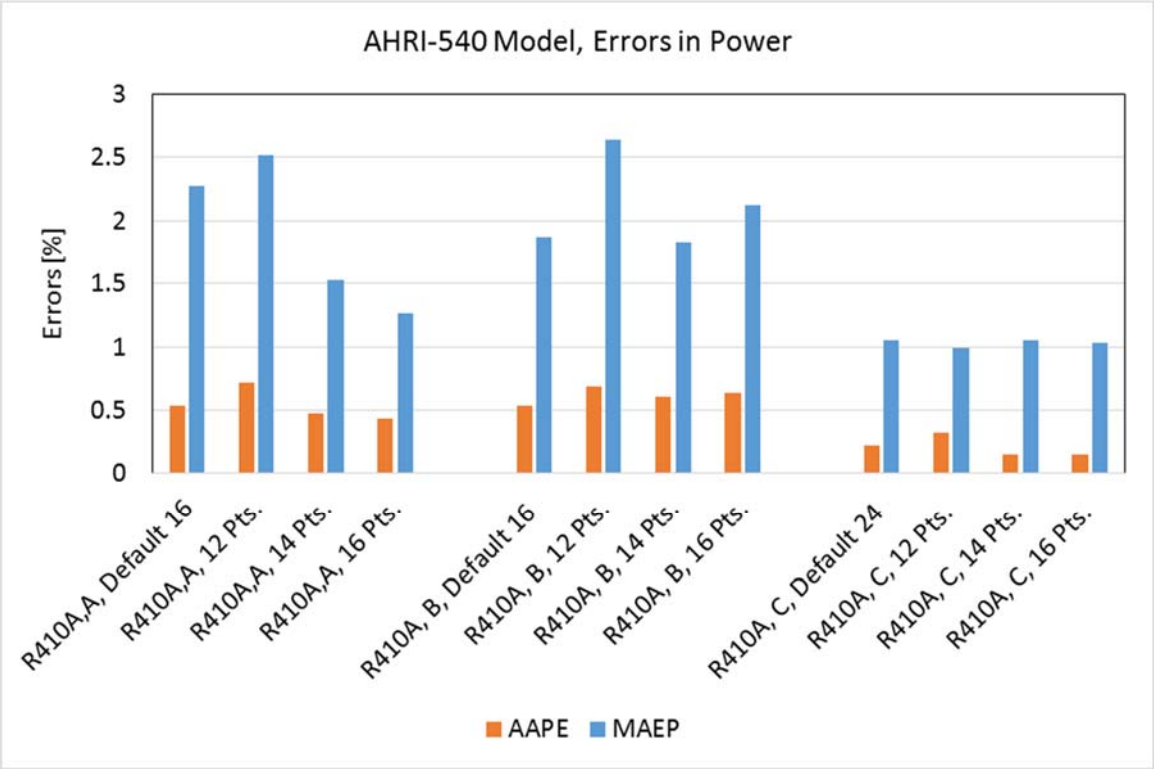

Figure 64: AHRI-540 Model, Errors in power prediction with default data set and PDOE sampling

8.2.2 Analysis of Map Data Sets

In this section, the previously developed sampling methods are used for the map data sets. We note here that this analysis is carried out for the sake of completeness and the results may be not be as reliable as the analysis presented in the previous section.

Each of the 43 compressor data sets has data points ranging from 12 to 50. In this analysis, 12 points are selected out of the available data set using design of experiments. The 12 points always include the convex hull of the operating envelope. The remaining points are selected based on the points that are closest to the center of the operating envelope. This approach was utilized because in this case, the points have already been evaluated and no other experiments can be carried out. To keep the analysis simple, only the AHRI540 and the QIAO model were compared. The results are presented in Figures 65 and 66. The x-axis labels show the compressor dataset name. The first part of this name is the refrigerant (i.e., R134a) and the second part (i.e., R, RO, S) represents the compressor type.

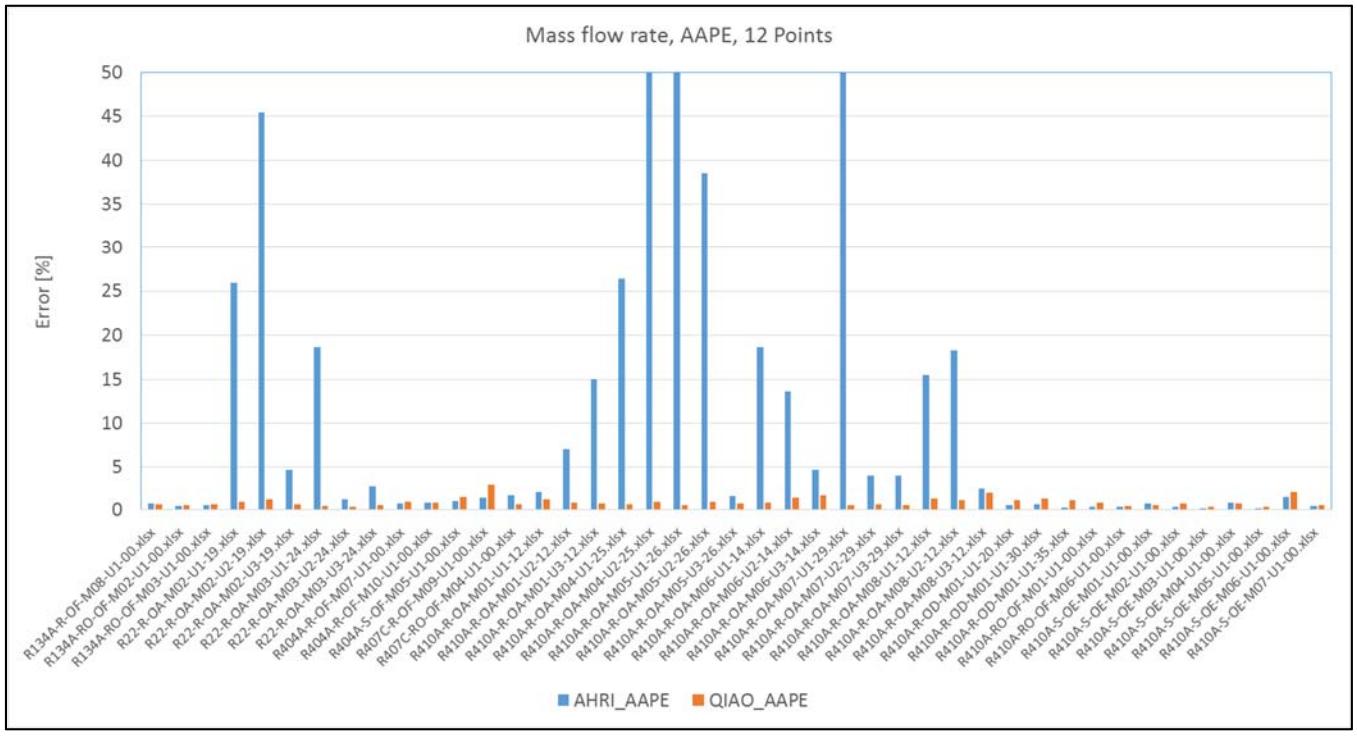

Figure 65: Average errors in mass flow rate prediction for 12 sample points

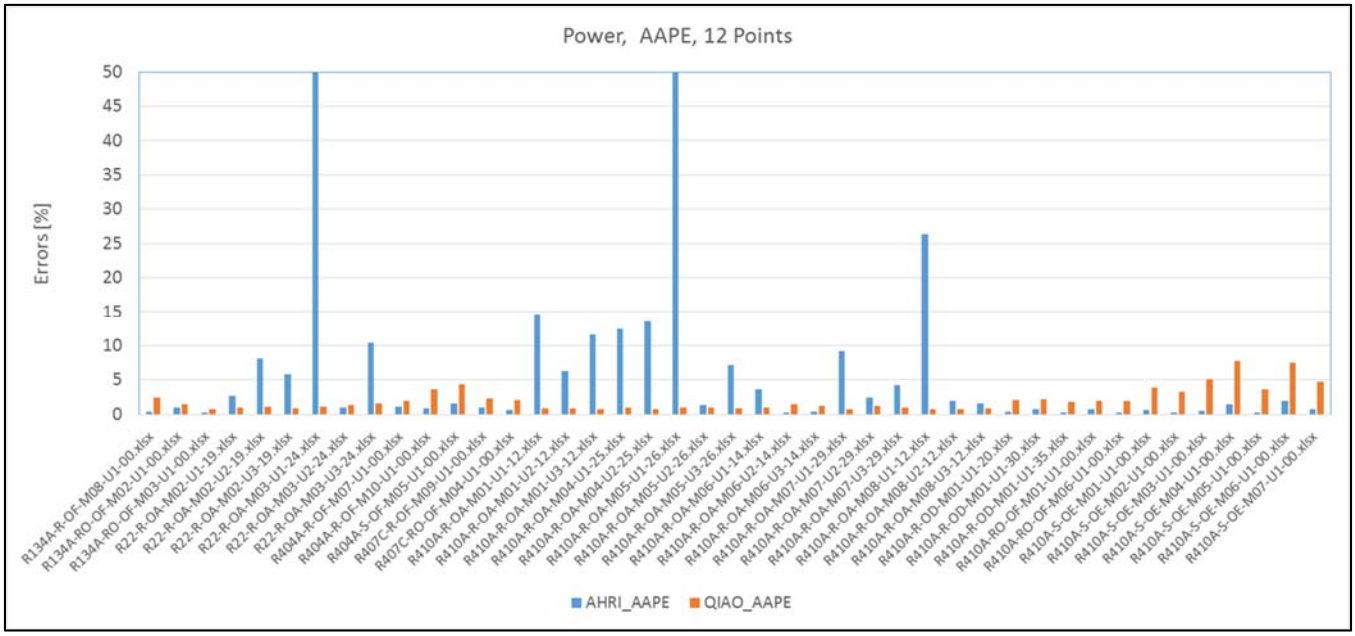

Figure 66: Average error in power prediction for 12 samples points

It can be seen that for several compressor models, the average absolute error in predicted mass flow rate is significantly higher for the AHRI540 model. This is true for the power prediction as well. This is expected, since the minimum number of points required for the AHRI540 model is 11 and with 12 points, there isn't enough information to develop a good regression model. The QIAO model, on the other hand, behaves much better since it requires only 6 data points and is partly physics based. It is also observed that the QIAO model has higher errors as compared to the AHRI540 model for most scroll compressors.

9 Conclusions and Recommendations

Conclusions are summarized in the subsections below and have been organized according to the different tasks conducted for Project 8013 completion. Note that additional queries regarding the analysis conducted for this project were addressed through a series of Project Update Meetings with the Project Committee. For completeness, responses to questions received that are not otherwise addressed in the report herein, are provided in Appendix D.

9.1 Manufacturer Survey

Most manufacturers indicated that more than 14 points were tested to develop the compressor performance map as per the AHRI540 standard. Most manufacturers also account for the unit to unit variation by testing at least three separate units for the same compressor model.

9.2 Uncertainty Analysis

There are several sources of uncertainty in the prediction of compressor performance using maps or models.

The most important amongst them are the uncertainty due to measurement and the uncertainty due to regression during model development. The measurement uncertainty has been quantified

in the literature. The regression uncertainty was studied in the present work for the AHRI540 model. The worst case maximum absolute error in predicted mass flow rate across all data sets was 17% and that for power was 9%. For most compressors, the high errors occur in the region of the envelope with low suction and low discharge dew point temperatures. The average uncertainty in power prediction can be as high as 5% and that in mass flow rate prediction can be as high as 4%.

9.3 Comprehensive Analysis of AHRI540 Method

Three data sets were available for comprehensive comparison of the AHRI540 model predictions over the entire operating envelope and beyond (for extrapolation). It was observed that within the operating envelope, the AHRI540 model predicted the mass flow rate and power within an average error of 1%. But for extrapolated areas, (10°F outside the operating envelope on suction and discharge dew point), the worst case errors were as high as 9% in power and 8% in mass flow prediction. This indicates that the AHRI540 performance map is not suitable for extrapolation purposes.

9.4 Method of Performance Representation

A comprehensive literature review was conducted to identify easy-to-use equations for compressor performance representation. A total of five methods were analyzed: AHRI540 (baseline), MPOLY, QIAO, KLEIN and EMILIO.

It should be noted that for the following conclusions, the model was used to predict source data, which was used to develop the model in the first place. Strictly speaking, a good regression model should predict the source data within 0.5% and reproduce the trend at the same time.

For most of the data sets, the average errors in mass flow rate prediction were better than 2% for the AHRI540, MPOLY and QIAO models. The maximum absolute errors were of the order of 2.5% for the three models.

Significant numerical challenges were encountered during regression for the KLEIN and EMILIO models. For these models, the average errors in mass flow rate predictions were of the order of 3%, but the maximum errors were more than 7%. In the case of power prediction, the AHRI540 and MPOLY models showed average errors of 3%, the QIAO model had errors around 4% and the KLEIN and EMILIO models exhibited errors greater than 15%.

The error metrics were also analyzed with regards to compressor type, compressor capacity and refrigerants. In general, the QIAO and the MPOLY models were more suited for rotary and reciprocating compressors than scroll compressors.

9.5 Effect of Superheat

As per the AHRI-540 standard, the source data is based on a fixed superheat value of 20°F. But in actual use, superheat values can vary. The models were analyzed to evaluate the effect of superheat on the power and mass flow rate prediction. Four data sets were available, each with 20°F and 40°F superheat data. It was found that the AHRI540 model had large (~6%) errors in prediction of mass flow rate at 40°F superheat, whereas the other models, which are mainly physics-based, showed lower (~3%) errors. The density-based correction proposed in the literature was applied to the AHRI540 model and it was found that the predictions were

acceptable. The errors in power prediction for the AHRI540 model were lower than 2%, even without correction, and were found to be acceptable. For the other models, a strong (approximately linear) correlation was observed between the errors in mass flow rate prediction and the ratio of suction densities. Similar correlation was observed in the case of power for the KLEIN and EMILIO models as well. There was no obvious correlation between the power errors and any input parameters for the case of the QIAO model, however this relationship needs further investigation.

9.6 Effect of Sample Size

Based on the manufacturer survey, at least 14 test points are used develop the AHRI-540 compressor performance map. It is desired to reduce this testing effort. The physics-based models such as QIAO, EMILIO and KLEIN require less than 8 points for model development. A study was conducted to evaluate the effect of sample size on the prediction capabilities for the various models. Three comprehensive datasets were available for this purpose. The number of points tested included [8, 10, 12, 14, 16] points. The number of tests points used for model verification was more than 475 for each data set and all were inside the operating envelope. The AHRI540 and the MPOLY models cannot be developed with less than 11 points.

One of the challenges was the selection of samples from the operating envelope. The conventional Latin Hypercube Sampling (LHS) method was used. A new method (PDOE) from the literature for sampling on non-rectangular domains was also implemented.

For the case of mass flow rate, it was found that the LHS method yielded average errors lower than 2% for all the sample sizes. However, the maximum absolute errors in mass flow rate were higher when there were a lower (<= 10) number of samples. In general, both the LHS and PDOE methods yielded similar errors for all models for samples sizes of 12, 14 and 16. Thus, for mass flow rate, it is possible to build a model with 12 systematically selected test points.

For power prediction, the average error for LHS and PDOE methods using AHRI540, QIAO and MPOLY was lower than 2% for all sample sizes. The KLEIN and EMILIO models exhibited significantly high errors. The maximum absolute errors in power prediction were less than 4% for the QIAO and MPOLY models for both sampling methods. The errors for 8 samples were slightly higher. But in general, the errors were of similar magnitude for 12, 14 and 16 samples. For some cases with the LHS method, the errors were unusually high, due the random nature of the algorithm.

A similar analysis was carried out on the 43 data sets that included only the points used to generate a map. In this case, only 12 points were selected and the errors were computed. It was observed that the QIAO model exhibited excellent prediction capabilities compared to the AHRI540 model. This is obvious since the QIAO model is physics-based and requires only 6 points for fitting; hence, 12 points provide sufficient information for a good regression. It was observed, however, that for most scroll compressors, the QIAO model exhibited higher errors than AHRI540 model.

9.7 Recommendations

Based on the results of the analysis conducted for this Project, the following observations and recommendations are made to improve compressor data representation:

1. Reducing the measurement uncertainty is important. Particular attention must be paid during measurements involving low suction and low discharge dew point temperatures.
2. The regression uncertainty has an additive effect on the overall model prediction when the measurement uncertainty is factored into the overall model uncertainty. As such, it is possible to define a lower bound on the expected uncertainty in model prediction. Higher bounds may be possible depending on the availability of data.
3. In order or reduce the regression uncertainty, numerically stable and linearly regressed models should be selected, though this is not always possible for a physics-based power prediction model. Mass flow models can be adapted to linear regression.
4. There is potential for reducing the number of tests used to develop the performance map for a compressor. In general, for the models analyzed as a part of this work, a sample size of 10 or 12 is recommended. This requires additional verification.
5. The use of a systematic DOE method is recommended for selection of samples once an operating envelope is determined. It should be noted, however, that most DOE methods are designed to work with rectangular-domains.

9.8 Potential Future Work

Analysis and findings from the present study identify several areas for future work, including the following:

1. The data available for analyses in this project was sufficient but not ideal. A comprehensive dataset would include test data for each compressor, based on different refrigerants, varying superheats and a wide operating envelope beyond the actual operating envelope. This will assist in calibrating physics-based models that typically require less than 10 test points and can be used for extrapolation.
2. In the present analysis, all of the available data was based on the standard superheat. It is possible to develop a test matrix with less than 16 points that will also be suitable for different superheat values and for reasonable extrapolation. Such a test matrix would involve tests at multiple suction superheat values.
3. A systematic DOE approach should be used when selecting points for model calibration (i.e., performance representation). Adaptive DOE methods are available in the literature that can improve model accuracy for the same number of tests. The drawback is that the tests need to be carried out in two or three steps and require model calibration in between the tests.

10 References

Abdelaziz O., and Shrestha, Som, 2013, Development of Versatile Compressor Modeling using Approximation Techniques for Alternative Refrigerants Evaluation, Manuscript to be published at ASHRAE 2014 Conference.

ANSI/AHRI., 2004. Standard for Performance Rating of Positive Displacement Refrigerant Compressors and Compressor Units. Standard 540. Arlington, VA: AHRI.

Aprea, C; Renno, C; Experimental model of a variable capacity compressor, International Journal of Energy Research 33 (2009) 29 – 37.

Arora, C.P.; Refrigeration and Air-Conditioning, Tata McGraw-Hill (2009).

ASHRAE, 2012, ASHRAE Handbook: HVAC Systems and Equipment, Atlanta, GA: ASHRAE.

Aute, V., Abdelaziz, O., Azarm, S., Radermacher, R. 2008, Cross-validation Based Single Response Adaptive Design of Experiments, 12th AIAA/ISSMO Multidisciplinary Analysis and Optimization Conference, Victoria, British Columbia, Canada10 - 12 Sep 2008.

Castaing-Lasvignottes, Jean; Gibout, Stephane; Dynamic simulation of reciprocating refrigeration compressors and experimental validation, International Journal of Refrigeration 33 (2010) 381 – 389.

Chen, Y., Halm, N.P., Groll, E.A., and Braun, J.E., 2002 (1), Mathematical modeling of scroll compressors – part I: compression process modeling, International J. of Refrigeration, 25, pp. 731-750.

Chen, Y., Halm, N.P., Braun, J.E, and Groll, E.A., 2002 (2), Mathematical modeling of scroll compressors – part II: overall scroll compressor modeling, International Journal of Refrigeration, 25, pp. 751-764.

Coleman, H. W., and Steele, W. G., 2009, Experimentation, Validation and Uncertainty Analysis for Engineers, Third Edition, John Wiley and Sons.

Dabiri A. E., and Rice, C. K., 1981, A Compressor Simulation Model with Corrections for the Level of Suction Gas Superheat, ASHRAE Transactions, V. 87, Pt. 2.

Draguljic D, Santner TJ, Dean AM. 2012, Noncollapsing Space-Filling Designs for Bounded Nonrectangular Regions, Technometrics 2012; 54(2):169–178.

Duprez, Marie-Eve; Dumont, Eric; Frere, Marc; Modeling of reciprocating and scroll compressors, International Journal of Refrigeration 30 (2007) 873 – 886.

Jahnig, Dagmar; Klein, S.A.; Reindl, D.T.; A semi-empirical method for modeling reciprocating compressors in household refrigerators and freezers (1999). MS Thesis.

Lee, Tzong-Shing; Liao, Ke-Yang; Lu, Wan Chen; Evaluation of the suitability of empirically based models for predicting energy performance of centrifugal water chillers with variable chilled water flow, Applied Energy 93 (2012) 583 – 595.

Lekivetz, R. and Jones, B., 2014, Fast Flexible Space-Filling Designs for Nonrectangular Regions, Research Article, Quality and Reliability Engineering International, DOI:10.1002/qre.1640.

Li, Wenhua; Simplified steady state modeling for hermetic compressors with focus on extrapolation, International Journal of Refrigeration 35 (2012) 1722 – 1733.

Mackensen, A., Klein, S. A., Reindl, D. T., 2002, Characterization of Refrigeration System Compressor Performance, International Refrigeration and Air Conditioning Conference at Purdue, July 2002.

Myers R. H., and Montgomery, D. C., Response Surface Methodology: Process and Product Optimization Using Designed Experiments (Wiley Series in Probability and Statistics).

Navarro, E.; Granryd, E.; Urchueguia, J.F.; Corberan, J.M.; A phenomenological model for analyzing reciprocating compressors, International Journal of Refrigeration 30 (2007), 1254 – 1265.

Prakash, R. and Singh, R.; Mathematical Modeling and Simulation of Refrigerating Compressors. International Compressor Engineering Conference. Paper 132, (1974).

Qiao, Hongtao; Kwon, Laeun; Aute, V; Radermacher, R; Transient Modeling of a Multi-evaporator Air Conditioning System and Control Method Investigation, IEA Heat Pump Conference (2014).

Rasmussen B.D., Jakobsen A., 2000, A Review of Compressor Models and Performance Characterizing Variables, International Compressor Engineering Conference, Paper 1429.

Sacks, J., Welch, W. J., Mitchell, T. J., and Wynn, H. P., 1989, Design and Analysis of Computer Experiments, Statistical Science, Vol.4, No.4, pp. 409–435.

Shao S.; Shi, W; Li, X.; Chen, H.; Performance representation of variable speed compressor for inverter air conditioners based on experimental data, International Journal of Refrigeration 27 (2004) 805 – 815.

Staley, D.M.; Bullard, C.W.; Crawford, R.R.; Steady state performance of a domestic refrigerator using R-12, R-134, Project 12, Air Conditioning and Refrigeration Center, University of Illinois, Urbana.

Wang, G. G. and Shan, S., 2007, Review of metamodeling techniques in support of engineering design optimization, Journal of Mechanical Design, Transactions of the ASME, 129(4), 370-380.

Winandy, Eric; Saavedra O.; Lebrun, Jean; Experimental analysis and simplified modeling of a hermetic scroll refrigeration compressor, Applied Thermal Engineering 22 (2002) 107-120.

Winkler, J. M., 2009, Development of a Component based Simulation Tool for the Steady State and Transient Analysis of Vapor Compression Systems, PhD Dissertation, University of Maryland College Park.

Zhao, Ling Xiao; Zhang, Chun Lu; Gu, Bo; Neural Network based polynomial correlation of single and variable speed compressor performance, HVAC&R Research, Volume 15, Number 2, 2009.

Zhao, Ling Xiao; Shao, Liang; Zhang, Chun Lu; Steady state hybrid modeling of economized screw water chillers using polynomial neural network compressor model, International Journal of Refrigeration 33 (2010), 729 – 738.

Appendix A: Scope of Work

The specific tasks for this project were defined as follows in the proposal prepared by OTS:

Task 1: Identify, Collect, and Characterize Representative Data

Approach

Using AHRI and OTS resources, OTS will identify pertinent performance metric data needed for review and analysis and collect such data from various manufacturers for multiple compressor types. Note that it is important that multiple data sets for each compressor type from different manufacturers are included in the analysis. It is expected that AHRI and manufacturers on the project monitoring subcommittee will assist in providing data. All data used in the analysis will be made anonymous.

In addition to performance data, OTS will conduct an informal survey with several manufacturers regarding the process used to develop their performance coefficients.

Task Details

This task will include the following sub-tasks:

a. Evaluate existing compressor performance data. Determine additional needs.
b. Reach out to industry contacts to obtain more compressor performance data, as required.
c. Conduct an informal survey of at least three compressor manufacturers to understand the methods used to develop and issue performance data.

Deliverables

There are no direct deliverables for this task. A summary of findings will be provided as part of the draft technical report issued at the completion of Task 3. Updates will be provided in the regular monthly reports.

Task 2: Review Uncertainty Sources and Recommend Methods to Estimate Uncertainties in Test Data

Approach

Using the data collected in Task 1, OTS will evaluate the potential uncertainty sources and values stemming from measurement uncertainty and product to product variation. OTS will use established techniques (Coleman and Steele, 2009; Taylor, 1997) for uncertainty analyses.

Task Details and Features

This task will include the following sub-tasks:

a. Review *ANSI/AHRI Standard 540-2004: Performance Rating of Positive Displacement Refrigerant Compressors and Compressor Units*.
b. Determine potential sources of uncertainty including, but not limited to, measurement uncertainty and product to product variation.
c. Using data collected in Task 1, quantify the level of uncertainty for each identified source.
d. Based on calculated results, develop a general methodology and/or guideline for estimating uncertainties of product performance.

Deliverables
There are no direct deliverables for this task. A summary of findings will be provided as part of the draft technical report issued at the completion of Task 3. Updates will be provided in the regular monthly reports.

Task 3: Survey and Evaluate Alternative Methods to Represent Data
Approach
Using the data collected from Task 1, and additional uncertainty information gathered in Task 2, OTS will identify and evaluate up to three alternative methods to represent compressor performance data. The alternative methods will include a mix of black-box (map-based) and efficiency based models described in Section I.B.6. Examples of each potential method will be developed using actual data collected in Task 1. The accuracy of each method will be evaluated based on the number and distribution of test points.

Task Details and Features
This task will include the following sub-tasks:

a. Identify potential alternative methods to represent data.
b. Evaluate potential methods using sample data collected in Task 1 and regression analysis.
c. Determine method accuracies based on the number and distribution of test points. The overall method accuracy can be quantified using regression errors. The effect of the number and distribution of various points will be evaluated using statistical techniques of bootstrapping (recursive sampling) and cross-validation (Aute et al, 2008). The cross-validation results will assist in finding data points that can be omitted without affecting the prediction accuracy.

Deliverables

a. Reference implementation code (in Matlab or C++, to be decided later) for each of the data representation method that is evaluated.
b. Draft technical report outlining the results and recommendations for Tasks 1, 2, and 3. This report will be further updated pending completion of Task 4 and feedback from the project monitoring subcommittee.
c. Web meeting to review the draft technical report and progress to date.

Task 4: Recommend a Preferred Method to Develop and Represent Data
Approach
With feedback from the project monitoring subcommittee and web meeting following Task 3, OTS will further develop one of the methodologies identified in Task 3 to provide a final recommendation on how best to develop and represent compressor performance data. Additional analysis and example generation will be conducted, to the extent required. One iteration of this final recommendation may be pursued upon receipt of additional feedback from the project monitoring subcommittee.

Ultimately, it would be best if the proposed methodology could be experimentally tested and validated. This would require cooperation of at least one compressor manufacturer. OTS would

propose a test matrix for the manufacturer to complete. Results would then be used to validate and further improve the proposed methodology. Experimentation would preferably be conducted twice: once for the initial data set provided and again for model verification.

Task Details and Features
This task will include the following sub-tasks:

a. Further develop the most promising method identified during Task 3. This will involve analyzing various design of experiments methods for use with the prediction model identified in Task 3.
b. Develop sample calculations that demonstrate the use of the predictions from the promising method in uncertainty estimation. The uncertainty estimation guidelines are proposed in Task 2 of this proposal.
c. Present recommendations in an updated technical report and review with the project monitoring subcommittee.
d. Revise the recommended method and technical report as per subcommittee feedback. Incorporate experimental validation results, if available through assistance from AHRI and committee compressor manufacturer(s).

Deliverables

a. Source code for reference implementation (Matlab or C++), for algorithms used to analyze the various representation methods.
b. Final technical report. An updated draft technical report will be provided after the completion of Task 4. Once reviewed by the project monitoring subcommittee, the report will be revised, as necessary, in order to produce the final technical report.
c. Two web meetings. The first web meeting will be conducted once the final methodology recommendation and updated draft technical report are developed. As noted above, the recommended methodology and technical report will then be updated, as necessary, based on feedback received during the first web meeting. A second web meeting will then follow to review the final recommendations and project deliverables.

Task 5: Project Management
Approach
OTS will provide monthly update reports, along with invoices, summarizing progress and task results to date. As appropriate, web meetings will be held with the AHRI team to review progress and share preliminary results and issues needing discussion. A kick-off meeting will be held at the start of the project to review overall approach and expectations. A close-out meeting will be held at the end of the project to review completed actions and any required steps moving forward. Our budget accounts for a total of four web meetings with AHRI over the course of the project.

As noted in the RFP, a technical journal article or technical presentation/paper of progress or final results may be desired for presentation at a U.S.-based conference. Should this be requested, OTS will modify the final technical report, as appropriate, to meet this request. No additional charge would be incurred for adding this task to the project.

Deliverables

a. Monthly invoices and summary reports indicating progress and task results to date.
b. A total of four web meetings: 1) project kick off; 2) completion of Task 3; 3) initial review of recommendations developed out of Task 4; and 4) completion of Task 4/project close out. As required, meeting notes will be issued in the form of a bulleted summary and action item list in a follow-up email to team members.
c. A technical journal article or conference paper, at the request of AHRI pending project progress and results.

Appendix B: Compressor Data Parameters

Data sets provided to OTS for project analysis included the following parameters:

Table 11: Parameters included in data sets requested for Project 8013 analysis

Parameter	Description
Compressor Type	Type of Compressor
Manufacturer	Identifier; does not have to be a real manufacturer name
Model	Can be real model number, or just an identifier
Application	Alphanumeric code to represent the application as described in 540.
Displacement	Numeric , theoretical/geometrical swept volume
Clearance Volume	Numeric, could be an estimate, or an average value
RPM	Numeric
Refrigerant	Refrigerant name as per ASRHAE Refrigerant nomenclature standard.
Unit	Unit of the same model, if multiple units of the same model are tested (indicate 0,1,2,…)
Test	Test number, if multiple tests are conducted on the same unit of the same model.
Tdew_Suction	Suction dew point
Tdew_Discharge	Discharge dew point
Suction_Superheat	Suction superheat (delta-T)
Discharge_Superheat	Discharge superheat (delta-T)
Discharge Shell Temperature	Shell temperature as measured.
P_Suction	Suction Pressure as measured
P_Discharge	Discharge pressure as measured
Power_Input	Power Input, as measured
Isentropic Efficiency	Compressor efficiency, as calculated from measured data
Massflow Rate	Mass flow rate, as measured
Current	Current , as measured
Capacity	Capacity, as calculated from measured data
Motor Efficiency	Motor efficiency if known.
T_Uncertainty	Uncertainty in temperature measurement, if available
P_Undertainty	Uncertainty in pressure measurement
M_Uncertainty	Uncertainty in mass flow measurement
A_Uncertainty	Uncertainty in Current measurement
Ambient Temperature	
Oil Circulation Ratio/Rate	
Purity of Refrigerant	Blend composition, variation from the standard.
Capacity Value	
Tdew_Suc_Min	Minimum suction dew point for which map is valid
Tdew_Suc_Max	Max suction dew point for which map is valid

Tdew_Dis_Min	Mininum discharge dew point
Tdew_Dis_Max	Max discharge dew point
Suction_Superheat	Suction superheat, as maintained during testing for each point in the map data
Discharge_Superheat	discharge superheat
Power Coefficients	
Mass Flow Rate Coefficients	
Capacity Coefficients	
Current Coefficients	

Appendix C: Manufacturer Survey Summary

A total of six responses were received and are summarized for each of the survey questions below.

Table 12: Manufacturer survey questions and results

Question	Summary of Responses Received
What data reduction equations are used?	AHRI Standard 540 10-coefficient polynomial
How many test points are used to generate the compressor data map?	Five of the six manufacturers indicated that they used at least 14 points. One manufacturer uses between 5 and 10 points.
How many total tests are conducted for a single compressor model? Are all these tests conducted for the same unit?	One manufacturer reported 150 tests over 3 units. Two manufacturers indicated that 38 tests were performed per compressor model. The other three indicated between 5 and 14 tests per model.
How many units of the same model type are tested?	One manufacturer tests three units of the same model. The other five use results from one unit only.
How are the test points generated (grid, DOE)?	Two manufacturers use a grid. The others use the rating points for the particular compressor model.
For extreme envelope operating conditions, how is the data generated?	One manufacturer uses extrapolation for low evaporating and high condensing temperatures, while another uses extrapolation only for points within 5K from a point at which measurement has been taken. The other manufacturers reported testing at points near the envelope boundaries and do not use extrapolation.
How are the end-points of the envelope determined? Are these end-points application specific? Are these end-points manufacturer specific?	All manufacturers reported that the compressor envelope was application specific. One manufacturer performs reliability tests to determine the envelope.
What kind of validation is conducted, if any, for extrapolated data points? Are these points simulated or experimentally tested?	All manufacturers indicated that there is no validation performed for extrapolated points.
How is data shifted, if at all, through the two rating points (for Unitary AC)?	One manufacturer reported that the data could be skewed to the rating points by repeating the data for those points in the data reduction process. Another indicated that data may be shifted directly through the two rating points or by shifting the rating curves a fixed percentage.
What errors, if any, are observed from this process?	Of the two manufacturers responding to the above question, one indicated that the errors at the extremes may increase. The other indicated that errors are calculated for tested vs. predicted values and for tested vs. shifted values.

Is testing done in-house, or at a third party laboratory? If both, what percentage of testing and what type of testing is conducted in-house vs. at a third party laboratory?	All six manufacturers reported testing done in-house.
What are typical accuracies of measurement instruments involved?	Responses varied significantly. Ultimately, these responses were not utilized for analysis.
Are there other methods for data reporting or representation your company has recently used or considered?	No other data representation methods were considered.
What is the standard practice in terms of assessing refrigerant purity?	There is no established practice. See the summary presented in Section 4 for additional details.
Please provide any additional comments you would like to share.	None were offered.

Appendix D: Responses to Additional Project Questions Presented by the Project Committee

The following section outlines several comments received from the Project Committee that are not otherwise addressed in the body of the report. Reviewer comments are in Red; OTS responses are in Black.

Have you considered using suction and discharge pressures rather than dew point temperatures as the parameters in the ARI-540 model? If so, is there any improvement?
>> There is no improvement across the board. This can also be deduced based on the logarithmic (or a rational-polynomial) relationship between dew point pressure and temperature. Substituting such relation into the current Temperature based equation essentially yields another polynomial with equivalent coefficients but no improvement in the prediction ability.

Is the comparison made in Section 6.4 comparing each model vs, the source data (in which case AHRI540 would obviously perform well), or against the more extensive validation data set(s)?
>> The comparison is made against the source-data itself. This is mentioned in the two sentences immediately following Table 9. We also agree with the observation that the AHRI540 model would obviously perform well but only for the cases wherein the source data was actually generated by using a fitted polynomial and NOT measured.

The last sentence in Section 6.3.1 indicates the Chebychev polynomials had much better fit measures, but did not represent the underlying physics. AHRI540 also does not represent underlying physics and is pointed out in Section 6.1, that extrapolation can result in significant prediction errors. Does the complexity of using the Chebychev polynomials a prohibitor from working further in that direction? Can you provide some further insight into the forms you evaluated?
>> Between any two given source points, the value of a Chebychev polynomial can practically go to infinity and it can still pass through the two given points. This is the challenge with Chebychev polynomials. Our statement in the report about not representing underlying physics is partially correct in this context. We tried various Chebychev polynomials with different orders, but were not able to find a consistent equation that would represent the given data.

I am somewhat disappointed that a better fitting physics based model with fewer regression terms didn't result from your study. I am also somewhat concerned that your study seems to suggest that 12 data points are sufficient for good model accuracy.
>> We agree with your observation. In the present study, we used all the data that we had available. There is not enough data to calibrate a better fitting physics based model. We have included several physics based models from the literature but their predictions are not as good as we would want them to be. This can be attributed to various factors including measurement uncertainty and limits of repeatability. The suggestion about 12 points implies that these are chosen in a systematic manner based on the underlying equation that you are trying to fit.

A plot of calculated mass flow rate against suction dew point temperature is presented in which the mass flow rate was negative.

>> It is possible for some of the polynomial equations to yield zero or negative values. Typically the higher order (3rd order terms in present case) terms are the ones that cause such behavior. One approach to avoid this is to solve the zero(s) of the resulting polynomial equation and check if the solution lies within the operating envelope.

In our analysis, we investigated this issue in quite a bit of detail. When we analyze Fit statistics for the current 10-coefficient polynomial, it is observed that several of the terms in the fit are not statistically significant. Regression analysis guidelines dictate that such terms should be removed from the fit.

There is an approach in the literature that facilitates the manipulation terms of an equation in an automated fashion. We used this approach to find the statistically "best" equation to represent mass flow rate and power consumption for each of the data sets.

Refer to the fit details for one particular case of fitting mass flow rate shown in Figures 67 and 68. In particular, refer to the column of p-Values in the first case, vs. the second case. Note that the second case has much better p-values and also a lower number of terms in the regression.

```
m =


Linear regression model:
    y ~ 1 + x1 + x2 + x3 + x4 + x5 + x6 + x7 + x8 + x9

Estimated Coefficients:
                    Estimate          SE         tStat      pValue
                    ________    __________    _________    _______

    (Intercept)          102.34        88.365       1.1582    0.28478
    x1                -0.16096        1.2503    -0.12873    0.90119
    x2                -0.91766        2.2476    -0.40829    0.69526
    x3                0.036647      0.020074      1.8256    0.11066
    x4                0.012911      0.015591     0.82805    0.43496
    x5               0.0049519      0.019223      0.2576    0.80412
    x6              -9.3042e-05    0.00016321    -0.57008    0.58645
    x7              -6.9669e-05    8.2666e-05    -0.84278    0.42721
    x8              -4.0026e-05    5.6213e-05    -0.71204    0.49948
    x9              -1.6672e-05    5.4517e-05    -0.30582    0.76864


Number of observations: 17, Error degrees of freedom: 7
Root Mean Squared Error: 0.676
R-squared: 1,  Adjusted R-Squared 1
F-statistic vs. constant model: 4.58e+03, p-value = 2.38e-12
```

Figure 67: Fit details for mass flow rate prediction

```
stp540mdot =


Linear regression model:
    y ~ 1 + x1 + x2 + x1^2 + x2^2

Estimated Coefficients:
                    Estimate        SE         tStat       pValue
                   ___________    _________    _______    __________

    (Intercept)         55.976       7.9864     7.0089    1.4165e-05
    x1                  1.1131      0.09065      12.28    3.7399e-08
    x2                0.031618       0.14281     0.2214        0.8285
    x1^2              0.018691    0.0012286     15.214    3.3053e-09
    x2^2             -0.0019394    0.00062183   -3.1189     0.0088728


Number of observations: 17, Error degrees of freedom: 12
Root Mean Squared Error: 0.626
R-squared: 1,  Adjusted R-Squared 1
F-statistic vs. constant model: 1.2e+04, p-value = 1.71e-21
```

Figure 68: Fit details for mass flow rate prediction, step-wise fit

We investigated various functional forms for mass flow rate and power fitting. As observed from the screenshots below in Figures 69 and 70, there was no consistent equation set applicable to all compressor types and all fluids.

	A	B	C	D	E	F	G	H	I	
1	DataSetNameMdot	Refrigerant	CompType	RowCount	Formula	Rsquared	RMSE	Fstat	pVal_Fsat	mir
2	R134A-R-OF-M08-U1-00.xlsx	R134A	R	y ~ 1 + x1 + x2 + x1^2 + x2^2	17	0.99975	0.625782	12000.51	0	
3	R134A-RO-OF-M02-U1-00.xlsx	R134A	RO	y ~ 1 + x1^2 + x1*x2 + x2^2 + x1^3 + (x1^2):x2	17	0.999916	0.729609	15222.33	0	
4	R134A-RO-OF-M03-U1-00.xlsx	R134A	RO	y ~ 1 + x1^2 + x1*x2 + x2^2	17	0.999903	0.330663	22659.87	0	
5	R22-R-OA-M02-U1-19-cond.xlsx	R22	R	y ~ 1 + x1^2 + x1*x2 + x2^2	16	0.999962	0.69889	53295.06	0	
6	R22-R-OA-M02-U2-19-cond.xlsx	R22	R	y ~ 1 + x1^2 + x1*x2 + x2^2	16	0.999881	1.252931	16872.78	0	
7	R22-R-OA-M02-U3-19-cond.xlsx	R22	R	y ~ 1 + x1^2 + x1*x2 + x2^2 + x2^3	17	0.999979	0.567251	79753.95	0	
8	R22-R-OA-M03-U1-24-cond.xlsx	R22	R	y ~ 1 + x1^2 + x1*x2 + x2^2 + (x1^2):x2 + x1:(x2^2) + x2^3	16	0.99999	0.515737	87369.66	0	
9	R22-R-OA-M03-U2-24-cond.xlsx	R22	R	y ~ 1 + x1^2 + x1*x2 + x2^2	16	0.999979	0.625259	96067.52	0	
10	R22-R-OA-M03-U3-24-cond.xlsx	R22	R	y ~ 1 + x1^2 + x1*x2 + x2^2	16	0.999969	0.751807	65274.42	0	
11	R32-S-OX-M01-U1-00-20F.xlsx	R32	S	y ~ 1 + x1 + x2 + x1^2 + x2^2 + x1^3 + x2^3	59	0.999591	1.020882	21156.96	0	
12	R404A-R-OF-M07-U1-00.xlsx	R404A	R	y ~ 1 + x1^2 + x1*x2 + x2^2 + x1^3 + (x1^2):x2 + x1:(x2^2)	21	0.999707	1.443271	5116.596	0	
13	R404A-R-OF-M10-U1-00.xlsx	R404A	R	y ~ 1 + x1 + x2 + x1^2 + x2^2	17	0.998567	2.006498	2090.78	0	
14	R404A-S-OF-M05-U1-00.xlsx	R404A	S	y ~ 1 + x1 + x2 + x1^2 + x2^2	22	0.998834	3.460825	3641.137	0	
15	R404A-S-OX-M02-U1-00-20F.xlsx	R404A	S	y ~ 1 + x1^2 + x1*x2 + x2^2 + x1:(x2^2)	63	0.99992	1.100794	117215.2	0	
16	R407C-R-OF-M09-U1-00.xlsx	R407C	R	y ~ 1 + x1^2 + x1*x2 + x2^2 + x1^3 + (x1^2):x2 + x1:(x2^2)	18	0.999362	5.043773	1762.466	0	
17	R407C-RO-OF-M04-U1-00.xlsx	R407C	RO	y ~ 1 + x1 + x2 + x1^2 + x1^3	19	0.995935	4.877099	857.4323	0	
18	R410A-R-OA-M01-U1-12-cond.xlsx	R410A	R	y ~ 1 + x1^2 + x1*x2 + x2^2 + x1^3 + (x1^2):x2 + x1:(x2^2) + x2^3	16	0.999984	0.522963	41401.09	0	
19	R410A-R-OA-M01-U2-12-cond.xlsx	R410A	R	y ~ 1 + x1^2 + x1*x2 + x2^2 + x1^3 + (x1^2):x2 + x1:(x2^2)	16	0.999947	0.834186	16642.54	0	
20	R410A-R-OA-M01-U3-12-cond.xlsx	R410A	R	y ~ 1 + x1^2 + x1*x2 + x2^2 + x1^3 + (x1^2):x2 + x1:(x2^2) + x2^3	16	0.999961	0.779769	17118.07	0	

Figure 69: Different equations for mass flow rate predictions

	A	B	C	D	E	F	G	H	I
1	DataSetNamePower	Refrigerar	CompType	RowCount	Formula	Rsquared	RMSE	Fstat	pVal_Fsat
2	R134A-R-OF-M08-U1-00.xlsx	R134A	R	y ~ 1 + x1^2 + x1*x2 + x2^2 + x1:(x2^2)	17	0.99937	4.455534	2645.069	0
3	R134A-RO-OF-M02-U1-00.xlsx	R134A	RO	y ~ 1 + x1^2 + x1*x2 + x2^2 + (x1^2):x2	17	0.999343	7.441265	2535.429	0
4	R134A-RO-OF-M03-U1-00.xlsx	R134A	RO	y ~ 1 + x1^2 + x1*x2 + x1^3 + (x1^2):x2	17	0.999879	1.415466	13785.38	0
5	R22-R-OA-M02-U1-19-cond.xlsx	R22	R	y ~ 1 + x1^2 + x1*x2 + x2^2 + x1^3 + (x1^2):x2 + x1:(x2^2) + x2^3	16	0.9999	4.552624	6677.263	0
6	R22-R-OA-M02-U2-19-cond.xlsx	R22	R	y ~ 1 + x1^2 + x1*x2 + x2^2 + (x1^2):x2	16	0.999563	7.81633	3431.916	0
7	R22-R-OA-M02-U3-19-cond.xlsx	R22	R	y ~ 1 + x1^2 + x1*x2 + x2^2 + x1^3 + (x1^2):x2	17	0.999797	5.299008	6339.753	0
8	R22-R-OA-M03-U1-24-cond.xlsx	R22	R	y ~ 1 + x1^2 + x1*x2 + x2^2 + x1^3 + (x1^2):x2 + x1:(x2^2) + x2^3	16	0.999943	4.151333	11642.89	0
9	R22-R-OA-M03-U2-24-cond.xlsx	R22	R	y ~ 1 + x1^2 + x1*x2 + x2^2 + x1^3 + (x1^2):x2 + x1:(x2^2) + x2^3	16	0.999867	6.364056	5027.801	0
10	R22-R-OA-M03-U3-24-cond.xlsx	R22	R	y ~ 1 + x1^2 + x1*x2 + x2^2 + x1^3 + (x1^2):x2 + x1:(x2^2) + x2^3	16	0.999944	4.159292	11903.03	0
11	R32-S-OX-M01-U1-00-20F.xlsx	R32	S	y ~ 1 + x1^2 + x1*x2 + x2^2 + x1:(x2^2) + x2^3	59	0.999068	13.96728	7806.765	0
12	R404A-R-OF-M07-U1-00.xlsx	R404A	R	y ~ 1 + x1^2 + x1*x2 + x2^2	21	0.993437	23.00516	454.1373	0
13	R404A-R-OF-M10-U1-00.xlsx	R404A	R	y ~ 1 + x1^2 + x1*x2 + (x1^2):x2	17	0.998224	18.37479	1236.773	0
14	R404A-S-OF-M05-U1-00.xlsx	R404A	S	y ~ 1 + x1 + x2 + x2^2	22	0.990388	51.95655	618.2072	0
15	R404A-S-OX-M02-U1-00-20F.xlsx	R404A	S	y ~ 1 + x1^2 + x1*x2 + x2^2 + (x1^2):x2 + x1:(x2^2) + x2^3	63	0.999975	3.336894	269255.7	0
16	R407C-R-OF-M09-U1-00.xlsx	R407C	R	y ~ 1 + x1^2 + x1*x2 + x2^2 + x1^3 + (x1^2):x2 + x2^3	18	0.997895	34.97763	533.3587	0
17	R407C-RO-OF-M04-U1-00.xlsx	R407C	RO	y ~ 1 + x1^2 + x1*x2 + x2^2	19	0.99972	5.810131	9271.037	0
18	R410A-R-OA-M01-U1-12-cond.xlsx	R410A	R	y ~ 1 + x1^2 + x1*x2 + x2^2 + x1:(x2^2) + x2^3	16	0.999795	4.673819	5585.102	0
19	R410A-R-OA-M01-U2-12-cond.xlsx	R410A	R	y ~ 1 + x1^2 + x1*x2 + x2^2 + (x1^2):x2 + x1:(x2^2)	16	0.999508	6.953506	2320.741	0
20	R410A-R-OA-M01-U3-12-cond.xlsx	R410A	R	y ~ 1 + x1^2 + x1*x2 + x2^2 + x1:(x2^2) + x2^3	16	0.999944	2.328977	20275.37	0

Figure 70: Different equations for power prediction

The interesting observation from this analysis is that the overall errors in prediction are essentially the same when using the full 10 coefficient equation vs. using only the statistically significant terms.

For the Section "Sampling Based on Non-Rectangular Domains," were simple changes in variable examined, where they may then have a rectangular domain to proceed with LHS sampling? For example, TE and Compression Ratio could be used as domain variables instead of TE, TC.

>> We did examine some of these variable changes, but they do not result in a rectangular domain. As an example, refer to the [Te,Tc] and [Te,Pr] plots below in Figures 71 and 72. Pr is the pressure/compression ratio.

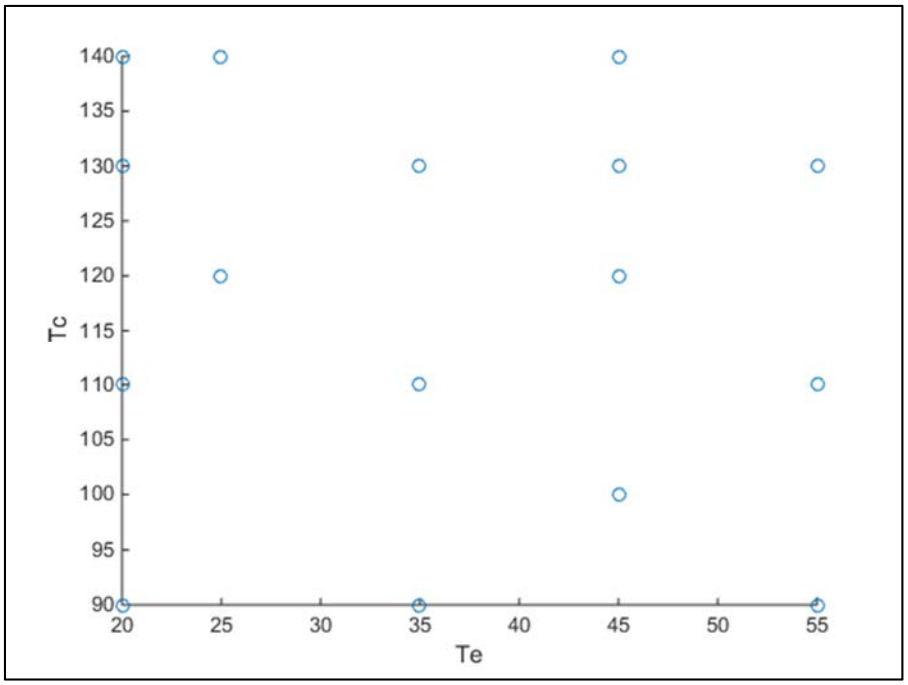

Figure 71: Compressor performance map, operating envelope, [Te,Tc]

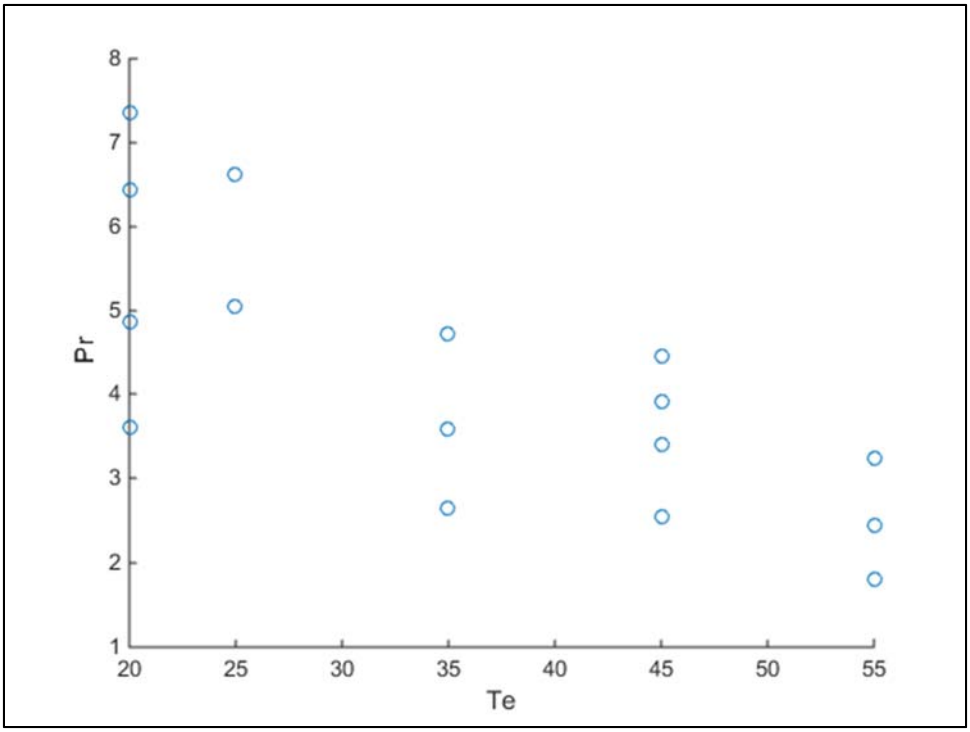

Figure 72: Compressor performance map, operating envelope [Te,Pr]

What were the standard deviations used for the ASHRAE 23 measurement accuracies for the Monte Carlo analysis?

>> The analysis was carried out assuming Normal distributions for all parameters. The standard deviation for temperature was 0.5F and for other parameters (mass flow and power), was 1%.